

NEAR-INFRARED PHOTOIMMUNOTHERAPY TARGETING
OF CANCER-ASSOCIATED FIBROBLASTS

By

Raisa A. Glabman

A DISSERTATION

Submitted to
Michigan State University
in partial fulfillment of the requirements
for the degree of

Comparative Medicine and Integrative Biology – Doctor of Philosophy

2023

ABSTRACT

Cancer-associated fibroblasts (CAFs) constitute a prominent cellular component of the tumor stroma, representing a heterogeneous group of activated fibroblasts. Within the tumor microenvironment (TME), CAFs play various pro-tumorigenic roles, including extracellular matrix remodeling, suppression of anti-tumor immunity, and modulation of tumor cell resistance to therapy. Fibroblast activation protein (FAP), a highly expressed marker on immunosuppressive CAFs, has been identified in several epithelial human cancers such as lung, colon, breast, and prostate cancer. Numerous attempts to target FAP+CAFs for inhibiting tumor progression and enhancing anti-tumor immunity have been reported, however, the translation of FAP-directed therapies into human clinical trials has been unsuccessful. Near-infrared photoimmunotherapy (NIR-PIT) is a highly selective tumor therapy that utilizes an antibody-photo-absorbing conjugate activated by near-infrared (NIR) light. In this study, we describe the therapeutic efficacy of anti-FAP near-infrared photoimmunotherapy (NIR-PIT) and subsequent immune activation in two immune-competent murine cancer models. Targeting FAP+ cells effectively suppressed tumor growth and reduced lung metastasis in a spontaneous mouse model of mammary cancer. These findings highlight a promising therapeutic approach for selectively and safely eliminating immunosuppressive FAP+ cells within the tumor microenvironment.

Copyright by
RAISA A. GLABMAN
2023

ACKNOWLEDGEMENTS

I am extremely grateful to have had the opportunity to be a trainee at both Michigan State University (MSU) and the National Cancer Institute (NCI). I recognize that I am uniquely fortunate to have this experience learning from MSU faculty and NCI clinicians, scientists and investigators all working towards the common goal of improving human and animal health.

Thank you to the Comparative Biomedical Scientist Training Program (CBSTP); Dr. Mark Simpson, Dr. Heather Shive, Jennifer Dwyer, Dr. Bih-Rong Wei, and the administrative staff for their invaluable support in ensuring the smooth operation of our fellowships. It has been an honor to work alongside the exceptionally talented CBSTP fellows, both past and present. Many thanks to the members of the Molecular Imaging Branch, as well as my colleagues in the Sato Lab – Colleen Olkowski, Dr. Qioaya Lin, Dr. Zuping Wang and Hannah Minor.

I am deeply thankful to my committee members: Dr. Peter Choyke, Dr. Noriko Sato, Dr. Dalen Agnew, Dr. Margaret Petroff, Dr. Mark Simpson, and my major faculty advisor, Dr. Gisela Soboll Hussey. Their guidance, support, and encouragement throughout my PhD program have been instrumental in shaping my research journey. Thank you to Dr. Colleen Hegg and Dimity Palazzola in the CMIB department for your tireless support of graduate students.

Lastly, I am eternally grateful to my family—Maureen, David, and Shira—and my extraordinary partner, Courtney. Your unwavering support has been my anchor and my strength during the most challenging moments of my journey.

TABLE OF CONTENTS

LIST OF ABBREVIATIONS vi

CHAPTER 1 INTRODUCTION AND LITERATURE REVIEW..... 1

 REFERENCES 23

 APPENDIX 1: TABLES & FIGURES 42

CHAPTER 2 ANTI-FIBROBLAST ACTIVATION PROTEIN NEAR-INFRARED
PHOTOIMMUNOTHERAPY TARGETING CANCER-ASSOCIATED FIBROBLASTS..... 48

 REFERENCES 72

 APPENDIX 2: TABLES & FIGURES 78

CHAPTER 3 CONCLUSIONS AND FUTURE DIRECTIONS..... 92

 REFERENCES 98

LIST OF ABBREVIATIONS

CAF	Cancer-associated fibroblast
ECM	Extracellular Matrix
FAP	Fibroblast activation protein
NIR-PIT	Near infrared photoimmunotherapy
PDPN	Podoplanin
α -SMA	alpha Smooth Muscle Actin

CHAPTER 1

INTRODUCTION AND LITERATURE REVIEW

Cancer-associated fibroblasts: Tumorigenicity and targeting for cancer therapy

Raisa A. Glabman^{1,2}, Peter L. Choyke¹, Noriko Sato^{1,*}

¹ Molecular Imaging Branch, Center for Cancer Research, National Cancer Institute, National Institutes of Health, Bethesda, MD 20892, USA

² Department of Pathobiology and Diagnostic Investigation, College of Veterinary Medicine, Michigan State University, East Lansing, MI 48824, USA

* Corresponding author: N. Sato, saton@mail.nih.gov; Molecular Imaging Branch, Center for Cancer Research, National Cancer Institute, National Institutes of Health, Bethesda, MD 20892, USA Tel.: 1-240-858-3079

ABSTRACT

Cancer-associated fibroblasts (CAFs) are a heterogeneous group of activated fibroblasts and major component of the tumor stroma. CAFs may be derived from fibroblasts, epithelial cells, endothelial cells, cancer stem cells, adipocytes, pericytes, or stellate cells. These complex origins may underlie their functional diversity, which includes pro-tumorigenic roles in extracellular matrix remodeling, suppression of anti-tumor immunity and resistance to cancer therapy. Several methods for targeting CAFs to inhibit tumor progression and enhance anti-tumor immunity have recently been reported. While preclinical studies have shown promise, to date they have been unsuccessful in human clinical trials against melanoma, breast cancer, pancreas cancer, and colorectal cancers. This review summarizes recent and major advances in CAF-targeting therapies, including DNA-based vaccines, anti-CAF CAR-T cells, and modifying and reprogramming CAF functions. Challenges in developing effective anti-CAF treatment are highlighted, which include CAF heterogeneity and plasticity, lack of specific target markers for CAFs, limitations in animal models recapitulating human cancer microenvironment, and undesirable off-target and systemic side effects. Overcoming these challenges and expanding our understanding of the basic biology of CAFs is necessary for making progress towards safe and effective therapeutic strategies against cancers in human patients.

Introduction

Over 1.9 million new cancer cases are expected in the United States in 2022, and solid tumors comprise approximately 90% of these cases [1]. As we continue to expand our knowledge of cancer, we now recognize the tumor microenvironment as a heterogenous, intricate system composed of tumor cells and nonmalignant host components including immune cells, stroma, and vasculature, which shapes the nature of the tumor. In many epithelial tumors, including pancreatic, lung, breast and colorectal cancers, the stroma can comprise up to 90% of the cancer mass [2]. Within the tumor stroma are both cellular and noncellular components, including collagen, fibroblasts, and mesenchymal stromal cells which provide structure and remodel the tissue. Activated stromal tissue, in the pathological context, forms desmoplasia or fibrosis, resulting in increased mass and stiffness which are considered negative prognostic indicators. Fibroblasts constitute one of the most abundant and critical cell types in the tumor stroma and are the major producers of connective tissue extracellular matrix (ECM). Within the tumor microenvironment, various inflammatory cytokines produced by cancer cells, host immune and stromal cells induce activation of fibroblasts. These activated fibroblasts are termed cancer-associated fibroblasts (CAFs). Through their production of soluble factors, such as cytokines and chemokines, and ECM, CAFs strongly influence surrounding cells. They support tumor progression and metastasis by promoting cancer cell growth, enhancing pro-tumor immune responses, remodeling the ECM, influencing tumor cell drug resistance, and promoting angiogenesis [3, 4]. In this review, we focus on CAFs, discuss their biologic tumor-promoting functions and recent advancements in the development of CAF-targeting cancer therapies.

Definitions, origins, and basic biology of CAFs

Definition of CAFs

Fibroblasts are found in virtually all organs and normal tissues and contribute to inflammation and fibrosis during wound healing. CAFs are activated fibroblasts with a mesenchymal lineage associated with cancer and contribute to tumor-promoting inflammation and fibrosis. CAFs are defined by a combination of their morphology, association with cancer cells, and lack of lineage markers for epithelial cells, endothelial cells, and hematopoietic cells [4]. CAFs maintain key roles in regulating the biologic function of the tumor stroma and contribute to immune regulation, angiogenesis, and ECM remodeling of the tumor, as well as generation and maintenance of cancer stem cells, thereby promoting therapeutic resistance.

Distinction of CAFs from resting fibroblasts

CAFs differ in several respects from resting fibroblasts residing in normal tissues. CAFs are generally larger than resting fibroblasts, spindle-shaped, and have indented nuclei and branching cytoplasm. However, the difference between the two is largely a functional distinction. CAFs possess enhanced proliferative, migratory, and secretory properties. CAFs are more metabolically active than untransformed fibroblasts, producing increased extracellular matrix factors such as tenascin, periostin (POSTN), and secreted protein acidic and rich in cysteine (SPARC) [5]. Collagen production by CAFs is abnormal, characterized by increased production and often a more rigid and contractile pattern of collagen deposition [6-8]. Several signaling mechanisms are recognized in the transition from resting fibroblast to CAF, including activation of the Hippo pathway, loss of p53, and activation of heat shock factor protein 1 triggered by inflammation and changes in the structure and composition of the ECM [6, 9]. CAFs are even found in circulation, akin to circulating tumor cells (CTCs) - circulating CAFs [identified based on expression of

fibroblast activation protein (FAP) and alpha-smooth muscle actin (α -SMA)] were found in 88% of patients with metastatic breast cancer and in 23% of patients with nonmetastatic disease [9], suggesting a role in metastasis and formation of the pre-metastatic niche.

Origin of CAFs

CAFs can arise from myriad cell precursors, which can also vary between tissues. The origins of all CAFs are not entirely and fully elucidated. Regardless of origin, the transition to CAF is largely irreversible, and yet remains plastic with regard to CAF phenotype within or across tumor types. CAFs often develop from local resident fibroblast populations but can also differentiate from mesenchymal stromal cells or mesenchymal stem cells (MSCs). MSCs express a similar, less abundant set of surface markers, and possess the ability to differentiate into osteoblasts, chondrocytes and adipocytes [10-12]. Quiescent resident fibroblasts in the liver and pancreas, also known as pancreatic stellate cells, can acquire a CAF phenotype upon activation by tumor growth factor beta (TGF- β) and platelet-derived growth factors (PDGFs) [13, 14]. Outside of the fibroblast lineage, CAFs can transdifferentiate from epithelial cells, blood vessels, adipocytes, pericytes, and smooth muscle cells via endothelial to mesenchymal transition (EMT) and endothelial to mesenchymal transition (EndMT). Fibrocytes, circulating mesenchymal cells derived from monocyte precursors can also become CAFs [15]. Both noninvasive and invasive cancer cells can express EMT markers β -catenin and vimentin or S100A4, so these are also not unique to CAFs. Importantly, CAFs can secrete proinflammatory cytokines, such as interleukin (IL)-6, which promotes EMT of cancer cells [16-18], forming a positive feedback loop. Recruitment and activation of CAFs is mediated by hypoxic conditions, oxidative stress, and certain growth factors produced by tumor cells. TGF- β , epidermal growth factor (EGF), fibroblast growth factor type 2 (FGF2) and PDGF are known to act as key regulators of CAF recruitment and activation [19, 20].

Additionally, IL-1 β from innate immune cells triggers NF- κ B activation and production of IL-6 in CAFs via the JAK-STAT pathway, contributing to CAF differentiation [21]. Lysophosphatidic acid produced by cancer cells synergizes with TGF- β to drive activation and increase contractility of CAFs [4]. Recent research has also shown that exosomes secreted by murine melanoma, human squamous cell carcinoma and human breast carcinoma can promote the differentiation of fibroblasts into CAFs, mediated by TGF- β and downstream SMAD signaling pathways [22, 23]. Overall, the precise origin and roles of fibroblast populations within the tumor microenvironment remain poorly understood. Further studies using lineage tracing for cell of origin [24, 25] will be essential in deepening our understanding on the origins of CAFs, as well as their evolution during tumorigenesis.

CAF phenotypic and functional heterogeneity

Tumors are spatially and functionally heterogeneous ecosystems [26], and the variety of sources from which CAFs can arise lend complexity to their phenotype, gene expression and function. Several biomarkers have been established to detect CAFs, however none are completely exclusive. To date, CAFs are defined as cells that lack expression of biomarkers for epithelial, endothelial, or hematopoietic cells but express mesenchymal biomarkers such as vimentin, α -SMA, FAP, and platelet-derived growth factor receptor alpha (PDGFR- α), and lack genetic mutations [27, 28]. As the phenotype of CAFs differs between tumor type, CAF studies necessitate the combined application of multiple biomarkers for detection and identification of these cells. As a result, CAFs are often identified by a combination of α -SMA, tenascin-C, periostin (POSTN), NG2 chondroitin sulfate proteoglycan, PDGFR- α/β and FAP expression. Other mesenchymal markers include vimentin, fibronectin, type I collagen, prolyl 4-hydroxylase, fibroblast surface protein, and

fibroblast specific protein-1 (FSP-1)/S100A4 [29]. Biomarkers expressed by CAFs are summarized in Table 1a and 1b.

Historically, activated fibroblasts expressing α -SMA were termed ‘myofibroblasts’ but are now recognized to be only one subset among several within the tumor microenvironment. **α -SMA+ CAFs** predominantly produce and modulate the ECM, facilitate cell-ECM adhesion, and regulate adaptive immunity [30]. **α -SMA+ CAFs** are also located more distally to tumor cells. **FAP+ CAFs** are immunosuppressive with increased ECM alignment and stiffness, and this is hypothesized to be a major factor in the transition from a tumor-resistant to tumor-permissive microenvironment [31]. Stiffness of the tumor stroma influences invasion through tumor cell integrin-dependent mechanotransduction signaling [32], and is correlated with increased metastasis [33, 34].

Newer analytic methods such as single-cell RNA sequencing (scRNAseq) and cytometry by time of flight (cyTOF) have begun to help answer questions concerning functional subsets. Functional CAF subsets maintain unique cytokine expression profiles which variably shape the tumor microenvironment. While some CAF subsets do not seem to affect immune cell populations, others in fact, modulate the immune microenvironment, often in pro-tumorigenic ways. The most recent scRNAseq transcriptome data suggest there are between 3-7 major subsets of fibroblasts [35-37] but some of these groups may have overlapping features, as well as context-dependent and tumor-dependent variability. Nonetheless, there is growing evidence for similar or shared phenotypes across tumor types as discussed in the following sections.

Functional CAF subsets in human cancers

Analysis of distinct CAF subpopulations at the single cell level has largely been performed in the context of human pancreatic cancer, with several studies also examining these cells in other human tumor types (Table 2). In human pancreatic cancer, at least two major CAF phenotypes are defined

by their expression of α -SMA and IL-6. A more matrix-secreting, TGF- β -responsive, high- α -SMA and low-cytokine (e.g., IL-6, IL-11)-expressing myofibroblastic, **myCAF** population, and inflammatory-type, **iCAFs**, that exhibit high IL-6 and IL-11 production and low α -SMA expression.[35, 38-40]. Spatial distribution of these two populations also differs - myCAFs are often found adjacent to neoplastic cells whereas iCAFs localize within dense stromal regions distant from neoplastic cells [39]. Interestingly, pancreatic CAFs, formerly quiescent pancreatic stellate cells, are able to transition between the **myCAF** and **iCAF** states, although the mechanism by which this occurs is not well understood [39]. A third CAF phenotype, **apCAFs**, are characterized by major histocompatibility complex (MHC) class II and CD74 expression and capable of presenting antigen to CD4 T cells, but lack classical costimulatory molecules expressed by professional antigen-presenting cells [35]. **MyCAF** and **iCAF** subpopulations have also been identified in human cholangiocarcinoma [41] and bladder cancer [42]. Human triple negative breast [43, 44] and ovarian [45] cancer studies have yielded 3-4 CAF subtypes, designated **CAF S1-S4** based on differential expression of six fibroblast markers (FAP, integrin β 1/CD29, α -SMA, S100-A4/FSP1, PDGFR- β , and CAV1). Other phenotyping studies in human lung [37], prostate [46], head and neck [47] and colorectal [48, 49] cancers similarly classify CAF subpopulations based on high versus low α -SMA expression and/or functional characteristics.

Functional CAF subsets in murine cancers

The three CAF subsets described in human tumors are also found in murine pancreatic cancer models by scRNAseq analysis; ECM-producing **myCAFs**, inflammatory **iCAFs**, and a third smaller population of antigen presenting **apCAFs**. CAF subsets in spontaneous mouse mammary tumor models (the MMTV-PyVT mouse model) have been categorized into four main groups, vascular CAFs (**vCAFs**), cycling CAFs (**cCAF**), matrix CAFs (**mCAF**), and developmental CAFs

(**dCAF**) [50]. **vCAFs** are angiogenic, predominantly located near vessels and thought to arise from perivascular cell precursors. **cCAFs** are considered the proliferating fraction of **vCAFs**, with similar transcriptional profiles as **vCAFs**, exhibiting upregulated cell cycle genes (e.g. *Nuf2*, *Mki67*, *Ccna2*, *Top2a*, *Cep55*). **mCAFs** are descendents of resident fibroblasts, expressing fibulin-1 and PDGFR α , which are often positioned at the invasive front of tumors. **dCAFs** express development-associated genes and are similar in phenotype and are proximal to cancer cells, suggesting they may originate from a malignant cell precursor. In 4T1 mouse mammary tumor models, eight subtypes of CAFs divided into in two main populations, **pCAF** and **sCAF**, are described based on selective expression of PDPN or S100A4. The ratio of **pCAFs** and **sCAFs** changes with tumor progression and is associated with disease outcome in triple negative breast cancer patients [51].

CAFs have been functionally categorized in other murine cancers, such as melanoma, as either immune (**S1**), desmoplastic (**S2**) or contractile (**S3**)[52], and in cholangiocarcinoma as either **myCAF**, **iCAF**, or mesothelial **mesCAF** [41]. Overall, the existence of both myofibroblastic and inflammatory CAF populations appears to be the most consistent observation in both human and mouse tumor models. Across cancer types, **myCAFs** are associated with high ECM production, whereas non-myofibroblastic **iCAFs** are generally characterized by a secretory, inflammatory phenotype. Lastly, CAFs can also be grouped based on location, e.g. primary tumor, circulation, or metastasis [53, 54].

Challenges in defining and detecting CAFs

By far, one of the greatest challenges in defining CAFs is the lack of a pan-specific biomarker. In addition, no standardization nor consensus of biomarkers to identify CAFs currently exist, adding to the difficulty in differentiating CAFs from other mesenchymal cells (e.g. adipocytes or

pericytes). This lack of uniform analysis makes interpretation of previous studies and understanding of the full biological implications of these cells difficult. Standardized functional and molecular definitions of fibroblast subtypes also do not yet exist. There is inherent plasticity between CAF subtypes, suggesting these are functional fibroblastic states, as opposed to static fibroblast types, adding to their complexity [55]. CAFs continue to evolve over time and eventually differentiate into subpopulations that promote tumor development in ways that are not only tissue specific but tumor specific. Identifying what triggers this plasticity will also be invaluable in future research, as phenotypic or functional subsets may not function comparably across tumor types. It is increasingly clear that the tumor microenvironment changes throughout cancer progression, and likely so do CAFs. Longitudinal studies, particularly focused on CAF plasticity, are necessary for further insight.

Pro-tumorigenic functions of CAFs

Various components of the tumor microenvironment promote tumor progression and resistance to cancer therapy. For instance, mesenchymal stem cells can secrete vascular endothelial growth factor (VEGF), promoting vessel growth, and prostaglandin E2 (PGE2), impeding the anti-tumor immune response through suppression of T cell function. Pericytes and adipocytes can produce pro-tumorigenic growth factors and cytokines and even contribute to T cell anergy [56]. Finally, immune cells such as TAMs promote EMT, inflammation-associated angiogenesis through VEGF, TIE2, and CD31 expression [57], and therapeutic resistance. Here, we focus specifically on the roles of CAFs.

Tumor promoting secretory factors

In general, CAFs secrete far more cytokines and chemokines than their resting counterparts. These secreted factors include TGF- β , PDGF, FGF, hepatocyte growth factor (HGF), VEGF, tumor

necrosis factor α (TNF- α), interferon- γ (IFN γ), CXCL12, IL-6, connective tissue growth factor (CTGF- β), EGF, growth arrest-specific protein 6 (GAS6), galectin-1, secreted frizzled-related protein 1 (SFRP1), sonic hedgehog protein (SHH), and bone morphogenetic protein (BMP), which are tumor-promoting [6]. As the master regulator of fibrosis and a major secreted factor of CAFs, TGF- β predominantly mediates cross-talk between CAFs and cancer cells. Inhibition of TGF- β signaling using a number of approaches has been shown to significantly inhibit tumor growth and metastasis [58].

CAFs have also been demonstrated to induce EMT and promote the growth and migration of cancer cells via IL-6 [59, 60]. Elevated levels of CAF-derived IL-6 induces activation of the JAK/STAT3 signaling pathway, leading to tumor cell proliferation mediated by activation of cyclin D1, among other cell cycle mediators. Tumor survival is enhanced by activation of downstream BCL2-like protein 1 (BCL2-L1). STAT3 also induces expression of angiogenic factor VEGF. During tumor neovascularization, degradation of the basement membrane and ECM occurs, with contribution from matrix metalloproteinases (MMPs) [61], to allow for endothelial cells to migrate and generate new vessels. This process, in turn, enhances cancer invasion and metastasis. The hyperactivation of STAT3 in anti-tumor immune cells exerts a negative regulatory effect which also contributes to an immunosuppressive tumor microenvironment [62]. Other signaling pathways governing the tumor-promoting ability of CAFs include PDGF-PDGFR, which acts through paracrine signaling on cancer cells to drive tumor growth [29].

Resistance to chemotherapies and radiation

Classic chemotherapy targets rapidly proliferating cells, but does not eliminate all CAFs, nor those cancer cells that become drug resistant. CAFs can also contribute to the development of resistant cancer phenotypes following cycles of chemotherapies. Several in vitro experiments demonstrate

that DNA damage induced by chemotherapies prompted increased cancer cell invasion and survival through stromal-derived paracrine signaling via cytokines and exosomes [6]. For example, this occurs via glial derived neurotrophic factor (GDNF) production in prostate cancer [63], IL-6 in lymphoma [64], and exosome secretion in colorectal cancer [65]. Chemotherapy-induced genotoxic stress can also trigger a DNA damage secretory program resulting in release of numerous inflammatory (IL-6/8), angiogenic (VEGF, CXCL1), mitogenic (amphiregulin) and pro-EMT (HGF) factors [55].

Several chemotherapy drugs have been reported to induce CAF-like phenotypes in resting fibroblasts and promote stemness in breast [66] and colorectal cancers [65]. This is thought to occur following an exposure of cancer cells to a hypoxic environment, which activates hypoxia-inducible factor (HIF-1 α) and sonic hedgehog-GLI signaling [66, 67]. CAF-mediated TGF- β signaling synergizes with HIF-1 α signaling and enhances the expression of GLI2 in cancer cells, inducing stemness. This results in resistance to chemotherapy. In fact, high expression of the HIF-1 α /TGF- β is associated with increased risk of colorectal cancer recurrence in patients undergoing chemotherapy [67]. Similarly, studies have found that CAFs contribute to drug resistance and reduce the efficacy of anti-EGFR cetuximab [68], gemcitabine [69], and tyrosine kinase inhibitor gefitinib [70].

As with the examples of chemotherapies described above, radiation therapy impedes cancer cell growth through DNA damage. Radiation affects not only cancer cells but also the tissue microenvironment surrounding cancer cells, which includes immune cells, endothelial cells, vasculature, and fibroblasts. Fibroblasts are highly resistant to radiation, even at high doses. Irradiated fibroblasts can overcome apoptotic signals and become senescent but have also been demonstrated to convert to a more activated CAF phenotype [71-73]. In one study, radiation

exposure activated CAFs and upregulated their expression of CXCL12, which directly acted on pancreatic cancer cells via CXCR4, promoting EMT and invasion in vitro and in vivo [74]. Enhanced expression of CXCL12, HGF, MMPs and TGF- β in irradiated fibroblasts was found to increase invasion and EMT in cancer cells as indicated by increased expression of vimentin, snail and beta-catenin, and decreased E-cadherin expression. [71-73].

CAF-directed resistance to radiotherapy and post-radiation recurrence of cancers is reported to be associated with activation of the autophagy pathway. It is likely this response is at least in part related to CAF-secreted IGF1/2, CXCL12 and β -hydroxybutyrate, leading to increased reactive oxygen species (ROS), enhancing protein phosphatase 2A (PP2A) activity, repressing mTOR activation, ultimately resulting in autophagy in cancer cells after irradiation [75, 76]. The IGF2 neutralizing antibody and autophagy inhibitor 3-MA consistently reduced the CAF-promoted tumor relapse in tumor-bearing mice after radiotherapy [75]. Combining CAF-targeted therapies and chemotherapy or radiation could yield a more powerful and robust anti-tumor response.

Immunomodulatory role of CAFs

Advances in immune checkpoint inhibitors, such as PD-1 and CTLA-4, have brought much attention to the immune cell-tumor crosstalk, however, less is known about the contribution of stromal components to the immune milieu. Recent studies suggest CAFs mediate the tumor immune landscape via the secretion of various cytokines, growth factors, chemokines, exosomes, and other effector molecules, ultimately shaping an immunosuppressive tumor microenvironment, enabling cancer cells to evade immune surveillance, and limiting immunotherapy strategies.

In general, CAFs shape the tumor microenvironment by production of proinflammatory cytokines, including IL-1 β and IL-6 [21, 77], and express the ligands CXCL12 [78], CXCL1 [79], and G-CSF [80] which can drive downstream immunosuppressive signaling pathways. For instance,

CXCL12 regulates interactions between tumor cells and surrounding cells in the tumor microenvironment, promoting tumor survival, proliferation, angiogenesis, and metastasis. It also promotes recruitment of immunosuppressive cells and their precursors, notably bone marrow mesenchymal stem cells and monocytes that differentiate into tumor-associated macrophages (TAMs). Inflammatory CAFs, or iCAF, highly express CXCL12 which binds to CXCR4 [35]. Blocking the CXCL12-CXCR4 interaction can induce cancer regression in pre-clinical models [78, 81]. CAFs also interact with T cells, NK cells, dendritic cells (DCs), myeloid-derived suppressor cells (MDSCs), mast cells, TANs and TAMs in the tumor microenvironment generally resulting in an immunopermissive environment.

CAFs prevent CD8⁺ cytotoxic T cell activity and recruitment within tumors, in part through TGF- β [82-84] and CXCL12 [85]. Both TGF- β and CXCL12 are known to contribute to cytotoxic T cell exclusion by attenuation of the anti-PD-L1 response [78]. While limiting anti-tumor cytotoxic T cells, CAFs can also increase intratumoral Treg recruitment and scRNAseq revealed upregulation of PD-1 and CTLA4 in Tregs. CAFs appear to attract, help accumulate and promote the survival of FOXP3⁺Tregs in human triple negative breast cancer [44]. FoxP3⁺Tregs are known to restrain host-antitumor-immunity, and thereby lend an unfavorable prognosis in number of cancers. Although the precise mechanism of crosstalk between Tregs and CAFs remains unclear, high numbers of both cell types are found in stromal regions and are associated with low survival in cancers such as lung adenocarcinoma [86].

NK cells are well-known innate effector cells; however, their function can be impaired by CAFs through inhibition of NK receptor activation, cytotoxic activity, and cytokine production [87, 88]. Netrin G1 (NetG1) expression on CAFs can suppress the cytotoxic function of NK cells and support survival of cancer cells in nutrient-deprived environments, and is thus, linked to poor

prognosis in cancers such as pancreatic ductal adenocarcinoma [89]. Tumor-infiltrating DCs are also critical to the anti-tumor immune response, and their functionality can similarly be impaired by CAFs. By activating the IL-6-mediated STAT3 pathway, CAFs in hepatocellular carcinoma transdifferentiated DCs into regulatory DCs (rDCs) that produce inhibitory cytokines and enzymes such as indoleamine 2,3-dioxygenase (IDO) [90]. VEGF produced by CAFs is also involved in the abnormal differentiation and impaired antigen presenting function of DCs via inhibition of NF- κ B activation [91].

MDSCs can be also be recruited to the tumor microenvironment by CAFs via CCL2 [92], thereby suppressing CD8 T cell proliferation and IFN- γ production [93]. Mast cells, which can be both tumor-suppressing and tumor promoting, can be recruited by CAFs via CXCL12 in a CXCR4-dependent manner [94]. In vitro, mast cells and CAFs can act together to induce the malignant transformation of benign epithelial cells [95]. Furthermore, N2, or protumorigenic, polarization of neutrophils within the tumor can be induced through CAF-derived cardiotrophin-like cytokine factor 1 (CLCF1), which upregulates CXCL6 and TGF- β on tumor cells [96]. Neutrophils may also be directly recruited by CAFs through secretion of CXCL12 or expression of CXCR2 thus becoming tumor associated neutrophils (TANs) [97, 98]. CAFs regulate the activation, survival, and function of TANs through the IL-6/STAT3-PDL1 signaling axis [97].

Like other cells in the tumor microenvironment, TAMs and CAFs have synergistic effects and are often detected in similar areas of tumor tissue. Their combined presence is a negative prognostic predictive indicator in human cancers [99]. Likewise, CAFs are involved in monocyte recruitment, macrophage differentiation and polarization toward tumor-promoting, or M2 phenotype [100, 101], through secretion of macrophage colony-stimulating factor 1 (M-CSF1), IL-6, CCL2 [102] and IL-8 [103]. M2 macrophages are reciprocally able to stimulate CAF activation through IL-6

and CXCL12 [100]. While research accumulates on the interactions of CAFs and immune cells in the tumor microenvironment, many ongoing questions remain unanswered. Undoubtedly, understanding CAF and immune cell interactions will provide the basis for novel strategies for targeted immunotherapies.

Targeting CAFs: Anti-cancer therapies

Significant advances have been made in CAF-targeted therapies in recent years. Predominantly, these methods aim to (1) directly or indirectly deplete CAFs, (2) reduce or eliminate the tumor-promoting and immunosuppressive functions of CAFs, or (3) normalize or reprogram CAFs to a more quiescent state. Those strategies are summarized here.

Chemotherapy targeting CAFs

As discussed previously, FAP is expressed on subsets of CAFs in various tumors. FAP is a membrane-bound serine postprolyl peptidase that differs from other dipeptidyl prolyl peptidases in that it also has endopeptidase activity [104]. A competitive inhibitor of prolyl peptidase, Val-boroPro (Talabostat) is an oral drug that showed some tumor growth control by degrading ECM in mice [105]. However, in human clinical trials for metastatic colorectal cancers, no therapeutic efficacy was observed [106]. Sibrotuzumab is a humanized anti-FAP monoclonal antibody (clone F19) that inhibits dipeptidyl peptidase activity of FAP [107]. Unlike F19, Sibrotuzumab did not demonstrate inhibitory activity and failed to suppress growth of pancreatic cancers in patients, despite documented evidence of accumulation of the antibody in the tumor using a radiolabeled version of the antibody (iodine-131-labeled Sibrotuzumab) imaged by single photon emission computed tomography (SPECT) [108].

Taking advantage of the unique enzymatic activity of FAP, anti-CAF prodrugs or protoxins contain cytotoxic agents coupled with a dipeptide containing a FAP cleavage site [104, 109]. These

prodrugs remain inactive when systemically delivered and are proteolytically activated upon cleavage by FAP, which is expressed on CAFs in the tumor. Intratumoral injection of these prodrugs produced tumor lysis and growth inhibition in human breast and prostate cancer xenografts [104, 109, 110]. Another class of drugs are the immunotoxins that use an antibody to specifically deliver a toxin to the target cells. Anti-FAP-PE39 demonstrated suppressed mammary tumor growth and increased recruitment of tumor infiltrating lymphocytes [111]. A monoclonal antibody conjugated with a tubulin binding drug maytansinoid and a bispecific antibody simultaneously targeting FAP on CAFs and death receptor 5 on tumor cells has shown potent anti-tumor effects [111, 112]. In another strategy, nanoparticles such as FAP-targeted liposomes have been explored as carriers to specifically deliver therapeutic drugs (e.g. doxorubicin, anti-Tenascin C) to CAFs [113, 114] or to remodel the tumor microenvironment [115, 116]. Despite the success of preclinical strategies, including substantially attenuating the growth of tumor xenografts in various cancer models with minimal to no toxicity [110, 117-119], clinical translation is still in its early stages.

Immunotherapy

Various strategies to enhance immunity against FAP expressing cells (i.e. CAFs) and to suppress cancer growth have been explored. Vaccination against FAP using dendritic cells transfected with FAP mRNA led to suppressed growth of implanted and intravenously injected tumors [120]. The efficacy was enhanced when a co-vaccination against FAP and a tumor cell-associated antigen was used. These DC vaccines, synergistically combined with an anti-fibrotic agent, showed promising activation of both innate and adaptive immunity. Enhanced NK cell activity, anti-tumoral humoral immunity, and cytotoxic CD8⁺ T cell response was observed in three different tumor models [120]. Similarly, adenoviral anti-FAP vaccines are able to selectively deplete CAFs by stimulating a

CD8⁺ T cell response, leading to inhibition of tumor growth and metastasis in several murine cancer models [121-124]. In a landmark study using a transgenic mouse expressing the diphtheria toxin receptor under the FAP promoter, depleting FAP⁺ CAFs by diphtheria toxin administration improved anti-cancer vaccination efficacy [125]. An orally administered anti-FAP DNA vaccine notably suppressed neoangiogenesis, tumor growth and metastasis of orthotopically injected breast carcinoma cells [121]. Adding doxorubicin substantially increased intratumoral uptake of the drug and prolonged lifespans of vaccinated mice [126].

Adoptive chimeric antigen receptor (CAR)-T cell therapy can also be used to directly target CAFs [117, 127, 128]. FAP-specific CAR-T cells deplete most FAP⁺ cells, including CAFs, and restrict tumor stroma generation, resulting in the improved uptake and anti-tumor effects of chemotherapeutic drugs. Unfortunately, several studies have observed severe side effects using this approach, such as significant bone marrow toxicity and cachexia [129, 130]. More selective and yet unknown targets may improve the precision of CAF-based therapies, which remains an active field of research [131].

Finally, near-infrared photoimmunotherapy (NIR-PIT) is an innovative approach to CAF depletion that has been used to directly and specifically deplete FAP expressing cells, including CAFs in the tumor microenvironment. Tumor growth was inhibited using a co-culture xenograft model of human esophageal squamous cell carcinoma without adverse effects [132]. Anti-FAP+CAF therapy combined with 5-fluorouracil (5-FU) could overcome chemoresistance compared with 5-FU alone [133].

Functional Modification/Reprogramming

Strategies that aim to revert activated CAFs to quiescence include use of all-trans-retinoic acid (ATRA) [134-136], minnelide (which de-regulates the TGF- β signaling pathway) [137, 138], and

calcipotriol, a vitamin D receptor ligand [139, 140]. The angiotensin receptor II antagonist losartan has been shown to decrease TGF- β -mediated activation of CAFs, reducing desmoplasia and increasing drug delivery and efficacy of immunotherapy [141-143]. Losartan in combination with other traditional chemotherapies to treat pancreatic cancer is currently under investigation in clinical trials [144]. Recent strategies seek to block immunosuppressive ligands of major CAF signaling pathways such as IL-6 [145, 146], LIF [147] and TGF- β [82, 84] in order to suppress or kill cancer cells.

The CXCL12/CXCR4 axis is important in cancer progression and immunosuppression. CXCL12 produced by CAFs recruits CXCR4 expressing endothelial progenitor cells and immune suppressive Tregs, which contributes to angiogenesis and tumor growth [43, 85]. Abrogation of CXCR4 signaling in CAFs using the CXCR4 inhibitor Plerixafor significantly reduced fibrosis, leading to vasculature normalization, increased cytotoxic T cell infiltration, decreased immunosuppressive cell populations, and increased checkpoint inhibitor efficacy [81]. Other strategies which inhibit CAF functions include TGF- β blockade [148], NF κ B inhibitors to overcome chemotherapy resistance [149], and Smoothed (SMO) hedgehog pathway inhibitors (IPI-926) [150].

Future Perspectives

CAFs play an integral role in the promotion of tumor growth. However, the origin and functional roles of unique CAF subsets are yet to be fully understood, as well as their niche within various tumor types. Determining the spatial and temporal dynamics of CAFs and their cell-to-cell interactions in the tumor microenvironment will add critical information to our knowledge on these fascinating cells. While much of CAF biology has been modeled in vitro, it has been repeatedly demonstrated that CAFs in culture do not fully recapitulate the heterogeneity of CAFs in vivo [47,

151, 152]. Increasing the strategic use of animal models, including humanized and genetically engineered mouse models, is critical to further understanding the origin, plasticity and phenotypes of CAFs over time. To this end, the future of the field will undoubtedly include new and emerging technologies such as fate mapping and scRNAseq to assess changes in both stromal cells and immune cells through tumor progression, digital or multiplex spatial profiling of proteins or RNA in tissue to assess spatial changes in the tumor microenvironment, spatial transcriptomics, digital pathology and three-dimensional tissue clearing and 3D culture systems. Intravital microscopy will provide live visualization of cell-to-cell interactions in vivo. These technologies will bring breakthroughs, such as the identification of even more CAF subpopulations, their cellular interactions, and further insights into CAF heterogeneity and plasticity.

In addition to these analytic methods, a consensus on CAF biomarkers will need to be reached, so that similar phenotypes may be compared across tumor types and preclinical models used in different laboratories. Improving therapeutic delivery methods, such as targeted CAF therapy, rather than stromal-directed therapy is now becoming more common. FAP shows promise as a CAF marker for CAR-targeted therapy. Recently emerged FAP imaging using gallium-68 labeled small-molecule FAP inhibitor (FAPI) as a tracer for positron emission tomography (PET) suggests superiority in detecting FAP+ cell containing cancers in patients compared with [fluorine-18]fluoro-deoxy-glucose PET in some cancers [153]. FAPI PET could be used to predetermine the candidacy for anti-FAP CAF-targeted therapies as well as to evaluate the therapy efficacy.

Conclusions

This review summarizes key advances in CAF directed therapies and highlights new techniques for the molecular targeting of CAFs. Although a dominant cell type in the tumor microenvironment, CAFs are difficult to precisely target for therapy because of their heterogeneity.

These challenges must be overcome to have meaningful impact from benchtop to clinical intervention. The origins of CAFs across cancer types remains elusive, as does the complete picture of subtypes and functional heterogeneity. Minimizing off target and systemic effects is an ongoing challenge. Finally, the combination of CAF immunotherapies with existing therapies may be valuable and remains an active area of investigation. These methods potentially add further insights to our knowledge of CAF biology but can also help improve precision cancer therapeutics and patient outcomes.

REFERENCES

1. Siegel RL, Miller KD, Fuchs HE, Jemal A. Cancer statistics, 2022. *CA Cancer J Clin*. 2022; 72: 7-33. doi: 10.3322/caac.21708.
2. D'Arcangelo E, Wu NC, Cadavid JL, McGuigan AP. The life cycle of cancer-associated fibroblasts within the tumour stroma and its importance in disease outcome. *Br J Cancer*. 2020; 122: 931-42. doi: 10.1038/s41416-019-0705-1.
3. Monteran L, Erez N. The Dark Side of Fibroblasts: Cancer-Associated Fibroblasts as Mediators of Immunosuppression in the Tumor Microenvironment. *Front Immunol*. 2019; 10: 1835. doi: 10.3389/fimmu.2019.01835.
4. Sahai E, Astsaturon I, Cukierman E, DeNardo DG, Egeblad M, Evans RM, Fearon D, Greten FR, Hingorani SR, Hunter T, Hynes RO, Jain RK, Janowitz T, et al. A framework for advancing our understanding of cancer-associated fibroblasts. *Nat Rev Cancer*. 2020; 20: 174-86. doi: 10.1038/s41568-019-0238-1.
5. Belhabib I, Zaghdoudi S, Lac C, Bousquet C, Jean C. Extracellular Matrices and Cancer-Associated Fibroblasts: Targets for Cancer Diagnosis and Therapy? *Cancers (Basel)*. 2021; 13. doi: 10.3390/cancers13143466.
6. Valkenburg KC, de Groot AE, Pienta KJ. Targeting the tumour stroma to improve cancer therapy. *Nat Rev Clin Oncol*. 2018; 15: 366-81. doi: 10.1038/s41571-018-0007-1.
7. Pankova D, Chen Y, Terajima M, Schliekelman MJ, Baird BN, Fahrenholtz M, Sun L, Gill BJ, Vadakkan TJ, Kim MP, Ahn YH, Roybal JD, Liu X, et al. Cancer-Associated Fibroblasts Induce a Collagen Cross-link Switch in Tumor Stroma. *Mol Cancer Res*. 2016; 14: 287-95. doi: 10.1158/1541-7786.MCR-15-0307.
8. Kalluri R. The biology and function of fibroblasts in cancer. *Nat Rev Cancer*. 2016; 16: 582-98. doi: 10.1038/nrc.2016.73.
9. Ao Z, Shah SH, Machlin LM, Parajuli R, Miller PC, Rawal S, Williams AJ, Cote RJ, Lippman ME, Datar RH, El-Ashry D. Identification of Cancer-Associated Fibroblasts in Circulating Blood from Patients with Metastatic Breast Cancer. *Cancer Res*. 2015; 75: 4681-7. doi: 10.1158/0008-5472.CAN-15-1633.
10. Lindner U, Kramer J, Rohwedel J, Schlenke P. Mesenchymal Stem or Stromal Cells: Toward a Better Understanding of Their Biology? *Transfus Med Hemother*. 2010; 37: 75-83. doi: 10.1159/000290897.
11. Paunescu V, Bojin FM, Tatu CA, Gavriliuc OI, Rosca A, Gruia AT, Tanasie G, Bunu C, Crisnic D, Gherghiceanu M, Tatu FR, Tatu CS, Vermesan S. Tumour-associated fibroblasts and mesenchymal stem cells: more similarities than differences. *J Cell Mol Med*. 2011; 15: 635-46. doi: 10.1111/j.1582-4934.2010.01044.x.

12. Dominici M, Le Blanc K, Mueller I, Slaper-Cortenbach I, Marini F, Krause D, Deans R, Keating A, Prockop D, Horwitz E. Minimal criteria for defining multipotent mesenchymal stromal cells. The International Society for Cellular Therapy position statement. *Cytotherapy*. 2006; 8: 315-7. doi: 10.1080/14653240600855905.
13. Helms E, Onate MK, Sherman MH. Fibroblast Heterogeneity in the Pancreatic Tumor Microenvironment. *Cancer Discov*. 2020; 10: 648-56. doi: 10.1158/2159-8290.CD-19-1353.
14. Norton J, Foster D, Chinta M, Titan A, Longaker M. Pancreatic Cancer Associated Fibroblasts (CAF): Under-Explored Target for Pancreatic Cancer Treatment. *Cancers (Basel)*. 2020; 12. doi: 10.3390/cancers12051347.
15. Liu T, Han C, Wang S, Fang P, Ma Z, Xu L, Yin R. Cancer-associated fibroblasts: an emerging target of anti-cancer immunotherapy. *J Hematol Oncol*. 2019; 12: 86. doi: 10.1186/s13045-019-0770-1.
16. Long KB, Tooker G, Tooker E, Luque SL, Lee JW, Pan X, Beatty GL. IL6 Receptor Blockade Enhances Chemotherapy Efficacy in Pancreatic Ductal Adenocarcinoma. *Mol Cancer Ther*. 2017; 16: 1898-908. doi: 10.1158/1535-7163.MCT-16-0899.
17. Jia C, Wang G, Wang T, Fu B, Zhang Y, Huang L, Deng Y, Chen G, Wu X, Chen J, Pan Y, Tai Y, Liang J, et al. Cancer-associated Fibroblasts induce epithelial-mesenchymal transition via the Transglutaminase 2-dependent IL-6/IL6R/STAT3 axis in Hepatocellular Carcinoma. *Int J Biol Sci*. 2020; 16: 2542-58. doi: 10.7150/ijbs.45446.
18. Sun Q, Zhang B, Hu Q, Qin Y, Xu W, Liu W, Yu X, Xu J. The impact of cancer-associated fibroblasts on major hallmarks of pancreatic cancer. *Theranostics*. 2018; 8: 5072-87. doi: 10.7150/thno.26546.
19. Lohr M, Schmidt C, Ringel J, Kluth M, Muller P, Nizze H, Jesnowski R. Transforming growth factor-beta1 induces desmoplasia in an experimental model of human pancreatic carcinoma. *Cancer Res*. 2001; 61: 550-5. doi:
20. Aoyagi Y, Oda T, Kinoshita T, Nakahashi C, Hasebe T, Ohkohchi N, Ochiai A. Overexpression of TGF-beta by infiltrated granulocytes correlates with the expression of collagen mRNA in pancreatic cancer. *Br J Cancer*. 2004; 91: 1316-26. doi: 10.1038/sj.bjc.6602141.
21. Erez N, Truitt M, Olson P, Arron ST, Hanahan D. Cancer-Associated Fibroblasts Are Activated in Incipient Neoplasia to Orchestrate Tumor-Promoting Inflammation in an NF-kappaB-Dependent Manner. *Cancer Cell*. 2010; 17: 135-47. doi: 10.1016/j.ccr.2009.12.041.
22. Ringuette Goulet C, Bernard G, Tremblay S, Chabaud S, Bolduc S, Pouliot F. Exosomes Induce Fibroblast Differentiation into Cancer-Associated Fibroblasts through TGFbeta Signaling. *Mol Cancer Res*. 2018; 16: 1196-204. doi: 10.1158/1541-7786.MCR-17-0784.

23. Yeon JH, Jeong HE, Seo H, Cho S, Kim K, Na D, Chung S, Park J, Choi N, Kang JY. Cancer-derived exosomes trigger endothelial to mesenchymal transition followed by the induction of cancer-associated fibroblasts. *Acta Biomater.* 2018; 76: 146-53. doi: 10.1016/j.actbio.2018.07.001.
24. LeBleu VS, Taduri G, O'Connell J, Teng Y, Cooke VG, Woda C, Sugimoto H, Kalluri R. Origin and function of myofibroblasts in kidney fibrosis. *Nat Med.* 2013; 19: 1047-53. doi: 10.1038/nm.3218.
25. Driskell RR, Lichtenberger BM, Hoste E, Kretzschmar K, Simons BD, Charalambous M, Ferron SR, Herault Y, Pavlovic G, Ferguson-Smith AC, Watt FM. Distinct fibroblast lineages determine dermal architecture in skin development and repair. *Nature.* 2013; 504: 277-81. doi: 10.1038/nature12783.
26. Hanahan D. Hallmarks of Cancer: New Dimensions. *Cancer Discov.* 2022; 12: 31-46. doi: 10.1158/2159-8290.CD-21-1059.
27. Nurmik M, Ullmann P, Rodriguez F, Haan S, Letellier E. In search of definitions: Cancer-associated fibroblasts and their markers. *Int J Cancer.* 2020; 146: 895-905. doi: 10.1002/ijc.32193.
28. Ping Q, Yan R, Cheng X, Wang W, Zhong Y, Hou Z, Shi Y, Wang C, Li R. Cancer-associated fibroblasts: overview, progress, challenges, and directions. *Cancer Gene Ther.* 2021; 28: 984-99. doi: 10.1038/s41417-021-00318-4.
29. Togo S, Polanska UM, Horimoto Y, Orimo A. Carcinoma-associated fibroblasts are a promising therapeutic target. *Cancers (Basel).* 2013; 5: 149-69. doi: 10.3390/cancers5010149.
30. Ozdemir BC, Pentcheva-Hoang T, Carstens JL, Zheng X, Wu CC, Simpson TR, Laklai H, Sugimoto H, Kahlert C, Novitskiy SV, De Jesus-Acosta A, Sharma P, Heidari P, et al. Depletion of Carcinoma-Associated Fibroblasts and Fibrosis Induces Immunosuppression and Accelerates Pancreas Cancer with Reduced Survival. *Cancer Cell.* 2015; 28: 831-3. doi: 10.1016/j.ccell.2015.11.002.
31. Barrett R, Pure E. Cancer-associated fibroblasts: key determinants of tumor immunity and immunotherapy. *Curr Opin Immunol.* 2020; 64: 80-7. doi: 10.1016/j.coi.2020.03.004.
32. Bayer SV, Grither WR, Brenot A, Hwang PY, Barcus CE, Ernst M, Pence P, Walter C, Pathak A, Longmore GD. DDR2 controls breast tumor stiffness and metastasis by regulating integrin mediated mechanotransduction in CAFs. *Elife.* 2019; 8. doi: 10.7554/eLife.45508.
33. Paszek MJ, Zahir N, Johnson KR, Lakins JN, Rozenberg GI, Gefen A, Reinhart-King CA, Margulies SS, Dembo M, Boettiger D, Hammer DA, Weaver VM. Tensional homeostasis and the malignant phenotype. *Cancer Cell.* 2005; 8: 241-54. doi: 10.1016/j.ccr.2005.08.010.

34. Zhang K, Grither WR, Van Hove S, Biswas H, Ponik SM, Eliceiri KW, Keely PJ, Longmore GD. Mechanical signals regulate and activate SNAIL1 protein to control the fibrogenic response of cancer-associated fibroblasts. *J Cell Sci.* 2016; 129: 1989-2002. doi: 10.1242/jcs.180539.
35. Elyada E, Bolisetty M, Laise P, Flynn WF, Courtois ET, Burkhart RA, Teinor JA, Belleau P, Biffi G, Lucito MS, Sivajothi S, Armstrong TD, Engle DD, et al. Cross-Species Single-Cell Analysis of Pancreatic Ductal Adenocarcinoma Reveals Antigen-Presenting Cancer-Associated Fibroblasts. *Cancer Discov.* 2019; 9: 1102-23. doi: 10.1158/2159-8290.CD-19-0094.
36. Dominguez CX, Muller S, Keerthivasan S, Koeppen H, Hung J, Gierke S, Breart B, Foreman O, Bainbridge TW, Castiglioni A, Senbabaoglu Y, Modrusan Z, Liang Y, et al. Single-Cell RNA Sequencing Reveals Stromal Evolution into LRRC15(+) Myofibroblasts as a Determinant of Patient Response to Cancer Immunotherapy. *Cancer Discov.* 2020; 10: 232-53. doi: 10.1158/2159-8290.CD-19-0644.
37. Lambrechts D, Wauters E, Boeckx B, Aibar S, Nittner D, Burton O, Bassez A, Decaluwe H, Pircher A, Van den Eynde K, Weynand B, Verbeken E, De Leyn P, et al. Phenotype molding of stromal cells in the lung tumor microenvironment. *Nat Med.* 2018; 24: 1277-89. doi: 10.1038/s41591-018-0096-5.
38. Biffi G, Oni TE, Spielman B, Hao Y, Elyada E, Park Y, Preall J, Tuveson DA. IL1-Induced JAK/STAT Signaling Is Antagonized by TGFbeta to Shape CAF Heterogeneity in Pancreatic Ductal Adenocarcinoma. *Cancer Discov.* 2019; 9: 282-301. doi: 10.1158/2159-8290.CD-18-0710.
39. Ohlund D, Handly-Santana A, Biffi G, Elyada E, Almeida AS, Ponz-Sarvisé M, Corbo V, Oni TE, Hearn SA, Lee EJ, Chio, II, Hwang CI, Tiriác H, et al. Distinct populations of inflammatory fibroblasts and myofibroblasts in pancreatic cancer. *J Exp Med.* 2017; 214: 579-96. doi: 10.1084/jem.20162024.
40. Avery D, Govindaraju P, Jacob M, Todd L, Monslow J, Pure E. Extracellular matrix directs phenotypic heterogeneity of activated fibroblasts. *Matrix Biol.* 2018; 67: 90-106. doi: 10.1016/j.matbio.2017.12.003.
41. Affo S, Nair A, Brundu F, Ravichandra A, Bhattacharjee S, Matsuda M, Chin L, Filliol A, Wen W, Song X, Decker A, Worley J, Caviglia JM, et al. Promotion of cholangiocarcinoma growth by diverse cancer-associated fibroblast subpopulations. *Cancer Cell.* 2021; 39: 883. doi: 10.1016/j.ccell.2021.05.010.
42. Chen Z, Zhou L, Liu L, Hou Y, Xiong M, Yang Y, Hu J, Chen K. Single-cell RNA sequencing highlights the role of inflammatory cancer-associated fibroblasts in bladder urothelial carcinoma. *Nat Commun.* 2020; 11: 5077. doi: 10.1038/s41467-020-18916-5.
43. Costa A, Kieffer Y, Scholer-Dahirel A, Pelon F, Bourachot B, Cardon M, Sirven P, Magagna I, Fuhrmann L, Bernard C, Bonneau C, Kondratova M, Kuperstein I, et al. Fibroblast Heterogeneity and Immunosuppressive Environment in Human Breast Cancer. *Cancer Cell.* 2018; 33: 463-79 e10. doi: 10.1016/j.ccell.2018.01.011.

44. Kieffer Y, Hocine HR, Gentric G, Pelon F, Bernard C, Bourachot B, Lameiras S, Albergante L, Bonneau C, Guyard A, Tarte K, Zinovyev A, Baulande S, et al. Single-Cell Analysis Reveals Fibroblast Clusters Linked to Immunotherapy Resistance in Cancer. *Cancer Discov.* 2020; 10: 1330-51. doi: 10.1158/2159-8290.CD-19-1384.
45. Givel AM, Kieffer Y, Scholer-Dahirel A, Sirven P, Cardon M, Pelon F, Magagna I, Gentric G, Costa A, Bonneau C, Mieulet V, Vincent-Salomon A, Mechta-Grigoriou F. miR200-regulated CXCL12beta promotes fibroblast heterogeneity and immunosuppression in ovarian cancers. *Nat Commun.* 2018; 9: 1056. doi: 10.1038/s41467-018-03348-z.
46. Chen S, Zhu G, Yang Y, Wang F, Xiao YT, Zhang N, Bian X, Zhu Y, Yu Y, Liu F, Dong K, Mariscal J, Liu Y, et al. Single-cell analysis reveals transcriptomic remodellings in distinct cell types that contribute to human prostate cancer progression. *Nat Cell Biol.* 2021; 23: 87-98. doi: 10.1038/s41556-020-00613-6.
47. Puram SV, Tirosh I, Parikh AS, Patel AP, Yizhak K, Gillespie S, Rodman C, Luo CL, Mroz EA, Emerick KS, Deschler DG, Varvares MA, Mylvaganam R, et al. Single-Cell Transcriptomic Analysis of Primary and Metastatic Tumor Ecosystems in Head and Neck Cancer. *Cell.* 2017; 171: 1611-24 e24. doi: 10.1016/j.cell.2017.10.044.
48. Li H, Courtois ET, Sengupta D, Tan Y, Chen KH, Goh JLL, Kong SL, Chua C, Hon LK, Tan WS, Wong M, Choi PJ, Wee LJK, et al. Reference component analysis of single-cell transcriptomes elucidates cellular heterogeneity in human colorectal tumors. *Nat Genet.* 2017; 49: 708-18. doi: 10.1038/ng.3818.
49. Zhang L, Li Z, Skrzypczynska KM, Fang Q, Zhang W, O'Brien SA, He Y, Wang L, Zhang Q, Kim A, Gao R, Orf J, Wang T, et al. Single-Cell Analyses Inform Mechanisms of Myeloid-Targeted Therapies in Colon Cancer. *Cell.* 2020; 181: 442-59 e29. doi: 10.1016/j.cell.2020.03.048.
50. Bartoschek M, Oskolkov N, Bocci M, Lovrot J, Larsson C, Sommarin M, Madsen CD, Lindgren D, Pekar G, Karlsson G, Ringner M, Bergh J, Bjorklund A, et al. Spatially and functionally distinct subclasses of breast cancer-associated fibroblasts revealed by single cell RNA sequencing. *Nat Commun.* 2018; 9: 5150. doi: 10.1038/s41467-018-07582-3.
51. Friedman G, Levi-Galibov, O., David, E. et al. Cancer-associated fibroblast compositions change with breast cancer progression linking the ratio of S100A4+ and PDPN+ CAFs to clinical outcome. *Nat Cancer* 2020; 1: 692–708. doi:
52. Davidson S, Efremova M, Riedel A, Mahata B, Pramanik J, Huuhtanen J, Kar G, Vento-Tormo R, Hagai T, Chen X, Haniffa MA, Shields JD, Teichmann SA. Single-Cell RNA Sequencing Reveals a Dynamic Stromal Niche That Supports Tumor Growth. *Cell Rep.* 2020; 31: 107628. doi: 10.1016/j.celrep.2020.107628.
53. Liao Z, Tan ZW, Zhu P, Tan NS. Cancer-associated fibroblasts in tumor microenvironment - Accomplices in tumor malignancy. *Cell Immunol.* 2019; 343: 103729. doi: 10.1016/j.cellimm.2017.12.003.

54. Biffi G, Tuveson DA. Diversity and Biology of Cancer-Associated Fibroblasts. *Physiol Rev.* 2021; 101: 147-76. doi: 10.1152/physrev.00048.2019.
55. Vickman RE, Faget DV, Beachy P, Beebe D, Bhowmick NA, Cukierman E, Deng WM, Granneman JG, Hildesheim J, Kalluri R, Lau KS, Lengyel E, Lundeberg J, et al. Deconstructing tumor heterogeneity: the stromal perspective. *Oncotarget.* 2020; 11: 3621-32. doi: 10.18632/oncotarget.27736.
56. Ribeiro AL, Okamoto OK. Combined effects of pericytes in the tumor microenvironment. *Stem Cells Int.* 2015; 2015: 868475. doi: 10.1155/2015/868475.
57. Kim OH, Kang GH, Noh H, Cha JY, Lee HJ, Yoon JH, Mamura M, Nam JS, Lee DH, Kim YA, Park YJ, Kim H, Oh BC. Proangiogenic TIE2(+)/CD31 (+) macrophages are the predominant population of tumor-associated macrophages infiltrating metastatic lymph nodes. *Mol Cells.* 2013; 36: 432-8. doi: 10.1007/s10059-013-0194-7.
58. Shi X, Young CD, Zhou H, Wang X. Transforming Growth Factor-beta Signaling in Fibrotic Diseases and Cancer-Associated Fibroblasts. *Biomolecules.* 2020; 10. doi: 10.3390/biom10121666.
59. Goulet CR, Champagne A, Bernard G, Vandal D, Chabaud S, Pouliot F, Bolduc S. Cancer-associated fibroblasts induce epithelial-mesenchymal transition of bladder cancer cells through paracrine IL-6 signalling. *BMC Cancer.* 2019; 19: 137. doi: 10.1186/s12885-019-5353-6.
60. Wang L, Zhang F, Cui JY, Chen L, Chen YT, Liu BW. CAFs enhance paclitaxel resistance by inducing EMT through the IL6/JAK2/STAT3 pathway. *Oncol Rep.* 2018; 39: 2081-90. doi: 10.3892/or.2018.6311.
61. Quintero-Fabián S, Arreola R, Becerril-Villanueva E, Torres-Romero JC, Arana-Argáez V, Lara-Riegos J, Ramírez-Camacho MA, Alvarez-Sánchez ME. Role of Matrix Metalloproteinases in Angiogenesis and Cancer. *Front Oncol.* 2019; 9: 1370. doi: 10.3389/fonc.2019.01370.
62. Johnson DE, O'Keefe RA, Grandis JR. Targeting the IL-6/JAK/STAT3 signalling axis in cancer. *Nat Rev Clin Oncol.* 2018; 15: 234-48. doi: 10.1038/nrclinonc.2018.8.
63. Huber RM, Lucas JM, Gomez-Sarosi LA, Coleman I, Zhao S, Coleman R, Nelson PS. DNA damage induces GDNF secretion in the tumor microenvironment with paracrine effects promoting prostate cancer treatment resistance. *Oncotarget.* 2015; 6: 2134-47. doi: 10.18632/oncotarget.3040.
64. Gilbert LA, Hemann MT. DNA damage-mediated induction of a chemoresistant niche. *Cell.* 2010; 143: 355-66. doi: 10.1016/j.cell.2010.09.043.
65. Hu Y, Yan C, Mu L, Huang K, Li X, Tao D, Wu Y, Qin J. Fibroblast-Derived Exosomes Contribute to Chemoresistance through Priming Cancer Stem Cells in Colorectal Cancer. *PLoS One.* 2015; 10: e0125625. doi: 10.1371/journal.pone.0125625.

66. Peiris-Pages M, Sotgia F, Lisanti MP. Chemotherapy induces the cancer-associated fibroblast phenotype, activating paracrine Hedgehog-GLI signalling in breast cancer cells. *Oncotarget*. 2015; 6: 10728-45. doi: 10.18632/oncotarget.3828.
67. Tang YA, Chen YF, Bao Y, Mahara S, Yatim S, Oguz G, Lee PL, Feng M, Cai Y, Tan EY, Fong SS, Yang ZH, Lan P, et al. Hypoxic tumor microenvironment activates GLI2 via HIF-1alpha and TGF-beta2 to promote chemoresistance in colorectal cancer. *Proc Natl Acad Sci U S A*. 2018; 115: E5990-E9. doi: 10.1073/pnas.1801348115.
68. Garvey CM, Lau R, Sanchez A, Sun RX, Fong EJ, Doche ME, Chen O, Jusuf A, Lenz HJ, Larson B, Mumenthaler SM. Anti-EGFR Therapy Induces EGF Secretion by Cancer-Associated Fibroblasts to Confer Colorectal Cancer Chemoresistance. *Cancers (Basel)*. 2020; 12. doi: 10.3390/cancers12061393.
69. Zhang D, Li L, Jiang H, Li Q, Wang-Gillam A, Yu J, Head R, Liu J, Ruzinova MB, Lim KH. Tumor-Stroma IL1 β -IRAK4 Feedforward Circuitry Drives Tumor Fibrosis, Chemoresistance, and Poor Prognosis in Pancreatic Cancer. *Cancer Res*. 2018; 78: 1700-12. doi: 10.1158/0008-5472.Can-17-1366.
70. Ishibashi M, Neri S, Hashimoto H, Miyashita T, Yoshida T, Nakamura Y, Udagawa H, Kirita K, Matsumoto S, Umemura S, Yoh K, Niho S, Tsuboi M, et al. CD200-positive cancer associated fibroblasts augment the sensitivity of Epidermal Growth Factor Receptor mutation-positive lung adenocarcinomas to EGFR Tyrosine kinase inhibitors. *Sci Rep*. 2017; 7: 46662. doi: 10.1038/srep46662.
71. Wang Z, Tang Y, Tan Y, Wei Q, Yu W. Cancer-associated fibroblasts in radiotherapy: challenges and new opportunities. *Cell Commun Signal*. 2019; 17: 47. doi: 10.1186/s12964-019-0362-2.
72. Ansems M, Span PN. The tumor microenvironment and radiotherapy response; a central role for cancer-associated fibroblasts. *Clin Transl Radiat Oncol*. 2020; 22: 90-7. doi: 10.1016/j.ctro.2020.04.001.
73. Ragnathan K, Upfold NLE, Oksenysh V. Interaction between Fibroblasts and Immune Cells Following DNA Damage Induced by Ionizing Radiation. *Int J Mol Sci*. 2020; 21. doi: 10.3390/ijms21228635.
74. Li D, Qu C, Ning Z, Wang H, Zang K, Zhuang L, Chen L, Wang P, Meng Z. Radiation promotes epithelial-to-mesenchymal transition and invasion of pancreatic cancer cell by activating carcinoma-associated fibroblasts. *Am J Cancer Res*. 2016; 6: 2192-206. doi: 10.1016/j.ajcr.2016.04.001.
75. Wang Y, Gan G, Wang B, Wu J, Cao Y, Zhu D, Xu Y, Wang X, Han H, Li X, Ye M, Zhao J, Mi J. Cancer-associated Fibroblasts Promote Irradiated Cancer Cell Recovery Through Autophagy. *EBioMedicine*. 2017; 17: 45-56. doi: 10.1016/j.ebiom.2017.02.019.
76. Yang N, Lode K, Berzaghi R, Islam A, Martinez-Zubiaurre I, Hellevik T. Irradiated Tumor Fibroblasts Avoid Immune Recognition and Retain Immunosuppressive Functions Over Natural Killer Cells. *Front Immunol*. 2020; 11: 602530. doi: 10.3389/fimmu.2020.602530.

77. Flint TR, Janowitz T, Connell CM, Roberts EW, Denton AE, Coll AP, Jodrell DI, Fearon DT. Tumor-Induced IL-6 Reprograms Host Metabolism to Suppress Anti-tumor Immunity. *Cell Metab.* 2016; 24: 672-84. doi: 10.1016/j.cmet.2016.10.010.
78. Feig C, Jones JO, Kraman M, Wells RJ, Deonaraine A, Chan DS, Connell CM, Roberts EW, Zhao Q, Caballero OL, Teichmann SA, Janowitz T, Jodrell DI, et al. Targeting CXCL12 from FAP-expressing carcinoma-associated fibroblasts synergizes with anti-PD-L1 immunotherapy in pancreatic cancer. *Proc Natl Acad Sci U S A.* 2013; 110: 20212-7. doi: 10.1073/pnas.1320318110.
79. Li J, Byrne KT, Yan F, Yamazoe T, Chen Z, Baslan T, Richman LP, Lin JH, Sun YH, Rech AJ, Balli D, Hay CA, Sela Y, et al. Tumor Cell-Intrinsic Factors Underlie Heterogeneity of Immune Cell Infiltration and Response to Immunotherapy. *Immunity.* 2018; 49: 178-93.e7. doi: 10.1016/j.immuni.2018.06.006.
80. Pickup MW, Owens P, Gorska AE, Chytil A, Ye F, Shi C, Weaver VM, Kalluri R, Moses HL, Novitskiy SV. Development of Aggressive Pancreatic Ductal Adenocarcinomas Depends on Granulocyte Colony Stimulating Factor Secretion in Carcinoma Cells. *Cancer Immunol Res.* 2017; 5: 718-29. doi: 10.1158/2326-6066.Cir-16-0311.
81. Chen IX, Chauhan VP, Posada J, Ng MR, Wu MW, Adstamongkonkul P, Huang P, Lindeman N, Langer R, Jain RK. Blocking CXCR4 alleviates desmoplasia, increases T-lymphocyte infiltration, and improves immunotherapy in metastatic breast cancer. *Proc Natl Acad Sci U S A.* 2019; 116: 4558-66. doi: 10.1073/pnas.1815515116.
82. Mariathasan S, Turley SJ, Nickles D, Castiglioni A, Yuen K, Wang Y, Kadel EE, III, Koeppen H, Astarita JL, Cubas R, Jhunjhunwala S, Banchereau R, Yang Y, et al. TGF β attenuates tumour response to PD-L1 blockade by contributing to exclusion of T cells. *Nature.* 2018; 554: 544-8. doi: 10.1038/nature25501.
83. Flavell RA, Sanjabi S, Wrzesinski SH, Licona-Limón P. The polarization of immune cells in the tumour environment by TGF β . *Nat Rev Immunol.* 2010; 10: 554-67. doi: 10.1038/nri2808.
84. Tauriello DVF, Palomo-Ponce S, Stork D, Berenguer-Llargo A, Badia-Ramentol J, Iglesias M, Sevillano M, Ibiza S, Cañellas A, Hernando-Momblona X, Byrom D, Matarin JA, Calon A, et al. TGF β drives immune evasion in genetically reconstituted colon cancer metastasis. *Nature.* 2018; 554: 538-43. doi: 10.1038/nature25492.
85. Orimo A, Gupta PB, SgROI DC, Arenzana-Seisdedos F, Delaunay T, Naeem R, Carey VJ, Richardson AL, Weinberg RA. Stromal fibroblasts present in invasive human breast carcinomas promote tumor growth and angiogenesis through elevated SDF-1/CXCL12 secretion. *Cell.* 2005; 121: 335-48. doi: 10.1016/j.cell.2005.02.034.
86. Kinoshita T, Ishii G, Hiraoka N, Hirayama S, Yamauchi C, Aokage K, Hishida T, Yoshida J, Nagai K, Ochiai A. Forkhead box P3 regulatory T cells coexisting with cancer associated fibroblasts are correlated with a poor outcome in lung adenocarcinoma. *Cancer Sci.* 2013; 104: 409-15. doi: 10.1111/cas.12099.

87. Balsamo M, Scordamaglia F, Pietra G, Manzini C, Cantoni C, Boitano M, Queirolo P, Vermi W, Facchetti F, Moretta A, Moretta L, Mingari MC, Vitale M. Melanoma-associated fibroblasts modulate NK cell phenotype and antitumor cytotoxicity. *Proc Natl Acad Sci U S A*. 2009; 106: 20847-52. doi: 10.1073/pnas.0906481106.
88. Li T, Yi S, Liu W, Jia C, Wang G, Hua X, Tai Y, Zhang Q, Chen G. Colorectal carcinoma-derived fibroblasts modulate natural killer cell phenotype and antitumor cytotoxicity. *Med Oncol*. 2013; 30: 663. doi: 10.1007/s12032-013-0663-z.
89. Francescone R, Barbosa Vendramini-Costa D, Franco-Barraza J, Wagner J, Muir A, Lau AN, Gabitova L, Pazina T, Gupta S, Luong T, Rollins D, Malik R, Thapa RJ, et al. Netrin G1 Promotes Pancreatic Tumorigenesis through Cancer-Associated Fibroblast-Driven Nutritional Support and Immunosuppression. *Cancer Discov*. 2021; 11: 446-79. doi: 10.1158/2159-8290.Cd-20-0775.
90. Cheng JT, Deng YN, Yi HM, Wang GY, Fu BS, Chen WJ, Liu W, Tai Y, Peng YW, Zhang Q. Hepatic carcinoma-associated fibroblasts induce IDO-producing regulatory dendritic cells through IL-6-mediated STAT3 activation. *Oncogenesis*. 2016; 5: e198. doi: 10.1038/oncsis.2016.7.
91. Rahma OE, Hodi FS. The Intersection between Tumor Angiogenesis and Immune Suppression. *Clin Cancer Res*. 2019; 25: 5449-57. doi: 10.1158/1078-0432.Ccr-18-1543.
92. Kumar V, Donthireddy L, Marvel D, Condamine T, Wang F, Lavilla-Alonso S, Hashimoto A, Vonteddu P, Behera R, Goins MA, Mulligan C, Nam B, Hockstein N, et al. Cancer-Associated Fibroblasts Neutralize the Anti-tumor Effect of CSF1 Receptor Blockade by Inducing PMN-MDSC Infiltration of Tumors. *Cancer Cell*. 2017; 32: 654-68.e5. doi: 10.1016/j.ccell.2017.10.005.
93. Xiang H, Ramil CP, Hai J, Zhang C, Wang H, Watkins AA, Afshar R, Georgiev P, Sze MA, Song XS, Curran PJ, Cheng M, Miller JR, et al. Cancer-Associated Fibroblasts Promote Immunosuppression by Inducing ROS-Generating Monocytic MDSCs in Lung Squamous Cell Carcinoma. *Cancer Immunol Res*. 2020; 8: 436-50. doi: 10.1158/2326-6066.Cir-19-0507.
94. Ma Y, Hwang RF, Logsdon CD, Ullrich SE. Dynamic mast cell-stromal cell interactions promote growth of pancreatic cancer. *Cancer Res*. 2013; 73: 3927-37. doi: 10.1158/0008-5472.Can-12-4479.
95. Pereira BA, Lister NL, Hashimoto K, Teng L, Flandes-Iparraguirre M, Eder A, Sanchez-Herrero A, Niranjana B. Tissue engineered human prostate microtissues reveal key role of mast cell-derived tryptase in potentiating cancer-associated fibroblast (CAF)-induced morphometric transition in vitro. *Biomaterials*. 2019; 197: 72-85. doi: 10.1016/j.biomaterials.2018.12.030.
96. Song M, He J, Pan QZ, Yang J, Zhao J, Zhang YJ, Huang Y, Tang Y, Wang Q, He J, Gu J, Li Y, Chen S, et al. Cancer-Associated Fibroblast-Mediated Cellular Crosstalk Supports Hepatocellular Carcinoma Progression. *Hepatology*. 2021; 73: 1717-35. doi: 10.1002/hep.31792.

97. Cheng Y, Li H, Deng Y, Tai Y, Zeng K, Zhang Y, Liu W, Zhang Q, Yang Y. Cancer-associated fibroblasts induce PDL1+ neutrophils through the IL6-STAT3 pathway that foster immune suppression in hepatocellular carcinoma. *Cell Death Dis.* 2018; 9: 422. doi: 10.1038/s41419-018-0458-4.
98. Fridlender ZG, Albelda SM. Tumor-associated neutrophils: friend or foe? *Carcinogenesis.* 2012; 33: 949-55. doi: 10.1093/carcin/bgs123.
99. Herrera M, Herrera A, Domínguez G, Silva J, García V, García JM, Gómez I, Soldevilla B, Muñoz C, Provencio M, Campos-Martin Y, García de Herreros A, Casal I, et al. Cancer-associated fibroblast and M2 macrophage markers together predict outcome in colorectal cancer patients. *Cancer Sci.* 2013; 104: 437-44. doi: 10.1111/cas.12096.
100. Comito G, Giannoni E, Segura CP, Barcellos-de-Souza P, Raspollini MR, Baroni G, Lanciotti M, Serni S, Chiarugi P. Cancer-associated fibroblasts and M2-polarized macrophages synergize during prostate carcinoma progression. *Oncogene.* 2014; 33: 2423-31. doi: 10.1038/onc.2013.191.
101. Mathew E, Brannon AL, Del Vecchio A, Garcia PE, Penny MK, Kane KT, Vinta A, Buckanovich RJ, di Magliano MP. Mesenchymal Stem Cells Promote Pancreatic Tumor Growth by Inducing Alternative Polarization of Macrophages. *Neoplasia.* 2016; 18: 142-51. doi: 10.1016/j.neo.2016.01.005.
102. Mace TA, Ameen Z, Collins A, Wojcik S, Mair M, Young GS, Fuchs JR, Eubank TD, Frankel WL, Bekaii-Saab T, Bloomston M, Lesinski GB. Pancreatic cancer-associated stellate cells promote differentiation of myeloid-derived suppressor cells in a STAT3-dependent manner. *Cancer Res.* 2013; 73: 3007-18. doi: 10.1158/0008-5472.Can-12-4601.
103. Zhang R, Qi F, Zhao F, Li G, Shao S, Zhang X, Yuan L, Feng Y. Cancer-associated fibroblasts enhance tumor-associated macrophages enrichment and suppress NK cells function in colorectal cancer. *Cell Death Dis.* 2019; 10: 273. doi: 10.1038/s41419-019-1435-2.
104. LeBeau AM, Brennen WN, Aggarwal S, Denmeade SR. Targeting the cancer stroma with a fibroblast activation protein-activated promelittin protoxin. *Molecular Cancer Therapeutics.* 2009; 8: 1378-86. doi: 10.1158/1535-7163.Mct-08-1170.
105. Adams S, Miller GT, Jesson MI, Watanabe T, Jones B, Wallner BP. PT-100, a small molecule dipeptidyl peptidase inhibitor, has potent antitumor effects and augments antibody-mediated cytotoxicity via a novel immune mechanism. *Cancer Res.* 2004; 64: 5471-80. doi: 10.1158/0008-5472.CAN-04-0447.
106. Narra K, Mullins SR, Lee HO, Strzemkowski-Brun B, Magalong K, Christiansen VJ, McKee PA, Egleston B, Cohen SJ, Weiner LM, Meropol NJ, Cheng JD. Phase II trial of single agent Val-boroPro (Talabostat) inhibiting Fibroblast Activation Protein in patients with metastatic colorectal cancer. *Cancer Biol Ther.* 2007; 6: 1691-9. doi: 10.4161/cbt.6.11.4874.

107. Hofheinz RD, al-Batran SE, Hartmann F, Hartung G, Jager D, Renner C, Tanswell P, Kunz U, Amelsberg A, Kuthan H, Stehle G. Stromal antigen targeting by a humanised monoclonal antibody: an early phase II trial of sibrotuzumab in patients with metastatic colorectal cancer. *Onkologie*. 2003; 26: 44-8. doi: 10.1159/000069863.
108. Scott AM, Wiseman G, Welt S, Adjei A, Lee F-T, Hopkins W, Divgi CR, Hanson LH, Mitchell P, Gansen DN, Larson SM, Ingle JN, Hoffman EW, et al. A Phase I Dose-Escalation Study of Sibrotuzumab in Patients with Advanced or Metastatic Fibroblast Activation Protein-positive Cancer1. *Clinical Cancer Research*. 2003; 9: 1639-47. doi:
109. Huang S, Fang R, Xu J, Qiu S, Zhang H, Du J, Cai S. Evaluation of the tumor targeting of a FAP α -based doxorubicin prodrug. *J Drug Target*. 2011; 19: 487-96. doi: 10.3109/1061186x.2010.511225.
110. Brennen WN, Isaacs JT, Denmeade SR. Rationale Behind Targeting Fibroblast Activation Protein-Expressing Carcinoma-Associated Fibroblasts as a Novel Chemotherapeutic Strategy. *Molecular Cancer Therapeutics*. 2012; 11: 257-66. doi: 10.1158/1535-7163.MCT-11-0340.
111. Fang J, Xiao L, Joo KI, Liu Y, Zhang C, Liu S, Conti PS, Li Z, Wang P. A potent immunotoxin targeting fibroblast activation protein for treatment of breast cancer in mice. *Int J Cancer*. 2016; 138: 1013-23. doi: 10.1002/ijc.29831.
112. Fang J, Hu B, Li S, Zhang C, Liu Y, Wang P. A multi-antigen vaccine in combination with an immunotoxin targeting tumor-associated fibroblast for treating murine melanoma. *Mol Ther Oncolytics*. 2016; 3: 16007. doi: 10.1038/mto.2016.7.
113. Tansi FL, Ruger R, Bohm C, Steiniger F, Kontermann RE, Teichgraeber UK, Fahr A, Hilger I. Activatable bispecific liposomes bearing fibroblast activation protein directed single chain fragment/Trastuzumab deliver encapsulated cargo into the nuclei of tumor cells and the tumor microenvironment simultaneously. *Acta Biomater*. 2017; 54: 281-93. doi: 10.1016/j.actbio.2017.03.033.
114. Rabenhold M, Steiniger F, Fahr A, Kontermann RE, Ruger R. Bispecific single-chain diabody-immunoliposomes targeting endoglin (CD105) and fibroblast activation protein (FAP) simultaneously. *J Control Release*. 2015; 201: 56-67. doi: 10.1016/j.jconrel.2015.01.022.
115. Chen B, Wang Z, Sun J, Song Q, He B, Zhang H, Wang X, Dai W, Zhang Q. A tenascin C targeted nanoliposome with navitoclax for specifically eradicating of cancer-associated fibroblasts. *Nanomedicine*. 2016; 12: 131-41. doi: 10.1016/j.nano.2015.10.001.
116. Truffi M, Mazzucchelli S, Bonizzi A, Sorrentino L, Allevi R, Vanna R, Morasso C, Corsi F. Nano-Strategies to Target Breast Cancer-Associated Fibroblasts: Rearranging the Tumor Microenvironment to Achieve Antitumor Efficacy. *Int J Mol Sci*. 2019; 20. doi: 10.3390/ijms20061263.

117. Ostermann E, Garin-Chesa P, Heider KH, Kalat M, Lamche H, Puri C, Kerjaschki D, Rettig WJ, Adolf GR. Effective immunoconjugate therapy in cancer models targeting a serine protease of tumor fibroblasts. *Clin Cancer Res.* 2008; 14: 4584-92. doi: 10.1158/1078-0432.CCR-07-5211.
118. Cheng JD, Dunbrack RL, Jr., Valianou M, Rogatko A, Alpaugh RK, Weiner LM. Promotion of Tumor Growth by Murine Fibroblast Activation Protein, a Serine Protease, in an Animal Model. *Cancer Research.* 2002; 62: 4767-72. doi:
119. Brünker P, Wartha K, Friess T, Grau-Richards S, Waldhauer I, Koller CF, Weiser B, Majety M, Runza V, Niu H, Packman K, Feng N, Daouti S, et al. RG7386, a Novel Tetravalent FAP-DR5 Antibody, Effectively Triggers FAP-Dependent, Avidity-Driven DR5 Hyperclustering and Tumor Cell Apoptosis. *Mol Cancer Ther.* 2016; 15: 946-57. doi: 10.1158/1535-7163.Mct-15-0647.
120. Lee J, Fassnacht M, Nair S, Boczkowski D, Gilboa E. Tumor immunotherapy targeting fibroblast activation protein, a product expressed in tumor-associated fibroblasts. *Cancer Res.* 2005; 65: 11156-63. doi: 10.1158/0008-5472.Can-05-2805.
121. Loeffler M, Kruger JA, Niethammer AG, Reisfeld RA. Targeting tumor-associated fibroblasts improves cancer chemotherapy by increasing intratumoral drug uptake. *J Clin Invest.* 2006; 116: 1955-62. doi: 10.1172/JCI26532.
122. Zhang Y, Ertl HC. Depletion of FAP+ cells reduces immunosuppressive cells and improves metabolism and functions CD8+T cells within tumors. *Oncotarget.* 2016; 7: 23282-99. doi: 10.18632/oncotarget.7818.
123. Xia Q, Zhang FF, Geng F, Liu CL, Xu P, Lu ZZ, Yu B, Wu H, Wu JX, Zhang HH, Kong W, Yu XH. Anti-tumor effects of DNA vaccine targeting human fibroblast activation protein α by producing specific immune responses and altering tumor microenvironment in the 4T1 murine breast cancer model. *Cancer Immunol Immunother.* 2016; 65: 613-24. doi: 10.1007/s00262-016-1827-4.
124. Freedman JD, Duffy MR, Lei-Rossmann J, Muntzer A, Scott EM, Hagel J, Campo L, Bryant RJ, Verrill C, Lambert A, Miller P, Champion BR, Seymour LW, et al. An Oncolytic Virus Expressing a T-cell Engager Simultaneously Targets Cancer and Immunosuppressive Stromal Cells. *Cancer Res.* 2018; 78: 6852-65. doi: 10.1158/0008-5472.Can-18-1750.
125. Kraman M, Bambrough PJ, Arnold JN, Roberts EW, Magiera L, Jones JO, Gopinathan A, Tuveson DA, Fearon DT. Suppression of antitumor immunity by stromal cells expressing fibroblast activation protein- α . *Science.* 2010; 330: 827-30. doi: 10.1126/science.1195300.
126. Geng F, Bao X, Dong L, Guo Q-Q, Guo J, Xie Y, Zhou Y, Yu B, Wu H, Wu J-X, Zhang H-H, Yu X-H, Kong W. Doxorubicin pretreatment enhances FAP α /survivin co-targeting DNA vaccine anti-tumor activity primarily through decreasing peripheral MDSCs in the 4T1 murine breast cancer model. *Oncoimmunology.* 2020; 9: 1747350-. doi: 10.1080/2162402X.2020.1747350.

127. Wang LC, Lo A, Scholler J, Sun J, Majumdar RS, Kapoor V, Antzis M, Cotner CE, Johnson LA, Durham AC, Solomides CC, June CH, Puré E, et al. Targeting fibroblast activation protein in tumor stroma with chimeric antigen receptor T cells can inhibit tumor growth and augment host immunity without severe toxicity. *Cancer Immunol Res.* 2014; 2: 154-66. doi: 10.1158/2326-6066.Cir-13-0027.
128. Lo A, Wang LS, Scholler J, Monslow J, Avery D, Newick K, O'Brien S, Evans RA, Bajor DJ, Clendenin C, Durham AC, Buza EL, Vonderheide RH, et al. Tumor-Promoting Desmoplasia Is Disrupted by Depleting FAP-Expressing Stromal Cells. *Cancer Res.* 2015; 75: 2800-10. doi: 10.1158/0008-5472.CAN-14-3041.
129. Roberts EW, Deonaraine A, Jones JO, Denton AE, Feig C, Lyons SK, Espeli M, Kraman M, McKenna B, Wells RJ, Zhao Q, Caballero OL, Larder R, et al. Depletion of stromal cells expressing fibroblast activation protein- α from skeletal muscle and bone marrow results in cachexia and anemia. *J Exp Med.* 2013; 210: 1137-51. doi: 10.1084/jem.20122344.
130. Tran E, Chinnasamy D, Yu Z, Morgan RA, Lee CC, Restifo NP, Rosenberg SA. Immune targeting of fibroblast activation protein triggers recognition of multipotent bone marrow stromal cells and cachexia. *J Exp Med.* 2013; 210: 1125-35. doi: 10.1084/jem.20130110.
131. Su S, Chen J, Yao H, Liu J, Yu S, Lao L, Wang M, Luo M, Xing Y, Chen F, Huang D, Zhao J, Yang L, et al. CD10(+)GPR77(+) Cancer-Associated Fibroblasts Promote Cancer Formation and Chemoresistance by Sustaining Cancer Stemness. *Cell.* 2018; 172: 841-56.e16. doi: 10.1016/j.cell.2018.01.009.
132. Watanabe S, Noma K, Ohara T, Kashima H, Sato H, Kato T, Urano S, Katsube R, Hashimoto Y, Tazawa H, Kagawa S, Shirakawa Y, Kobayashi H, et al. Photoimmunotherapy for cancer-associated fibroblasts targeting fibroblast activation protein in human esophageal squamous cell carcinoma. *Cancer Biol Ther.* 2019; 20: 1234-48. doi: 10.1080/15384047.2019.1617566.
133. Katsube R, Noma K, Ohara T, Nishiwaki N, Kobayashi T, Komoto S, Sato H, Kashima H, Kato T, Kikuchi S, Tazawa H, Kagawa S, Shirakawa Y, et al. Fibroblast activation protein targeted near infrared photoimmunotherapy (NIR PIT) overcomes therapeutic resistance in human esophageal cancer. *Sci Rep.* 2021; 11: 1693. doi: 10.1038/s41598-021-81465-4.
134. Ene-Obong A, Clear AJ, Watt J, Wang J, Fatah R, Riches JC, Marshall JF, Chin-Aleong J, Chelala C, Gribben JG, Ramsay AG, Kocher HM. Activated pancreatic stellate cells sequester CD8⁺ T cells to reduce their infiltration of the juxtatumoral compartment of pancreatic ductal adenocarcinoma. *Gastroenterology.* 2013; 145: 1121-32. doi: 10.1053/j.gastro.2013.07.025.
135. Froeling FE, Feig C, Chelala C, Dobson R, Mein CE, Tuveson DA, Clevers H, Hart IR, Kocher HM. Retinoic acid-induced pancreatic stellate cell quiescence reduces paracrine Wnt- β -catenin signaling to slow tumor progression. *Gastroenterology.* 2011; 141: 1486-97, 97.e1-14. doi: 10.1053/j.gastro.2011.06.047.

136. Han X, Li Y, Xu Y, Zhao X, Zhang Y, Yang X, Wang Y, Zhao R, Anderson GJ, Zhao Y, Nie G. Reversal of pancreatic desmoplasia by re-educating stellate cells with a tumour microenvironment-activated nanosystem. *Nat Commun.* 2018; 9: 3390. doi: 10.1038/s41467-018-05906-x.
137. Banerjee S, Modi S, McGinn O, Zhao X, Dudeja V, Ramakrishnan S, Saluja AK. Impaired Synthesis of Stromal Components in Response to Minnelide Improves Vascular Function, Drug Delivery, and Survival in Pancreatic Cancer. *Clin Cancer Res.* 2016; 22: 415-25. doi: 10.1158/1078-0432.Ccr-15-1155.
138. Dauer P, Zhao X, Gupta VK, Sharma N, Kesh K, Gnamlin P, Dudeja V, Vickers SM, Banerjee S, Saluja A. Inactivation of Cancer-Associated-Fibroblasts Disrupts Oncogenic Signaling in Pancreatic Cancer Cells and Promotes Its Regression. *Cancer Res.* 2018; 78: 1321-33. doi: 10.1158/0008-5472.Can-17-2320.
139. Ding N, Yu RT, Subramaniam N, Sherman MH, Wilson C, Rao R, Leblanc M, Coulter S, He M, Scott C, Lau SL, Atkins AR, Barish GD, et al. A vitamin D receptor/SMAD genomic circuit gates hepatic fibrotic response. *Cell.* 2013; 153: 601-13. doi: 10.1016/j.cell.2013.03.028.
140. Sherman MH, Yu RT, Engle DD, Ding N, Atkins AR, Tiriack H, Collisson EA, Connor F, Van Dyke T, Kozlov S, Martin P, Tseng TW, Dawson DW, et al. Vitamin D receptor-mediated stromal reprogramming suppresses pancreatitis and enhances pancreatic cancer therapy. *Cell.* 2014; 159: 80-93. doi: 10.1016/j.cell.2014.08.007.
141. Chauhan VP, Chen IX, Tong R, Ng MR, Martin JD, Naxerova K, Wu MW, Huang P, Boucher Y, Kohane DS, Langer R, Jain RK. Reprogramming the microenvironment with tumor-selective angiotensin blockers enhances cancer immunotherapy. *Proc Natl Acad Sci U S A.* 2019; 116: 10674-80. doi: 10.1073/pnas.1819889116.
142. Chauhan VP, Martin JD, Liu H, Lacorre DA, Jain SR, Kozin SV, Stylianopoulos T, Mousa AS, Han X, Adstamongkonkul P, Popovic Z, Huang P, Bawendi MG, et al. Angiotensin inhibition enhances drug delivery and potentiates chemotherapy by decompressing tumour blood vessels. *Nat Commun.* 2013; 4: 2516. doi: 10.1038/ncomms3516.
143. Diop-Frimpong B, Chauhan VP, Krane S, Boucher Y, Jain RK. Losartan inhibits collagen I synthesis and improves the distribution and efficacy of nanotherapeutics in tumors. *Proc Natl Acad Sci U S A.* 2011; 108: 2909-14. doi: 10.1073/pnas.1018892108.
144. Murphy JE, Wo JY, Ryan DP, Clark JW, Jiang W, Yeap BY, Drapek LC, Ly L, Baglini CV, Blaszkowsky LS, Ferrone CR, Parikh AR, Weekes CD, et al. Total Neoadjuvant Therapy With FOLFIRINOX in Combination With Losartan Followed by Chemoradiotherapy for Locally Advanced Pancreatic Cancer: A Phase 2 Clinical Trial. *JAMA Oncol.* 2019; 5: 1020-7. doi: 10.1001/jamaoncol.2019.0892.
145. Mace TA, Shakya R, Pitarresi JR, Swanson B, McQuinn CW, Loftus S, Nordquist E, Cruz-Monserrate Z, Yu L, Young G, Zhong X, Zimmers TA, Ostrowski MC, et al. IL-6 and PD-L1 antibody blockade combination therapy reduces tumour progression in murine models of pancreatic cancer. *Gut.* 2018; 67: 320-32. doi: 10.1136/gutjnl-2016-311585.

146. Zhang Y, Yan W, Collins MA, Bednar F, Rakshit S, Zetter BR, Stanger BZ, Chung I, Rhim AD, di Magliano MP. Interleukin-6 is required for pancreatic cancer progression by promoting MAPK signaling activation and oxidative stress resistance. *Cancer Res.* 2013; 73: 6359-74. doi: 10.1158/0008-5472.Can-13-1558-t.
147. Shi Y, Gao W, Lytle NK, Huang P, Yuan X, Dann AM, Ridinger-Saison M, DelGiorno KE, Antal CE, Liang G, Atkins AR, Erikson G, Sun H, et al. Targeting LIF-mediated paracrine interaction for pancreatic cancer therapy and monitoring. *Nature.* 2019; 569: 131-5. doi: 10.1038/s41586-019-1130-6.
148. Grauel AL, Nguyen B, Ruddy D, Laszewski T, Schwartz S, Chang J, Chen J, Piquet M, Pelletier M, Yan Z, Kirkpatrick ND, Wu J, deWeck A, et al. TGF β -blockade uncovers stromal plasticity in tumors by revealing the existence of a subset of interferon-licensed fibroblasts. *Nat Commun.* 2020; 11: 6315. doi: 10.1038/s41467-020-19920-5.
149. Godwin P, Baird AM, Heavey S, Barr MP, O'Byrne KJ, Gately K. Targeting nuclear factor-kappa B to overcome resistance to chemotherapy. *Front Oncol.* 2013; 3: 120. doi: 10.3389/fonc.2013.00120.
150. Steele NG, Biffi G, Kemp SB, Zhang Y, Drouillard D, Syu L, Hao Y, Oni TE, Brosnan E, Elyada E, Doshi A, Hansma C, Espinoza C, et al. Inhibition of Hedgehog Signaling Alters Fibroblast Composition in Pancreatic Cancer. *Clinical cancer research : an official journal of the American Association for Cancer Research.* 2021; 27: 2023-37. doi: 10.1158/1078-0432.CCR-20-3715.
151. Tirosh I, Izar B, Prakadan SM, Wadsworth MH, 2nd, Treacy D, Trombetta JJ, Rotem A, Rodman C, Lian C, Murphy G, Fallahi-Sichani M, Dutton-Regester K, Lin JR, et al. Dissecting the multicellular ecosystem of metastatic melanoma by single-cell RNA-seq. *Science.* 2016; 352: 189-96. doi: 10.1126/science.aad0501.
152. Waise S, Parker R, Rose-Zerilli MJJ, Layfield DM, Wood O, West J, Ottensmeier CH, Thomas GJ, Hanley CJ. An optimised tissue disaggregation and data processing pipeline for characterising fibroblast phenotypes using single-cell RNA sequencing. *Sci Rep.* 2019; 9: 9580. doi: 10.1038/s41598-019-45842-4.
153. Giesel FL, Kratochwil C, Schlittenhardt J, Dendl K, Eiber M, Staudinger F, Kessler L, Fendler WP, Lindner T, Koerber SA, Cardinale J, Sennung D, Roehrich M, et al. Head-to-head intra-individual comparison of biodistribution and tumor uptake of (68)Ga-FAPI and (18)F-FDG PET/CT in cancer patients. *Eur J Nucl Med Mol Imaging.* 2021; 48: 4377-85. doi: 10.1007/s00259-021-05307-1.
154. Arnold JN, Magiera L, Kraman M, Fearon DT. Tumoral immune suppression by macrophages expressing fibroblast activation protein-alpha and heme oxygenase-1. *Cancer Immunol Res.* 2014; 2: 121-6. doi: 10.1158/2326-6066.CIR-13-0150.

155. Yang X, Lin Y, Shi Y, Li B, Liu W, Yin W, Dang Y, Chu Y, Fan J, He R. FAP Promotes Immunosuppression by Cancer-Associated Fibroblasts in the Tumor Microenvironment via STAT3-CCL2 Signaling. *Cancer Res.* 2016; 76: 4124-35. doi: 10.1158/0008-5472.CAN-15-2973.
156. Farahani RM, Xaymardan M. Platelet-Derived Growth Factor Receptor Alpha as a Marker of Mesenchymal Stem Cells in Development and Stem Cell Biology. *Stem Cells International.* 2015; 2015: 362753. doi: 10.1155/2015/362753.
157. Sugimoto H, Mundel TM, Kieran MW, Kalluri R. Identification of fibroblast heterogeneity in the tumor microenvironment. *Cancer Biol Ther.* 2006; 5: 1640-6. doi: 10.4161/cbt.5.12.3354.
158. Kitano H, Kageyama S, Hewitt SM, Hayashi R, Doki Y, Ozaki Y, Fujino S, Takikita M, Kubo H, Fukuoka J. Podoplanin expression in cancerous stroma induces lymphangiogenesis and predicts lymphatic spread and patient survival. *Arch Pathol Lab Med.* 2010; 134: 1520-7. doi: 10.5858/2009-0114-oa.1.
159. Astarita JL, Acton SE, Turley SJ. Podoplanin: emerging functions in development, the immune system, and cancer. *Front Immunol.* 2012; 3: 283. doi: 10.3389/fimmu.2012.00283.
160. Kerrigan AM, Navarro-Nuñez L, Pyz E, Finney BA, Willment JA, Watson SP, Brown GD. Podoplanin-expressing inflammatory macrophages activate murine platelets via CLEC-2. *J Thromb Haemost.* 2012; 10: 484-6. doi: 10.1111/j.1538-7836.2011.04614.x.
161. Shindo K, Aishima S, Ohuchida K, Fujiwara K, Fujino M, Mizuuchi Y, Hattori M, Mizumoto K, Tanaka M, Oda Y. Podoplanin expression in cancer-associated fibroblasts enhances tumor progression of invasive ductal carcinoma of the pancreas. *Mol Cancer.* 2013; 12: 168. doi: 10.1186/1476-4598-12-168.
162. Augsten M. Cancer-associated fibroblasts as another polarized cell type of the tumor microenvironment. *Front Oncol.* 2014; 4: 62. doi: 10.3389/fonc.2014.00062.
163. Zhu CQ, Popova SN, Brown ER, Barsyte-Lovejoy D, Navab R, Shih W, Li M, Lu M, Jurisica I, Penn LZ, Gullberg D, Tsao MS. Integrin alpha 11 regulates IGF2 expression in fibroblasts to enhance tumorigenicity of human non-small-cell lung cancer cells. *Proc Natl Acad Sci U S A.* 2007; 104: 11754-9. doi: 10.1073/pnas.0703040104.
164. Blandin AF, Renner G, Lehmann M, Lelong-Rebel I, Martin S, Dontenwill M. $\beta 1$ Integrins as Therapeutic Targets to Disrupt Hallmarks of Cancer. *Front Pharmacol.* 2015; 6: 279. doi: 10.3389/fphar.2015.00279.
165. Navab R, Strumpf D, To C, Pasko E, Kim KS, Park CJ, Hai J, Liu J, Jonkman J, Barczyk M, Bandarchi B, Wang YH, Venkat K, et al. Integrin $\alpha 11\beta 1$ regulates cancer stromal stiffness and promotes tumorigenicity and metastasis in non-small cell lung cancer. *Oncogene.* 2016; 35: 1899-908. doi: 10.1038/onc.2015.254.

166. Zeltz C, Primac I, Erusappan P, Alam J, Noel A, Gullberg D. Cancer-associated fibroblasts in desmoplastic tumors: emerging role of integrins. *Semin Cancer Biol.* 2020; 62: 166-81. doi: 10.1016/j.semcancer.2019.08.004.
167. Simpkins SA, Hanby AM, Holliday DL, Speirs V. Clinical and functional significance of loss of caveolin-1 expression in breast cancer-associated fibroblasts. *J Pathol.* 2012; 227: 490-8. doi: 10.1002/path.4034.
168. Chen D, Che G. Value of caveolin-1 in cancer progression and prognosis: Emphasis on cancer-associated fibroblasts, human cancer cells and mechanism of caveolin-1 expression (Review). *Oncol Lett.* 2014; 8: 1409-21. doi: 10.3892/ol.2014.2385.
169. Shimizu K, Kirita K, Aokage K, Kojima M, Hishida T, Kuwata T, Fujii S, Ochiai A, Funai K, Yoshida J, Tsuboi M, Ishii G. Clinicopathological significance of caveolin-1 expression by cancer-associated fibroblasts in lung adenocarcinoma. *J Cancer Res Clin Oncol.* 2017; 143: 321-8. doi: 10.1007/s00432-016-2285-2.
170. Scatena C, Fanelli G, Fanelli GN, Menicagli M, Aretini P, Ortenzi V, Civitelli SP, Innocenti L, Sotgia F, Lisanti MP, Naccarato AG. New insights in the expression of stromal caveolin 1 in breast cancer spread to axillary lymph nodes. *Sci Rep.* 2021; 11: 2755. doi: 10.1038/s41598-021-82405-y.
171. Kisselbach L, Merges M, Bossie A, Boyd A. CD90 Expression on human primary cells and elimination of contaminating fibroblasts from cell cultures. *Cytotechnology.* 2009; 59: 31-44. doi: 10.1007/s10616-009-9190-3.
172. Takahashi K, Yamanaka S. A decade of transcription factor-mediated reprogramming to pluripotency. *Nat Rev Mol Cell Biol.* 2016; 17: 183-93. doi: 10.1038/nrm.2016.8.
173. Schliekelman MJ, Creighton CJ, Baird BN, Chen Y, Banerjee P, Bota-Rabassedas N, Ahn YH, Roybal JD, Chen F, Zhang Y, Mishra DK, Kim MP, Liu X, et al. Thy-1(+) Cancer-associated Fibroblasts Adversely Impact Lung Cancer Prognosis. *Sci Rep.* 2017; 7: 6478. doi: 10.1038/s41598-017-06922-5.
174. Sauzay C, Voutetakis K, Chatziioannou A, Chevet E, Avril T. CD90/Thy-1, a Cancer-Associated Cell Surface Signaling Molecule. *Front Cell Dev Biol.* 2019; 7: 66. doi: 10.3389/fcell.2019.00066.
175. Satelli A, Li S. Vimentin in cancer and its potential as a molecular target for cancer therapy. *Cell Mol Life Sci.* 2011; 68: 3033-46. doi: 10.1007/s00018-011-0735-1.
176. Hsia LT, Ashley N, Ouaret D, Wang LM, Wilding J, Bodmer WF. Myofibroblasts are distinguished from activated skin fibroblasts by the expression of AOC3 and other associated markers. *Proc Natl Acad Sci U S A.* 2016; 113: E2162-71. doi: 10.1073/pnas.1603534113.
177. Strutz F, Okada H, Lo CW, Danoff T, Carone RL, Tomaszewski JE, Neilson EG. Identification and characterization of a fibroblast marker: FSP1. *J Cell Biol.* 1995; 130: 393-405. doi: 10.1083/jcb.130.2.393.

178. Österreicher CH, Penz-Österreicher M, Grivennikov SI, Guma M, Koltsova EK, Datz C, Sasik R, Hardiman G, Karin M, Brenner DA. Fibroblast-specific protein 1 identifies an inflammatory subpopulation of macrophages in the liver. *Proc Natl Acad Sci U S A*. 2011; 108: 308-13. doi: 10.1073/pnas.1017547108.
179. Zhang J, Chen L, Liu X, Kammertoens T, Blankenstein T, Qin Z. Fibroblast-specific protein 1/S100A4-positive cells prevent carcinoma through collagen production and encapsulation of carcinogens. *Cancer Res*. 2013; 73: 2770-81. doi: 10.1158/0008-5472.Can-12-3022.
180. De Wever O, Nguyen QD, Van Hoorde L, Bracke M, Bruyneel E, Gespach C, Mareel M. Tenascin-C and SF/HGF produced by myofibroblasts in vitro provide convergent pro-invasive signals to human colon cancer cells through RhoA and Rac. *Faseb j*. 2004; 18: 1016-8. doi: 10.1096/fj.03-1110fje.
181. Lowy CM, Oskarsson T. Tenascin C in metastasis: A view from the invasive front. *Cell Adh Migr*. 2015; 9: 112-24. doi: 10.1080/19336918.2015.1008331.
182. Yoshida T, Akatsuka T, Imanaka-Yoshida K. Tenascin-C and integrins in cancer. *Cell Adh Migr*. 2015; 9: 96-104. doi: 10.1080/19336918.2015.1008332.
183. Planche A, Bacac M, Provero P, Fusco C, Delorenzi M, Stehle JC, Stamenkovic I. Identification of prognostic molecular features in the reactive stroma of human breast and prostate cancer. *PLoS One*. 2011; 6: e18640. doi: 10.1371/journal.pone.0018640.
184. Chen SX, Xu XE, Wang XQ, Cui SJ, Xu LL, Jiang YH, Zhang Y, Yan HB, Zhang Q, Qiao J, Yang PY, Liu F. Identification of colonic fibroblast secretomes reveals secretory factors regulating colon cancer cell proliferation. *J Proteomics*. 2014; 110: 155-71. doi: 10.1016/j.jprot.2014.07.031.
185. Qin X, Yan M, Zhang J, Wang X, Shen Z, Lv Z, Li Z, Wei W, Chen W. TGF β 3-mediated induction of Periostin facilitates head and neck cancer growth and is associated with metastasis. *Sci Rep*. 2016; 6: 20587. doi: 10.1038/srep20587.
186. Yu B, Wu K, Wang X, Zhang J, Wang L, Jiang Y, Zhu X, Chen W, Yan M. Periostin secreted by cancer-associated fibroblasts promotes cancer stemness in head and neck cancer by activating protein tyrosine kinase 7. *Cell Death Dis*. 2018; 9: 1082. doi: 10.1038/s41419-018-1116-6.
187. Jia D, Liu Z, Deng N, Tan TZ, Huang RY, Taylor-Harding B, Cheon DJ, Lawrenson K, Wiedemeyer WR, Walts AE, Karlan BY, Orsulic S. A COL11A1-correlated pan-cancer gene signature of activated fibroblasts for the prioritization of therapeutic targets. *Cancer Lett*. 2016; 382: 203-14. doi: 10.1016/j.canlet.2016.09.001.
188. Nishishita R, Morohashi S, Seino H, Wu Y, Yoshizawa T, Haga T, Saito K, Hakamada K, Fukuda S, Kijima H. Expression of cancer-associated fibroblast markers in advanced colorectal cancer. *Oncol Lett*. 2018; 15: 6195-202. doi: 10.3892/ol.2018.8097.

189. Vázquez-Villa F, García-Ocaña M, Galván JA, García-Martínez J, García-Pravia C, Menéndez-Rodríguez P, González-del Rey C, Barneo-Serra L, de Los Toyos JR. COL11A1/(pro)collagen 11A1 expression is a remarkable biomarker of human invasive carcinoma-associated stromal cells and carcinoma progression. *Tumour Biol.* 2015; 36: 2213-22. doi: 10.1007/s13277-015-3295-4.
190. Gascard P, Tlsty TD. Carcinoma-associated fibroblasts: orchestrating the composition of malignancy. *Genes Dev.* 2016; 30: 1002-19. doi: 10.1101/gad.279737.116.
191. Pelon F, Bourachot B, Kieffer Y, Magagna I, Mermet-Meillon F, Bonnet I, Costa A, Givel AM, Attieh Y, Barbazan J, Bonneau C, Fuhrmann L, Descroix S, et al. Cancer-associated fibroblast heterogeneity in axillary lymph nodes drives metastases in breast cancer through complementary mechanisms. *Nat Commun.* 2020; 11: 404. doi: 10.1038/s41467-019-14134-w.
192. Wu SZ, Roden DL, Wang C, Holliday H, Harvey K, Cazet AS, Murphy KJ, Pereira B, Al-Eryani G, Bartonicek N, Hou R, Torpy JR, Junankar S, et al. Stromal cell diversity associated with immune evasion in human triple-negative breast cancer. *Embo j.* 2020; 39: e104063. doi: 10.15252/emboj.2019104063.
193. Valdés-Mora F, Salomon R, Gloss BS, Law AMK, Venhuizen J, Castillo L, Murphy KJ, Magenau A, Papanicolaou M, Rodriguez de la Fuente L, Roden DL, Colino-Sanguino Y, Kikhtyak Z, et al. Single-cell transcriptomics reveals involution mimicry during the specification of the basal breast cancer subtype. *Cell Rep.* 2021; 35: 108945. doi: 10.1016/j.celrep.2021.108945.

APPENDIX 1: TABLES & FIGURES

Table 1a: Surface biomarkers used to identify fibroblasts and cancer-associated fibroblasts.

Marker	Localization	Expressed by	Role in tumor functionality/progression	References
Fibroblast Activation Protein (FAP)	membrane	Fibroblasts, immune cells	Tumor progression and metastasis, shaping the immunosuppressive TME, ECM remodeling, fibrogenesis	[78, 128, 154, 155]
PDGFRa/b	membrane	Fibroblasts, vascular smooth muscle cells, pericytes	M2 polarization, angiogenesis	[27, 156, 157]
Podoplanin (PDPN)	membrane	Endothelial cells	Immunosuppression, tumor growth	[158-162]
α11β1 integrin (ITGA11)	membrane	Mesenchymal cells	Cancer cell migration, adhesion, tumor cell invasion, desmoplasia	[163-166]
Caveolin-1 (CAV1)	membrane	Many cells	Vascular and pleural invasion of cancer cells, metastasis	[43, 167-170]
CD10	membrane	Bone marrow mesenchymal stem cells, pre-B lymphocytes	Sustaining cancer stemness, cancer formation, chemoresistance	[131]
CD74	membrane	Fibroblasts, monocytes, macrophages, epithelial cells	Antigen presentation	[35, 38]
Ly6C	membrane	Inflammatory CAFs, myeloid cells	Protumorigenic inflammation	[35, 38]
Thy-1 (CD90)	membrane	Fibroblasts, neurons, endothelial cells, tumor cells, immune cells	Tumor cell invasion, migration, tumor-associated endothelial cells	[171-174]

TME: tumor microenvironment, ECM: extracellular matrix

Table 1b: Intracellular biomarkers used to identify fibroblasts and cancer-associated fibroblasts.

Marker	Localization	Expressed by:	Role in tumor functionality/progression:	References
Vimentin	cytoplasmic	Fibroblasts, mesenchymal cells	Tumor growth, invasion, migration, endothelial to mesenchymal transition	[175, 176]
α-SMA	cytoplasmic	Fibroblasts, smooth muscle cells	Tumor cell proliferation, protection mechanism, impediment to drug delivery, ECM remodeling, desmoplasia, cancer stemness	[30, 39, 43]
FSP-1/S100A4	cytoplasmic, nuclear	Normal fibroblasts, epithelial and endothelial cells	Promotion of metastasis, immune evasion, immune surveillance, cell motility, fibrosis	[157, 177-179]
Tenascin-C	ECM protein	Tumor cells, stromal cells	Driver of metastasis, Epithelial-mesenchymal transition, desmoplasia, angiogenesis	[180-182]
Periostin (POSTN, OSF-2)	Secreted ECM protein	Many cells	Cancer cell stemness, promotes tumor progression and metastasis	[183-186]
COL1 and COL11A1	cytoplasmic	Activated stromal cells	Epithelial-mesenchymal transition, metastasis	[157, 187-190]

Table 2: Cancer-associated fibroblast subtypes across different cancers.

Tumor type	Species	CAF subtype	Relevant Biomarker(s) or Major Feature(s)	Reference(s)
Pancreatic cancer	Patient samples, Murine tumors (KPC)	myCAF – ECM producing	FAP, α -SMA ^{hi} , Thy1, TAGLN	[35, 36, 38, 39]
		iCAF - inflammatory	Ly6C ^{hi} , α -SMA ^{lo} , PDGFR α ^{hi} , IL-1, IL-6	
		ApCAF – Ag presenting	MHCII	
Colorectal cancer	Patient samples	CAF-A	α -SMA ^{lo} , FAP, MMP2, DCN, ECM remodeling	[48, 49]
		CAF-B	α -SMA ^{hi} , TAGLN ^{hi} , PDGFR α , FAP-; activated myofibroblasts	
Head and neck cancer	Patient samples	Myofibroblast	α -SMA ^{hi} , MYL9, MYLK, contractile	[47]
		Activated CAFs (2 subclusters; CAF1 and CAF2)	FAP, PDPN, PDGFR α ; ECM producing	
Lung cancer	Patient samples	Cluster 1	ECM-producing, TGF- β signature	[37]
		Cluster 2	α -SMA ^{hi}	
		Cluster 4	Enriched at leading edge	
		Cluster 5	High mTOR; enriched at tumor core	
		Cluster 7	High mTOR; enriched at leading edge	
Melanoma	Murine tumors (B16-F10)	S1 – immune CAFs	CD34 ^{hi} , CXCL12, C3, immunosuppressive	[52]
		S2 – desmoplastic CAFs	CD34 ^{lo} , CTGF, TNC; PDGFR α , ECM producing	
		S3 – contractile CAFs	α -SMA ^{hi} , RGS5	
Breast cancer and ovarian cancer	Patient samples	CAF-S1	FAP ^{hi} , α -SMA ^{hi} , CXCL12, IL-6	[43-45, 191]
		CAF-S2	Low/no marker expression; contractile	
		CAF-S3	α -SMA ^{lo} , FSP1, PDGFR β +	
		CAF-S4	CD29 ^{hi} , α -SMA ^{hi} , FAP ^{lo}	
Breast cancer	Patient samples	iCAF	CXCL12	[192]
		myCAF	α -SMA, FAP, PDPN, COL1A1, COL1A2	

Table 2 (cont'd)

Breast cancer	Murine tumors (MMTV-PyVT)	Vascular CAF (vCAF)	α -SMA, PDGFR β ; angiogenesis	[50, 193]
		Matrix CAF (mCAF)	α -SMA ^{lo} , PDGFR α ; ECM producing	
		Cycling CAF (cCAF)	PDGFR β ^{hi} , angiogenesis	
		Developmental CAF (dCAF)	PDGFR β -, SCRG1, SOX9; differentiation	
Breast cancer	Murine tumors (4T1)	PDPN-CAF	6 subclusters	[51]
		S100A4-CAF	2 subclusters	
Bladder cancer	Patient samples	Myo-CAF	RGS5, MYL9, MYH11	[42]
		iCAF	PDGFR α , CXCL12, IL-6, CXCL14, CXCL1, CXCL2	
Prostate cancer	Patient samples	CAF-S1	α -SMA, PDGFR β	[46]
		CAF-S2	PDGFR α , PLAGL1	
		CAF-S3	α -SMA, HOXB2, MAFB	
Cholangio carcinoma	Patient samples, Murine tumors (KRAS ^{G12D} /p19-induced, YAP ^{S127A} /AKT-induced)	myCAF	COL1A1, α -SMA	[41]
		iCAF	COL8A1, COL15A1, SERPINF1	
		mesCAF	CXCL12, HGF, RGS5 Mesothelin	

TAGLN: transgelin, MHCII: major histocompatibility complex class II, DCN: decorin, MY: myosin, CTGF: connective tissue growth factor, TNC: tenascin-C, RGS5: regulator of G protein signaling 5, FSP1: fibroblast-specific protein-1, SCRG1: stimulator of chondrogenesis 1, SOX9: SRY-Box Transcription Factor 9, PLAGL1: pleomorphic adenoma gene 1, HOXB2: homeobox B2, MAFB: musculoaponeurotic fibrosarcoma oncogene homolog B, SERPINF1: serpin family F member 1

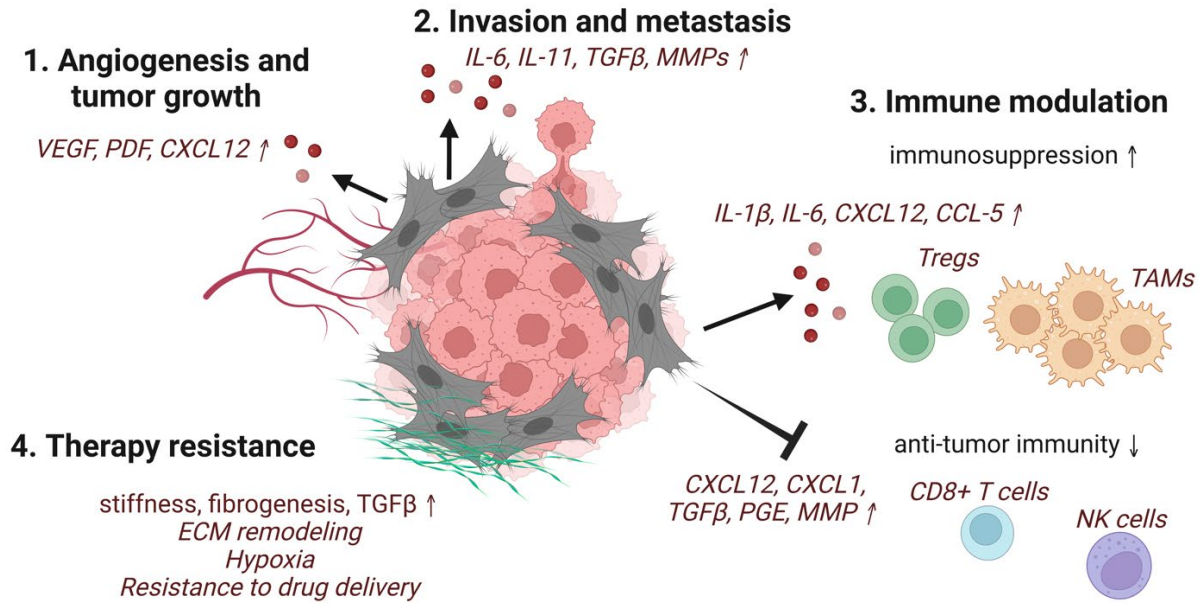


Figure 1. Schematic representation of selected pro-tumorigenic functions of CAFs.

CAFs induce (1) angiogenesis and tumor growth, (2) invasion and metastasis of cancer cells, (3) modulation of the immune system, including recruitment and activation of immune suppressors and inhibition of anti-tumor effector cells, and (4) therapy-resistance through ECM production and remodeling (created with BioRender.com).

FUNDING

This article was prepared with funding from the Intramural Research Programs of the National Cancer Institute at the National Institutes of Health.

CHAPTER 2

ANTI-FIBROBLAST ACTIVATION PROTEIN NEAR-INFRARED PHOTOIMMUNOTHERAPY TARGETING CANCER-ASSOCIATED FIBROBLASTS

Anti-fibroblast activation protein near-infrared photoimmunotherapy targeting cancer-associated fibroblasts

Raisa A. Glabman^{1,2}, Peter L. Choyke¹, Noriko Sato^{1,*}

¹ Molecular Imaging Branch, Center for Cancer Research, National Cancer Institute, National Institutes of Health, Bethesda, MD 20892, USA

² Department of Pathobiology and Diagnostic Investigation, College of Veterinary Medicine, Michigan State University, East Lansing, MI 48824, USA

* Corresponding author: N. Sato, saton@mail.nih.gov; Molecular Imaging Branch, Center for Cancer Research, National Cancer Institute, National Institutes of Health, Bethesda, MD 20892, USA Tel.: 1-240-858-3079

ABSTRACT

Cancer-associated fibroblasts (CAFs) constitute a prominent cellular component of the tumor stroma, representing a heterogeneous group of activated fibroblasts. Within the tumor microenvironment (TME), CAFs play various pro-tumorigenic roles, including extracellular matrix remodeling, suppression of anti-tumor immunity, and modulation of tumor cell resistance to therapy. Fibroblast activation protein (FAP), a highly expressed marker on immunosuppressive CAFs, has been identified in several epithelial human cancers such as lung, colon, breast, and prostate cancer. Numerous attempts to target FAP⁺CAFs for inhibiting tumor progression and enhancing anti-tumor immunity have been reported, however, the translation of FAP-directed therapies into human clinical trials has been unsuccessful. Near-infrared photoimmunotherapy (NIR-PIT) is a highly selective tumor therapy that utilizes an antibody-photo-absorbing conjugate activated by near-infrared (NIR) light. In this study, we examined the therapeutic efficacy of CAF depletion by anti-FAP NIR-PIT in two mouse models. Using CAF-rich syngeneic lung and spontaneous mammary tumors, anti-FAP NIR-PIT effectively depleted FAP⁺ CAFs, as well as FAP⁺ myeloid cells, and suppressed tumor growth. Activation of CD8⁺T and natural killer cells to produce interferon-gamma was induced within hours after anti-FAP NIR-PIT. Lung metastasis was reduced in the spontaneous mammary cancer model. These findings highlight a promising therapeutic approach for selectively and safely eliminating immunosuppressive FAP⁺ cells within the tumor microenvironment.

KEY WORDS

Fibroblast Activation Protein

Near-Infrared Photoimmunotherapy

Cancer-Associated Fibroblast

Tumor Microenvironment

Cancer therapy

ABBREVIATIONS

α -SMA: alpha Smooth Muscle Actin

CAF: Cancer-Associated Fibroblast

FAP: Fibroblast Activation Protein

GCV: Ganciclovir

NIR-PIT: Near-Infrared Photoimmunotherapy

PDGFR- α : platelet derived growth factor receptor alpha

PDGFR- β : platelet derived growth factor receptor beta

PDPN: Podoplanin

TME: Tumor Microenvironment

TGF- β : Tumor Growth Factor beta

INTRODUCTION

The tumor microenvironment (TME) contains various elements that contribute to both immune evasion and immune suppression. Among them, cancer-associated fibroblasts (CAFs) constitute a key cellular component of the tumor stroma, serving a number of immunosuppressive functions within the TME. Pro-tumorigenic roles of CAFs include remodeling of the extracellular matrix (ECM), suppressing anti-tumor immunity, and aiding tumor cells in resistance to therapy. Targeting CAFs presents several challenges owing to their diverse origins, plasticity, expression of heterogeneous markers and phenotypic variation across different cancer and tissue types. Regardless, controlling or reducing CAFs in the TME presents a promising approach to improve current cancer therapies. CAFs are more genetically stable compared with neoplastic cells, and less likely to develop resistant phenotypes due to high mutation rates and clonal selection. They maintain epigenetic differences compared with normal resting stromal cells and contribute to the physical structure and function of the extracellular matrix (ECM). CAFs support neoplastic cells throughout the disease spectrum, from early seeding to metastasis. Targeting or reducing CAFs has the potential to impact angiogenesis, epithelial-mesenchymal transition (EMT), and immune evasion, further augmenting cancer treatment outcomes [1].

Fibroblast activation protein (FAP) is a type II transmembrane serine protease family glycoprotein which is a member of the serine protease family [2]. FAP is minimally expressed by fibroblasts in health [3], but highly upregulated by CAFs in cancer as well as other fibroproliferative diseases (idiopathic pulmonary fibrosis, hepatic fibrosis, rheumatoid arthritis and myocardial infarction) [4, 5]. High FAP expression has been correlated to higher tumor grade, high recurrence rates and poor survival across a wide range of human cancers including breast [6-8], oral squamous cell carcinoma [9], gastric [10, 11], renal [12], colorectal [13, 14], lung [5, 15], ovarian [16], pancreatic

[17, 18] and melanoma [19, 20]. FAP promotes tumor growth by promoting angiogenesis and ECM remodeling [21] and facilitates the progression of tumors by suppressing the anti-cancer immune response [22, 23]. FAP is upregulated in vitro and in vivo by TGF- β and IL-1 β [24]. Despite abundant evidence that FAP is critical in the TME, and FAP-targeted therapies have shown preclinical success [15, 25, 26], this has not translated into human clinical trials [27-30].

Near-infrared photoimmunotherapy (NIR-PIT) is a novel technique to selectively target and deplete cells locally within a tumor. Using an antibody conjugated to a phthalocyanine dye, IR700, followed by exposure to NIR-light, target cells rapidly undergo necrosis [31, 32]. Currently, epidermal growth factor receptor (EGFR)-targeted NIR-PIT is in phase 3 clinical trials in head and neck cancer ([http://clinicaltrials.gov/ Identifier: NCT02422979](http://clinicaltrials.gov/Identifier:NCT02422979)) and has been approved for clinical use in Japan [33] (Rakuten Medical Inc.). In addition to directly targeting tumor antigens, immunosuppressive cells in the TME can be selectively depleted with NIR-PIT. For instance, CD25⁺ Treg cells have been locally depleted using NIR-PIT to augment the anti-tumor immune response [34]. In a similar manner, fibroblasts can be selectively targeted using anti-FAP NIR-PIT [35-37]. In this study, we investigated the therapeutic effect and subsequent immune response to FAP⁺ targeted NIR-PIT (**Figure 1.1**). Using CAF-rich syngeneic lung and spontaneous mammary tumors, we demonstrate that anti-FAP NIR-PIT can effectively deplete endogenous CAFs in the tumor microenvironment, induce anti-tumor effect cell activation and IFN- γ production and suppress tumor growth.

MATERIALS AND METHODS

Synthesis of IR700-conjugated anti-FAP and anti-PDPN antibody

Conjugation of IR700 with monoclonal antibodies was performed according to previous reports [32]. Briefly, 500 mg of anti-FAP (Clone 983802; R&D Systems) or anti-podoplanin (PDPN) (Clone 8.1.1; BioXCell) antibody was incubated with molar excess of IR700 (LI-COR Biosciences) in 0.1 mol/L sodium phosphate buffer (Sigma) at room temperature for 1 hour. The mixture was purified with a desalting column (PD-10 Sephadex column; GE Healthcare and Life Science) followed by protein concentration using a 500,000 MW spin column (Vivaspin™; Cytiva) and resuspended in PBS at 500 µg/mL. The quality of anti-FAP or anti-PDPN antibody-IR700 (FAP-IR700 or PDPN-IR700) was confirmed with UV-Vis (Agilent Technologies) where absorption of the elute was measured at a wavelength of 280 and 689 nm. The IR700 to antibody: dye ratio was 3:1 for FAP-IR700 and 4:1 for PDPN-IR700. Unconjugated antibody was used for the antibody control group.

Cell culture

NIH3T3 mouse fibroblasts, LL/2 Lewis lung carcinoma, MOC2 squamous cell carcinoma cells EL-4 T lymphoblast, EO771 mammary carcinoma, 4T1 mammary carcinoma, and PAN02 pancreatic adenocarcinoma cells were purchased from ATCC. MC38 colon adenocarcinoma cells were purchased from Kerablast. NIH3T3 cells were maintained in DMEM (Thermo Fisher Scientific) supplemented with 10 % fetal calf serum (FCS, Gemini), 100 IU/ml penicillin/streptomycin, and 0.05 mM 2-mercaptoethanol. LL/2, MOC2, EL-4, EO771, 4T1, PAN02 and MC38 cells were cultured in RPMI1640 (Thermo Fisher Scientific) supplemented with 0.05 mM 2-Mercaptoethanol, 10% FCS and 100 IU/mL penicillin/streptomycin. All cell lines were tested negative via Molecular Testing of Biological Materials by Frederick National Laboratory

for Cancer Research and *Mycoplasma* via PCR using a Mycoplasma PCR detection kit (ABM). All cells were cultured in a humidified incubator at 37°C with 5% CO₂.

In vitro NIR-PIT

NIH3T3 cells (3x10⁵ cells) were seeded into 12-well plates and incubated with TGF-β (20 ng/ml; Peprotech) in complete media at 37°C. After 48h, cells were washed and incubated with or without antibody conjugate (FAP-IR700 or PDPN-IR700) at 20 μl/mL in phosphate buffered saline (PBS) and incubated for 1h at 37°C. Cells were then washed with PBS and NIR irradiation performed (150 mW/cm²; ML7710 Laser System, Modulight). After 1h incubation at 37°C, cells were gently detached using PBS with 1 mM ethylenediaminetetraacetic acid (EDTA) and a cell scraper. Cell suspensions were then stained using fluorochrome-conjugated antibodies and analyzed using flow cytometry for NIR-PIT efficacy.

Animal Experiments

Mice

All animals were housed in the NIH Clinical Center animal facility, and all procedures were performed in accordance with NIH guidelines and approved by the NIH Institutional Animal Care and Use Committee.

Wild-type C57BL/6 (strain #000664), Ly 5.1 (B6.SJL-*Ptprc*^a *Pepc*^b/BoyJ; strain # 002014), B6 MMTV-PyVT (B6.FVB-Tg(MMTV-PyVT)634Mul/LelJ; strain #022974) mice expressing the polyoma virus middle T oncoprotein (PyMT) under the Mouse Mammary Tumor Virus (MMTV) promoter in a C57BL/6 background, FAP-TK mice (B6.Cg-Tg(Fap-TK)MRkl/J; strain #034655), IFN-γ-enhanced yellow fluorescent protein (eYFP) reporter GREAT mice (C.129S4(B6)-Ifngtm3.1Lky/J; strain #017580), and green fluorescent protein (GFP) transgenic mice (C57BL/6-

Tg(CAG-EGFP)131Osb/LeySopJ; strain #006567) were purchased from The Jackson Laboratory and maintained in our facility.

Subcutaneous tumors were generated by inoculating 3×10^5 LL/2, MOC2, EL-4, EO771, 4T1, PAN02 or MC38 tumor cells in 100 μ l PBS subcutaneously into the right dorsum of mice. Tumor size was measured using electronic calipers (Mitutoyo) and tumor volume (V) was calculated as $V = (\text{major axis}) \times (\text{minor axis})^2 \times \frac{1}{2}$ and followed until endpoint of $V=4000 \text{ mm}^3$. Mice with tumor size of approximately 100 mm^3 were randomly grouped for subsequent experiments. In the MMTV-PyMT mouse, expression of the PyMT oncoprotein is restricted to the mammary epithelium, which results in the appearance of mammary tumors starting from 6-8 weeks after birth in C57BL/6 background mice and pulmonary metastases at 18 weeks in a C57BL/6 mouse background [38, 39].

GREAT mice (IFN- γ reporter with endogenous polyA tail) [40] were used to evaluate IFN γ -eYFP expression using flow cytometry. FAP-TK mice [41] were used to achieve systemic depletion of FAP⁺ expressing cells by administration of ganciclovir (GCV; Sagent Pharmaceuticals) interperitoneally every 12 hours at 100 mg/kg of bodyweight (2.5 mg per 25 g mouse) for 2 days (total of 4 doses).

In vivo NIR-PIT

To evaluate the efficacy of FAP-targeted NIR-PIT, tumor-bearing mice were randomized into 4 groups as follows: (1) no treatment (untreated control); (2) 50 μ g of anti-FAP antibody intravenously (IV), without NIR laser-light exposure (antibody alone); (3) 50 μ g of anti-rat IgG1-IR700 antibody IV with NIR laser-light exposure (isotype control) or (4) 50 μ g of anti-FAP-IR700 IV with NIR laser-light exposure (anti-FAP NIR-PIT). Anti-FAP-IR700, unconjugated anti-FAP or anti-rat IgG1-IR700 was IV administered when tumors reached 100 mm^3 (Day 0). NIR laser-light

(690 nm, 150 mW/cm², 50 J/cm²) exposure of the tumor occurred 24 hours later (Day 1). During NIR laser-light delivery, non-tumoral regions were covered with aluminum foil to prevent NIR exposure.

Bone Marrow Chimeras

Bone marrow chimera mice were generated by whole body lethal irradiation (9.5 Gy) of recipient mice (either MMTV-PyVT, FAP-TK or Ly5.1) using a Cesium-137 irradiator followed by intravenous injection of donor bone marrow cells within 3 hours of irradiation. Bone marrow was collected from donor mice (either FAP-TK or Ly 5.1) immediately after euthanasia by flushing the epiphysis of the femur and tibia with sterile PBS. MMTV-PyVT recipients (expressing Ly 5.2) received bone marrow from either FAP-TK (expressing Ly 5.2) mice (FAP-TK→MMTV) or Ly5.1 mice (Ly5.1→MMTV). FAP-TK and Ly5.1 recipients received bone marrow from Ly5.1 (Ly5.1→FAP-TK) and FAP-TK (FAP-TK→Ly5.1) mice, respectively. Six weeks later, established chimerism was examined using peripheral blood, by distinguishing the recipient- and donor-derived cells by Ly5.2 and Ly5.1 markers using flow cytometry, where applicable. Mice with >95% chimerism in peripheral blood were used for subsequent experiments.

In vivo depletion of FAP-TK⁺ cells by ganciclovir

FAP-TK mice or bone marrow chimera mice generated using FAP-TK either as recipients or donors underwent depletion of FAP expressing cells by intraperitoneal administration of ganciclovir (GCV; Sagent Pharmaceuticals) every 12 hours at 100 mg/kg of bodyweight (2.5 mg per 25 g mouse) in PBS for 2 days (total of 4 doses).

Flow Cytometry

Tumors were harvested, minced using scissors, and digested using 5 µg/mL collagenase (Liberase TM™, Sigma) in 500 µL RPMI for 30 minutes at 37°C. Digestion was stopped by the addition of

FBS to neutralize protease activity. Digested tissues were then filtered through a 70 µm nylon mesh filter (BD Biosciences), centrifuged, washed, and incubated with Fc block (CD16, Thermo Fisher Scientific) for 10 minutes at 4°C. LiveDead™ (Invitrogen™) was used for dead cell exclusion. Single cell suspensions were stained with fluorochrome-conjugated antibodies and analyzed using a CytoFLEX (Beckman Coulter). Antibodies and secondary reagents were titrated to determine optimal concentrations. BD™ CompBeads were used for single-color compensation to create multi-color compensation matrices. Data was analyzed using FlowJo 10.8 (BD Biosciences). Antibodies used for flow cytometry can be found in **Supplementary Table S1**.

Histologic and Multiplex Immunofluorescence Staining

Whole tumors and endpoint MMTV-PyMT mouse lung tissue were harvested immediately following euthanasia and placed in 10% neutral buffered formalin (NBF) for 24-48 hours followed by 70% ethanol for paraffin embedding. Formalin-fixed, paraffin-embedded (FFPE) sections of 3-5 µm thickness were baked for 30 min at 60°C and processed for immunohistochemical (IHC) and immunofluorescent (IF) staining. Opal™ Fluorescent Automation IHC Kits (Akoya Bioscience) were used on FFPE tissue according to the manufacturer's instructions. FFPE tissue slides were stained using a Leica Bond RX autostainer and coverslipped using ProLong Diamond Antifade Mountant (Invitrogen). Antibodies used for histology can be found in **Supplementary Table S2**.

Digital pathology image analysis

IHC and IF slides were scanned using a Zeiss AxioScan Z1 whole slide scanner. Multiplex stained slides were scanned in their entirety using a 20x objective lens. Digital image analysis was performed using HALO® Imaging Analysis platform v3.5 (Indica Labs). A HALO® random forest classifier was used to train a classifier to segment epithelial, stromal, or necrotic tumor regions on H&E-stained whole tumor scanned slides (LL/2 and MMTV-PyVT). Specifically, the classifier

was trained based on 5-10 manual annotations of these regions. The classifier was visually and iteratively improved to prevent any inaccurate classification by manually adding additional training examples as needed. A HALO® AI DenseNet v2 classifier was trained to detect metastasis in lung tissue. Whole slide images taken every 20 µm of the entire lung were first annotated to exclude non-lung tissue (esophagus, thyroid, bronchial lymph nodes). Subsequent classified regions were validated by two board-certified veterinary pathologists in consensus. The percentage of each measure (tumor to lung ratio) was determined by dividing the total area classified as tumor by total area classified as lung.

The HALO® High-Plex FL algorithm was used to analyze fluorescent cells and colocalization of markers. Thresholds of each stain were set using the real-time tuning window. User-defined cell phenotypes were created to make the algorithm quantify single, double, or triple positive cells. Cell segmentation was performed with the help of multiple parameters including minimum nuclear intensity, nuclear contrast threshold, and nuclear and membrane segmentation aggressiveness. Cell phenotype used to create heat maps was defined based on the antigen expressions as the following: $\text{DAPI}^+\text{FAP}^+ = \text{FAP}^+$ cell, $\text{DAPI}^+\text{PDPN}^+ = \text{PDPN}^+$ cell, $\text{DAPI}^+\text{CD8}^+ = \text{CD8}^+$ T cell. To assess the validity of the unsupervised cell phenotyping algorithm, random areas were selected for manual visual counting of positive cell numbers.

Statistical Analysis

Graphing and statistical analyses were carried out using GraphPad Prism 9 (GraphPad Software). P-values were calculated using two-tailed Student's t-test when comparing two experimental groups, or one-way ANOVA when comparing more than two experimental groups. Parametric or non-parametric tests were applied accordingly. Error bars represent standard error of the mean unless specified in the figure legends. Asterisks indicate significant differences between experimental groups (* P value < 0.05, ** P value < 0.01, *** P value < 0.001) and N.S. = no statistically significant difference.

Figures and schematics were created using BioRender (Biorender.com).

RESULTS

CAFs are present in the TME across several tumor models at steady state.

As CAFs are known to be variably abundant in syngeneic murine cancer models, we first examined the expression of five commonly reported CAF markers [42], including FAP, α -SMA, Podoplanin (PDPN), platelet derived growth factor receptor alpha (PDGFR- α) and platelet derived growth factor receptor beta (PDGFR- β) on seven murine cancer cell lines, EL-4, MC38, EO771, PAN02, LL/2, MOC2, 4T1 in vitro (**Figure S1A-B**). All cell lines examined highly expressed α -SMA. FAP and PDPN expression was low to absent. Among these cell lines, LL/2, 4T1 and MC38 demonstrated a steady subcutaneous tumor growth in mice (data not shown). To optimize downstream experiments, these three murine tumor models were compared for presence of the immunosuppressive CD45⁻ α -SMA⁺FAP⁺ CAF subtype [43, 44]. Flow cytometry analysis indicated the highest frequency of the CD45⁻ α -SMA⁺FAP⁺ fraction in the LL/2 tumor model compared with 4T1 and MC38 tumors (**Figure 2A-B**). Histological analysis of the LL/2 tumors confirmed the presence of α -SMA⁺ and FAP⁺ cells (**Figure 2C**), and a heat map analysis showed FAP⁺ cells were concentrated predominantly at the stromal margin near the tumor invasive front (**Figure 2C**).

Because growth of subcutaneously inoculated tumors is more rapid than naturally occurring cancers, which affects CAF development and distribution, we performed similar expression analysis on a genetically engineered mouse model (GEMM) of spontaneous mammary cancer, the MMTV-PyVT mouse [38, 39]. Mammary tumors in these GEMMs have similar characteristics to human breast carcinoma including tumor progression [45] and CAF subsets [46]. Histologically, the MMTV-PyVT tumors also had high prevalence of α -SMA⁺FAP⁺ cells at the tumor periphery

(**Figure S2A**). We further analyzed Ki67 expression and found that these cells demonstrated Ki67⁺ staining, indicating their active proliferation (**Figure S2B**).

Anti-FAP-IR700 NIR-PIT induces cell death of FAP expressing fibroblasts in vitro.

To test the efficacy of anti-FAP NIR-PIT, we next performed depletion of FAP⁺ cells in vitro. Murine fibroblasts (NIH3T3) were stimulated with TGF- β to induce FAP expression [47, 48]. NIH3T3 cells upregulated FAP⁺ in a TGF- β dose-dependent manner observed via flow cytometry analysis (**Figure 3A**). In vitro anti-FAP NIR-PIT targeting of FAP-induced NIH3T3 cells resulted in decrease of live cells dependent on NIR light intensity (**Figure 3B**), confirming the efficacy of anti-FAP NIR-PIT. Based on these results, we chose 50J of NIR light exposure for subsequent in vivo PIT experiments.

Anti-FAP NIR-PIT suppresses tumor growth and lung metastasis in vivo.

In vivo anti-FAP NIR-PIT was performed in two murine tumor models, one subcutaneously inoculated (LL/2) and one spontaneously developed (MMTV-PyVT) to evaluate therapeutic efficacy on tumor growth. In both models, tumor-bearing mice were administered anti-FAP-IR700 conjugate (Day -1), NIR-PIT performed 24 hours later (Day 0), and tumors measured for 10-30 days until endpoint (**Figure 4A**). Anti-FAP NIR-PIT significantly suppressed LL/2 tumor growth compared with an anti-FAP Ab alone, rat IgG1 isotype control plus NIR-PIT light exposure, or an untreated control group (**Figure 4B**). Similarly, MMTV-PyVT tumor growth was significantly suppressed in the anti-FAP NIR-PIT group compared with an anti-FAP Ab alone, or an untreated control group (**Figure 4C**). Digital image analysis to segment tumor regions (as tumor, stroma, necrosis, muscle, skin or glass) was performed on H&E-stained scanned sections of MMTV-PyVT control and anti-FAP NIR-PIT treatment groups using a random forest classifier. Average stromal area (total stromal area divided by total classified area) was reduced by approximately 50% at 24

hours post NIR-PIT compared to untreated controls (**Figure 4D**). Moreover, in contrast to the multiple lung metastasis observed in untreated MMTV-PyVT tumors, lung metastasis was significantly reduced in the anti-FAP NIR-PIT group (**Figure 4E**).

Anti-PDPN-IR700 NIR-PIT induces cell death of PDPN expressing fibroblasts in vitro, but did not suppress tumor growth in vivo.

In addition to FAP, a second CAF marker, Podoplanin (PDPN), was tested for efficacy as an anti-CAF NIR-PIT target. As with FAP, PDPN expression increased on NIH3T3 cells in vitro after stimulation with TGF- β (**Figure S3A**). Anti-PDPN NIR-PIT demonstrated killing of NIH3T3 cells compared to untreated control cells (**Figure S3B**). PDPN expression levels varied among tumor types in vivo (**Figure S3C**) with highest expression in MOC2 tumors but absent in MOC2 tumor cells. PDPN-expressing cells were observed predominantly at the tumor periphery, near the invasive front (**Figure S3D**). Anti-PDPN NIR-PIT was performed on mice inoculated with subcutaneous MOC2 tumors, however, no difference in tumor growth was observed between the anti-PDPN NIR-PIT group, anti-PDPN Ab alone, or an untreated control group (**Figure S3E**).

Anti-FAP NIR-PIT increases immune effector cells and their IFN- γ expression in the tumor microenvironment.

To understand how tumor growth suppression was occurring, the frequency of key anti-tumor effector cells cytotoxic CD8⁺T and natural killer (NK) cells, as well as their IFN- γ production was measured within the tumor. As the primary anti-tumor effector cells, CD8⁺T and NK cells were enumerated in the tumor before and 24h after anti-FAP NIR-PIT. Flow cytometry showed an increase in frequency of CD8⁺ T cells after anti-FAP NIR-PIT for both LL/2 (**Figure 5A**). and MMTV-PyVT tumor models (**Figure 5B**). Multiplex immunohistochemistry revealed distribution of CD8⁺ T cells 24h after anti-FAP NIR-PIT was particularly increased in stromal regions

compared to untreated controls (**Figure 5C**). To examine IFN- γ production, ‘GREAT’ eYFP-IFN- γ reporter mice were inoculated with LL/2 tumors and analyzed for the induction of eYFP signal in intratumoral CD8⁺T and NK cells by flow cytometry. As early as 3h after treatment, CD8⁺ T cells and NK cells began to express eYFP, indicating activation of these anti-tumor effector cells and production of IFN- γ (**Figure 5D**). eYFP positivity in CD8⁺ T and NK cells increased from 3h to 24h (**Figure 5D-E**), suggesting IFN- γ production continues at least up to 24 hours after anti-FAP NIR-PIT. Because eYFP protein can remain within a cell after IFN- γ is no longer produced, it is difficult to determine the true peak of IFN- γ production using the GREAT eYFP mouse model (**Figure S4**).

Depletion of FAP⁺ hematopoietic cells contributes to tumor growth suppression.

Flow cytometry characterization of the FAP⁺ population using GFP mice inoculated with LL/2 tumors demonstrated that many endogenous FAP⁺ cells also expressed CD45 (**Figure 6A**), a pan-leukocyte marker. Additional analysis of this FAP⁺CD45⁺ population in anti-FAP NIR-PIT treated LL/2 tumors suggested that FAP⁺ macrophages (CD45⁺Ly6C^{int}F4/80^{hi}), circulating monocytes (CD45⁺Ly6C^{hi}F4/80^{int}), and resting monocytes (CD45⁺Ly6C^{lo}F4/80^{int}), were depleted 1h after anti-FAP NIR-PIT (**Figure 6B**).

To determine whether the tumor suppressive effect observed with anti-FAP NIR-PIT was due to ablation of FAP⁺CD45⁻ mesenchymal stromal cells or FAP⁺CD45⁺ hematopoietic cells, a series of FAP-TK bone marrow chimeras were generated to allow for selective FAP⁺ cell depletion of either stromal or hematopoietic cells. GCV treatment depleted FAP⁺ cells in LL/2 tumors in FAP-TK mice (**Figure S5A**). Reconstitution of bone marrow by recipients was confirmed to be >95% by flow cytometry analysis using Ly5.1 and Ly5.2 congenic markers (**Figure S5B**). Generated bone marrow chimeras and control FAP-TK or wild type mice received 4 doses of 100 mg/ kg GCV intraperitoneal injections every 12 hours (**Figure 6C**). In the chimeras, GCV treatment selectively depleted actively dividing FAP⁺ cells in either the stromal (when FAP-TK mice were recipients) or hematopoietic compartments (when bone marrow from FAP-TK mice were transferred as donor bone marrow). Suppression of tumor growth was observed for the LL/2 stromal FAP⁺ depletion group (Ly5.1 → FAP-TK) and, to a lesser extent, for the hematopoietic FAP⁺ depletion group (FAP-TK → Ly5.1) compared with PBS injected controls (**Figure 6D**). Tumor suppression was also observed for the MMTV-PyVT hematopoietic FAP⁺ depletion group (FAP-TK → MMTV) compared with a bone marrow transfer control group (Ly5.1 → MMTV) receiving GCV, and an untreated control group (**Figure 6E**). This data indicates that depletion of FAP⁺ CAFs or FAP⁺

hematopoietic cells alone can suppress tumor growth, and suggests that the tumor suppression of anti-FAP NIR-PIT, which depletes both the FAP⁺ CAFs and FAP⁺ hematopoietic cells, may occur through combined effects.

DISCUSSION

In this study, we investigated the therapeutic and immune effects of FAP-targeted NIR-PIT in subcutaneously inoculated syngeneic tumor and spontaneously developing MMTV-PyVT mammary tumor mouse models. Previous studies have indicated that anti-FAP therapies such as binding of FAP- α or blocking the enzymatic activity of FAP- α are safe and effective in preclinical studies but do not translate into human clinical trial success [29, 49]. As NIR-PIT targeting EGFR-expressing cancer cells has been approved for use in Japan (Rakuten Medical Inc.) and currently in Phase 3 clinical trials in the US ([ClinicalTrials.gov Identifier: NCT02422979](https://clinicaltrials.gov/ct2/show/study/NCT02422979)) [33], there is clear safety and efficacy in using the NIR-PIT model in humans. Novel use of this established system to deplete immunosuppressive cells within the tumor has been established by targeting CD25 to deplete Treg cells [34, 50] and FAP to deplete CAFs [35, 37, 51] from the TME. As NIR light is carefully applied only at the tumor site, off-target effects are low in NIR-PIT [34, 50]. We demonstrate that local, anti-FAP NIR-PIT can successfully and selectively deplete FAP⁺ immunosuppressive cells, both CAFs and myeloid cells, in the TME which resulted in activation of CD8⁺ T and NK cells, production of IFN- γ , and suppression of tumor growth in both the subcutaneous LL/2 and spontaneous MMTV-PyVT tumors examined. Although anti-FAP NIR-PIT alone did not result in complete tumor remission, lung metastasis in MMTV-PyVT tumor mice was significantly reduced. To our knowledge, this work is the first to use anti-FAP NIR-PIT to deplete CAFs physiologically differentiated in the TME. Moreover, our use of MMTV-PyVT mouse mammary tumors more closely mimic the human tumor microenvironment, including cellular and spatial heterogeneity, tumor growth, and CAF subsets [45].

It has been reported that higher PDPN expression is associated with poorer outcomes in human colorectal carcinomas [52] and is considered to be another promising CAF target [53]. Aside from

high expression on CAFs, PDPN is also highly expressed on lymphatic endothelium, both in normal tissues and during tumorigenesis. Additionally, PDPN serves important functions during development [54-56] and may not be an ideal target molecule for systemic depletion. We hypothesized that NIR-PIT could allow selective depletion of PDPN⁺ cells within the TME and examined the efficacy of anti-PDPN NIR-PIT in a syngeneic MOC2 tumor model. Despite being effective in vitro against murine fibroblasts (NIH3T3) with upregulated PDPN expression, anti-PDPN NIR-PIT was not successful in successfully reducing tumor volume in vivo in our study. Possible explanations include ineffective antibody distribution in the tumor, or less specificity of the PDPN-IR700 conjugate for CAFs in vivo. Taken together, from our data, we concluded that anti-PDPN NIR-PIT was a less favorable strategy for targeting CAFs compared with anti-FAP NIR-PIT.

In this study, non-stromal, CD45⁺ cells within the tumor microenvironment expressed FAP. Our flow cytometry analysis data indicated that these FAP⁺CD45⁺ cells were likely myeloid, consistent with previous work demonstrating that macrophages, specifically M2 or tumor associated macrophages (TAMs), based on F4/80^{hi}/CCR2⁺/CD206⁺ expression, also express FAP [57]. From our data bone marrow chimera mice, depletion of FAP⁺ hematopoietic cells by GCV had a suppressive tumor effect. This result supports the hypothesis that the FAP⁺ hematopoietic cell subset likely contributed to the total observed tumor suppression of anti-FAP NIR-PIT in non-chimeric mice. This hypothesis is also consistent with previous observations that ablation of FAP⁺/F4/80^{hi} TAMs using a diphtheria toxin receptor (DTR) model results in suppression of tumor growth [57]. We observed a similar tumor suppressive effect of FAP-TK cell depletion by GCV injection between the bone marrow chimeras expressing FAP-TK in the stromal cells and the bone marrow chimeras expressing FAP-TK in the hematopoietic cell compartment. In the intratumoral

FAP⁺ cell depletion by anti-FAP NIR-PIT, it is likely that depletion of the stromal cells (CAFs) and that of hematopoietic FAP expressing cells (myeloid cells) both contributed to the observed therapeutic effect. This highlights a strength of anti-FAP NIR-PIT in targeting different immunosuppressive cell types in the TME with one treatment.

A limitation to the chimera models using the FAP-TK/GCV system was toxicity of ganciclovir. To achieve FAP depletion in the FAP-TK chimeras, a near-toxic systemic dose (100 mg/kg IP twice daily for two days) was used, which likely caused off-target effects. Some studies have reported that systemic depletion of FAP⁺ cells induces bone marrow hypocellularity, anemia and cachexia in mice [58, 59]. With the dose of GCV used in our study, we cannot exclude the possibility of inducing some off-target effects in GCV-treated mice.

In summary, this work provides evidence to support anti-FAP NIR-PIT as a viable method for depletion of immunosuppressive CAFs. The selective depletion of FAP⁺ cells using NIR-PIT successfully suppressed tumor growth in subcutaneous mouse tumor model and lung metastasis in a spontaneous mouse mammary tumor model. Our findings highlight a promising therapeutic approach for selectively and safely eliminating FAP⁺ cells within the tumor microenvironment.

ACKNOWLEDGEMENTS

The authors would like to acknowledge Dr. Aki Furasawa for assistance with multiplex immunostaining, Colleen Olkowski for technical assistance, Hannah Minor for assistance with flow cytometry, Ross Lake for whole slide scanning, and Dr. Noemi Kedei and Dr. Laura Bassel for providing constructive feedback and assistance with HALO analysis. Analysis and management of images and associated metadata was supported in part by the NCI HALO Image Analysis Resource. RG would like to thank Dr. Mark Simpson, the NIH Comparative Biomedical Scientist Training Program as well as Michigan State University for lending expertise and insight.

REFERENCES

1. Toledo B, Picon-Ruiz M, Marchal JA, Peran M. Dual Role of Fibroblasts Educated by Tumour in Cancer Behavior and Therapeutic Perspectives. *Int J Mol Sci.* 2022; 23. doi: 10.3390/ijms232415576.
2. Liu R, Li H, Liu L, Yu J, Ren X. Fibroblast activation protein: A potential therapeutic target in cancer. *Cancer Biol Ther.* 2012; 13: 123-9. doi: 10.4161/cbt.13.3.18696.
3. Niedermeyer J, Garin-Chesa P, Kriz M, Hilberg F, Mueller E, Bamberger U, Rettig WJ, Schnapp A. Expression of the fibroblast activation protein during mouse embryo development. *Int J Dev Biol.* 2001; 45: 445-7. doi:
4. Huang Y, Wang S, Kelly T. Seprase promotes rapid tumor growth and increased microvessel density in a mouse model of human breast cancer. *Cancer Res.* 2004; 64: 2712-6. doi: 10.1158/0008-5472.can-03-3184.
5. Kilvaer TK, Rakaee M, Hellevik T, Ostman A, Strell C, Bremnes RM, Busund LT, Donnem T, Martinez-Zubiaurre I. Tissue analyses reveal a potential immune-adjuvant function of FAP-1 positive fibroblasts in non-small cell lung cancer. *PLoS One.* 2018; 13: e0192157. doi: 10.1371/journal.pone.0192157.
6. Kelly T. Fibroblast activation protein-alpha and dipeptidyl peptidase IV (CD26): cell-surface proteases that activate cell signaling and are potential targets for cancer therapy. *Drug Resist Updat.* 2005; 8: 51-8. doi: 10.1016/j.drug.2005.03.002.
7. Bernard V, Semaan A, Huang J, San Lucas FA, Mulu FC, Stephens BM, Guerrero PA, Huang Y, Zhao J, Kamyabi N, Sen S, Scheet PA, Taniguchi CM, et al. Single-Cell Transcriptomics of Pancreatic Cancer Precursors Demonstrates Epithelial and Microenvironmental Heterogeneity as an Early Event in Neoplastic Progression. *Clin Cancer Res.* 2019; 25: 2194-205. doi: 10.1158/1078-0432.Ccr-18-1955.
8. Park SY, Kim HM, Koo JS. Differential expression of cancer-associated fibroblast-related proteins according to molecular subtype and stromal histology in breast cancer. *Breast Cancer Res Treat.* 2015; 149: 727-41. doi: 10.1007/s10549-015-3291-9.
9. Wang LC, Lo A, Scholler J, Sun J, Majumdar RS, Kapoor V, Antzis M, Cotner CE, Johnson LA, Durham AC, Solomides CC, June CH, Puré E, et al. Targeting fibroblast activation protein in tumor stroma with chimeric antigen receptor T cells can inhibit tumor growth and augment host immunity without severe toxicity. *Cancer Immunol Res.* 2014; 2: 154-66. doi: 10.1158/2326-6066.Cir-13-0027.
10. Saadi A, Shannon NB, Lao-Sirieix P, O'Donovan M, Walker E, Clemons NJ, Hardwick JS, Zhang C, Das M, Save V, Novelli M, Balkwill F, Fitzgerald RC. Stromal genes discriminate preinvasive from invasive disease, predict outcome, and highlight inflammatory pathways in digestive cancers. *Proc Natl Acad Sci U S A.* 2010; 107: 2177-82. doi: 10.1073/pnas.0909797107.

11. Hu M, Qian C, Hu Z, Fei B, Zhou H. Biomarkers in Tumor Microenvironment? Upregulation of Fibroblast Activation Protein- α Correlates with Gastric Cancer Progression and Poor Prognosis. *OMICS*. 2017; 21: 38-44. doi: 10.1089/omi.2016.0159.
12. Errarte P, Guarch R, Pulido R, Blanco L, Nunes-Xavier CE, Beitia M, Gil J, Angulo JC, Lopez JI, Larrinaga G. The Expression of Fibroblast Activation Protein in Clear Cell Renal Cell Carcinomas Is Associated with Synchronous Lymph Node Metastases. *PLoS One*. 2016; 11: e0169105. doi: 10.1371/journal.pone.0169105.
13. Lopez JI, Errarte P, Erramuzpe A, Guarch R, Cortes JM, Angulo JC, Pulido R, Irazusta J, Llarena R, Larrinaga G. Fibroblast activation protein predicts prognosis in clear cell renal cell carcinoma. *Hum Pathol*. 2016; 54: 100-5. doi: 10.1016/j.humpath.2016.03.009.
14. Chen L, Qiu X, Wang X, He J. FAP positive fibroblasts induce immune checkpoint blockade resistance in colorectal cancer via promoting immunosuppression. *Biochem Biophys Res Commun*. 2017; 487: 8-14. doi: 10.1016/j.bbrc.2017.03.039.
15. Santos AM, Jung J, Aziz N, Kissil JL, Pure E. Targeting fibroblast activation protein inhibits tumor stromagenesis and growth in mice. *J Clin Invest*. 2009; 119: 3613-25. doi: 10.1172/JCI38988.
16. Mhawech-Fauceglia P, Yan L, Sharifian M, Ren X, Liu S, Kim G, Gayther SA, Pejovic T, Lawrenson K. Stromal Expression of Fibroblast Activation Protein Alpha (FAP) Predicts Platinum Resistance and Shorter Recurrence in patients with Epithelial Ovarian Cancer. *Cancer Microenviron*. 2015; 8: 23-31. doi: 10.1007/s12307-014-0153-7.
17. Shi M, Yu DH, Chen Y, Zhao CY, Zhang J, Liu QH, Ni CR, Zhu MH. Expression of fibroblast activation protein in human pancreatic adenocarcinoma and its clinicopathological significance. *World J Gastroenterol*. 2012; 18: 840-6. doi: 10.3748/wjg.v18.i8.840.
18. Kawase T, Yasui Y, Nishina S, Hara Y, Yanatori I, Tomiyama Y, Nakashima Y, Yoshida K, Kishi F, Nakamura M, Hino K. Fibroblast activation protein- α -expressing fibroblasts promote the progression of pancreatic ductal adenocarcinoma. *BMC Gastroenterol*. 2015; 15: 109. doi: 10.1186/s12876-015-0340-0.
19. Sorrentino C, Miele L, Porta A, Pinto A, Morello S. Activation of the A2B adenosine receptor in B16 melanomas induces CXCL12 expression in FAP-positive tumor stromal cells, enhancing tumor progression. *Oncotarget*. 2016; 7: 64274-88. doi: 10.18632/oncotarget.11729.
20. Tulley S, Chen WT. Transcriptional regulation of seprase in invasive melanoma cells by transforming growth factor- β signaling. *J Biol Chem*. 2014; 289: 15280-96. doi: 10.1074/jbc.M114.568501.
21. Cao D, Hou M, Guan YS, Jiang M, Yang Y, Gou HF. Expression of HIF-1 α and VEGF in colorectal cancer: association with clinical outcomes and prognostic implications. *BMC Cancer*. 2009; 9: 432. doi: 10.1186/1471-2407-9-432.

22. Kraman M, Bambrough PJ, Arnold JN, Roberts EW, Magiera L, Jones JO, Gopinathan A, Tuveson DA, Fearon DT. Suppression of antitumor immunity by stromal cells expressing fibroblast activation protein-alpha. *Science*. 2010; 330: 827-30. doi: 10.1126/science.1195300.
23. Joyce JA, Fearon DT. T cell exclusion, immune privilege, and the tumor microenvironment. *Science*. 2015; 348: 74-80. doi: 10.1126/science.aaa6204.
24. Chung KM, Hsu SC, Chu YR, Lin MY, Jiaang WT, Chen RH, Chen X. Fibroblast activation protein (FAP) is essential for the migration of bone marrow mesenchymal stem cells through RhoA activation. *PLoS One*. 2014; 9: e88772. doi: 10.1371/journal.pone.0088772.
25. Adams S, Miller GT, Jesson MI, Watanabe T, Jones B, Wallner BP. PT-100, a small molecule dipeptidyl peptidase inhibitor, has potent antitumor effects and augments antibody-mediated cytotoxicity via a novel immune mechanism. *Cancer Res*. 2004; 64: 5471-80. doi: 10.1158/0008-5472.CAN-04-0447.
26. LeBeau AM, Brennen WN, Aggarwal S, Denmeade SR. Targeting the cancer stroma with a fibroblast activation protein-activated promelittin protoxin. *Mol Cancer Ther*. 2009; 8: 1378-86. doi: 10.1158/1535-7163.MCT-08-1170.
27. Eager RM, Cunningham CC, Senzer N, Richards DA, Raju RN, Jones B, Uprichard M, Nemunaitis J. Phase II trial of talabostat and docetaxel in advanced non-small cell lung cancer. *Clin Oncol (R Coll Radiol)*. 2009; 21: 464-72. doi: 10.1016/j.clon.2009.04.007.
28. Eager RM, Cunningham CC, Senzer NN, Stephenson J, Jr., Anthony SP, O'Day SJ, Frenette G, Pavlick AC, Jones B, Uprichard M, Nemunaitis J. Phase II assessment of talabostat and cisplatin in second-line stage IV melanoma. *BMC Cancer*. 2009; 9: 263. doi: 10.1186/1471-2407-9-263.
29. Hofheinz RD, al-Batran SE, Hartmann F, Hartung G, Jager D, Renner C, Tanswell P, Kunz U, Amelsberg A, Kuthan H, Stehle G. Stromal antigen targeting by a humanised monoclonal antibody: an early phase II trial of sibrotuzumab in patients with metastatic colorectal cancer. *Onkologie*. 2003; 26: 44-8. doi: 10.1159/000069863.
30. Narra K, Mullins SR, Lee HO, Strzemkowski-Brun B, Magalong K, Christiansen VJ, McKee PA, Egleston B, Cohen SJ, Weiner LM, Meropol NJ, Cheng JD. Phase II trial of single agent Val-boroPro (Talabostat) inhibiting Fibroblast Activation Protein in patients with metastatic colorectal cancer. *Cancer Biol Ther*. 2007; 6: 1691-9. doi: 10.4161/cbt.6.11.4874.
31. Kobayashi H, Choyke PL. Near-Infrared Photoimmunotherapy of Cancer. *Acc Chem Res*. 2019; 52: 2332-9. doi: 10.1021/acs.accounts.9b00273.
32. Mitsunaga M, Ogawa M, Kosaka N, Rosenblum LT, Choyke PL, Kobayashi H. Cancer cell-selective in vivo near infrared photoimmunotherapy targeting specific membrane molecules. *Nat Med*. 2011; 17: 1685-91. doi: 10.1038/nm.2554.

33. Cognetti DM, Johnson JM, Curry JM, Kochuparambil ST, McDonald D, Mott F, Fidler MJ, Stenson K, Vasan NR, Razaq MA, Campana J, Ha P, Mann G, et al. Phase 1/2a, open-label, multicenter study of RM-1929 photoimmunotherapy in patients with locoregional, recurrent head and neck squamous cell carcinoma. *Head Neck*. 2021; 43: 3875-87. doi: 10.1002/hed.26885.
34. Sato K, Sato N, Xu B, Nakamura Y, Nagaya T, Choyke PL, Hasegawa Y, Kobayashi H. Spatially selective depletion of tumor-associated regulatory T cells with near-infrared photoimmunotherapy. *Sci Transl Med*. 2016; 8: 352ra110. doi: 10.1126/scitranslmed.aaf6843.
35. Katsube R, Noma K, Ohara T, Nishiwaki N, Kobayashi T, Komoto S, Sato H, Kashima H, Kato T, Kikuchi S, Tazawa H, Kagawa S, Shirakawa Y, et al. Fibroblast activation protein targeted near infrared photoimmunotherapy (NIR PIT) overcomes therapeutic resistance in human esophageal cancer. *Sci Rep*. 2021; 11: 1693. doi: 10.1038/s41598-021-81465-4.
36. Sato H, Noma K, Ohara T, Kawasaki K, Akai M, Kobayashi T, Nishiwaki N, Narusaka T, Komoto S, Kashima H, Katsura Y, Kato T, Kikuchi S, et al. Dual-targeted near-infrared photoimmunotherapy for esophageal cancer and cancer-associated fibroblasts in the tumor microenvironment. *Sci Rep*. 2022; 12: 20152. doi: 10.1038/s41598-022-24313-3.
37. Watanabe S, Noma K, Ohara T, Kashima H, Sato H, Kato T, Urano S, Katsube R, Hashimoto Y, Tazawa H, Kagawa S, Shirakawa Y, Kobayashi H, et al. Photoimmunotherapy for cancer-associated fibroblasts targeting fibroblast activation protein in human esophageal squamous cell carcinoma. *Cancer Biol Ther*. 2019; 20: 1234-48. doi: 10.1080/15384047.2019.1617566.
38. Guy CT, Cardiff RD, Muller WJ. Induction of mammary tumors by expression of polyomavirus middle T oncogene: a transgenic mouse model for metastatic disease. *Mol Cell Biol*. 1992; 12: 954-61. doi: 10.1128/mcb.12.3.954-961.1992.
39. Lin EY, Jones JG, Li P, Zhu L, Whitney KD, Muller WJ, Pollard JW. Progression to malignancy in the polyoma middle T oncoprotein mouse breast cancer model provides a reliable model for human diseases. *Am J Pathol*. 2003; 163: 2113-26. doi: 10.1016/S0002-9440(10)63568-7.
40. Reinhardt RL, Liang HE, Locksley RM. Cytokine-secreting follicular T cells shape the antibody repertoire. *Nat Immunol*. 2009; 10: 385-93. doi: 10.1038/ni.1715.
41. McAndrews KM, Miyake T, Ehsanipour EA, Kelly PJ, Becker LM, McGrail DJ, Sugimoto H, LeBleu VS, Ge Y, Kalluri R. Dermal alphaSMA(+) myofibroblasts orchestrate skin wound repair via beta1 integrin and independent of type I collagen production. *EMBO J*. 2022; 41: e109470. doi: 10.15252/embj.2021109470.
42. Nurmik M, Ullmann P, Rodriguez F, Haan S, Letellier E. In search of definitions: Cancer-associated fibroblasts and their markers. *Int J Cancer*. 2020; 146: 895-905. doi: 10.1002/ijc.32193.

43. Feig C, Jones JO, Kraman M, Wells RJ, Deonaraine A, Chan DS, Connell CM, Roberts EW, Zhao Q, Caballero OL, Teichmann SA, Janowitz T, Jodrell DI, et al. Targeting CXCL12 from FAP-expressing carcinoma-associated fibroblasts synergizes with anti-PD-L1 immunotherapy in pancreatic cancer. *Proc Natl Acad Sci U S A*. 2013; 110: 20212-7. doi: 10.1073/pnas.1320318110.
44. Yang X, Lin Y, Shi Y, Li B, Liu W, Yin W, Dang Y, Chu Y, Fan J, He R. FAP Promotes Immunosuppression by Cancer-Associated Fibroblasts in the Tumor Microenvironment via STAT3-CCL2 Signaling. *Cancer Res*. 2016; 76: 4124-35. doi: 10.1158/0008-5472.CAN-15-2973.
45. Attalla S, Taifour T, Bui T, Muller W. Insights from transgenic mouse models of PyMT-induced breast cancer: recapitulating human breast cancer progression in vivo. *Oncogene*. 2021; 40: 475-91. doi: 10.1038/s41388-020-01560-0.
46. Bartoschek M, Oskolkov N, Bocci M, Lovrot J, Larsson C, Sommarin M, Madsen CD, Lindgren D, Pekar G, Karlsson G, Ringner M, Bergh J, Bjorklund A, et al. Spatially and functionally distinct subclasses of breast cancer-associated fibroblasts revealed by single cell RNA sequencing. *Nat Commun*. 2018; 9: 5150. doi: 10.1038/s41467-018-07582-3.
47. Lee SW, Kwak HS, Kang MH, Park YY, Jeong GS. Fibroblast-associated tumour microenvironment induces vascular structure-networked tumouroid. *Sci Rep*. 2018; 8: 2365. doi: 10.1038/s41598-018-20886-0.
48. Miyake M, Hori S, Morizawa Y, Tatsumi Y, Nakai Y, Anai S, Torimoto K, Aoki K, Tanaka N, Shimada K, Konishi N, Toritsuka M, Kishimoto T, et al. CXCL1-Mediated Interaction of Cancer Cells with Tumor-Associated Macrophages and Cancer-Associated Fibroblasts Promotes Tumor Progression in Human Bladder Cancer. *Neoplasia*. 2016; 18: 636-46. doi: 10.1016/j.neo.2016.08.002.
49. Scott AM, Wiseman G, Welt S, Adjei A, Lee FT, Hopkins W, Divgi CR, Hanson LH, Mitchell P, Gansen DN, Larson SM, Ingle JN, Hoffman EW, et al. A Phase I dose-escalation study of sibrotuzumab in patients with advanced or metastatic fibroblast activation protein-positive cancer. *Clin Cancer Res*. 2003; 9: 1639-47. doi:
50. Kurebayashi Y, Olkowski CP, Lane KC, Vasalatiy OV, Xu BC, Okada R, Furusawa A, Choyke PL, Kobayashi H, Sato N. Rapid Depletion of Intratumoral Regulatory T Cells Induces Synchronized CD8 T- and NK-cell Activation and IFN γ -Dependent Tumor Vessel Regression. *Cancer Res*. 2021; 81: 3092-104. doi: 10.1158/0008-5472.CAN-20-2673.
51. Jin J, Barnett JD, Krishnamachary B, Mironchik Y, Luo CK, Kobayashi H, Bhujwala ZM. Evaluating near-infrared photoimmunotherapy for targeting fibroblast activation protein-alpha expressing cells in vitro and in vivo. *Cancer Sci*. 2023; 114: 236-46. doi: 10.1111/cas.15601.

52. Astarita JL, Keerthivasan S, Husain B, Senbabaoglu Y, Verschueren E, Gierke S, Pham VC, Peterson SM, Chalouni C, Pierce AA, Lill JR, Gonzalez LC, Martinez-Martin N, et al. The neutrophil protein CD177 is a novel PDPN receptor that regulates human cancer-associated fibroblast physiology. *PLoS One*. 2021; 16: e0260800. doi: 10.1371/journal.pone.0260800.
53. Kato T, Furusawa A, Okada R, Inagaki F, Wakiyama H, Furumoto H, Fukushima H, Okuyama S, Choyke PL, Kobayashi H. Near-Infrared Photoimmunotherapy Targeting Podoplanin-Expressing Cancer Cells and Cancer-Associated Fibroblasts. *Mol Cancer Ther*. 2023; 22: 75-88. doi: 10.1158/1535-7163.MCT-22-0313.
54. Astarita JL, Acton SE, Turley SJ. Podoplanin: emerging functions in development, the immune system, and cancer. *Front Immunol*. 2012; 3: 283. doi: 10.3389/fimmu.2012.00283.
55. Renart J, Carrasco-Ramirez P, Fernandez-Munoz B, Martin-Villar E, Montero L, Yurrita MM, Quintanilla M. New insights into the role of podoplanin in epithelial-mesenchymal transition. *Int Rev Cell Mol Biol*. 2015; 317: 185-239. doi: 10.1016/bs.ircmb.2015.01.009.
56. Suzuki-Inoue K, Osada M, Ozaki Y. Physiologic and pathophysiologic roles of interaction between C-type lectin-like receptor 2 and podoplanin: partners from in utero to adulthood. *J Thromb Haemost*. 2017; 15: 219-29. doi: 10.1111/jth.13590.
57. Arnold JN, Magiera L, Kraman M, Fearon DT. Tumoral immune suppression by macrophages expressing fibroblast activation protein-alpha and heme oxygenase-1. *Cancer Immunol Res*. 2014; 2: 121-6. doi: 10.1158/2326-6066.CIR-13-0150.
58. Roberts EW, Deonaraine A, Jones JO, Denton AE, Feig C, Lyons SK, Espeli M, Kraman M, McKenna B, Wells RJ, Zhao Q, Caballero OL, Larder R, et al. Depletion of stromal cells expressing fibroblast activation protein-alpha from skeletal muscle and bone marrow results in cachexia and anemia. *J Exp Med*. 2013; 210: 1137-51. doi: 10.1084/jem.20122344.
59. Tran E, Chinnasamy D, Yu Z, Morgan RA, Lee CC, Restifo NP, Rosenberg SA. Immune targeting of fibroblast activation protein triggers recognition of multipotent bone marrow stromal cells and cachexia. *J Exp Med*. 2013; 210: 1125-35. doi: 10.1084/jem.20130110.

APPENDIX 2: TABLES & FIGURES

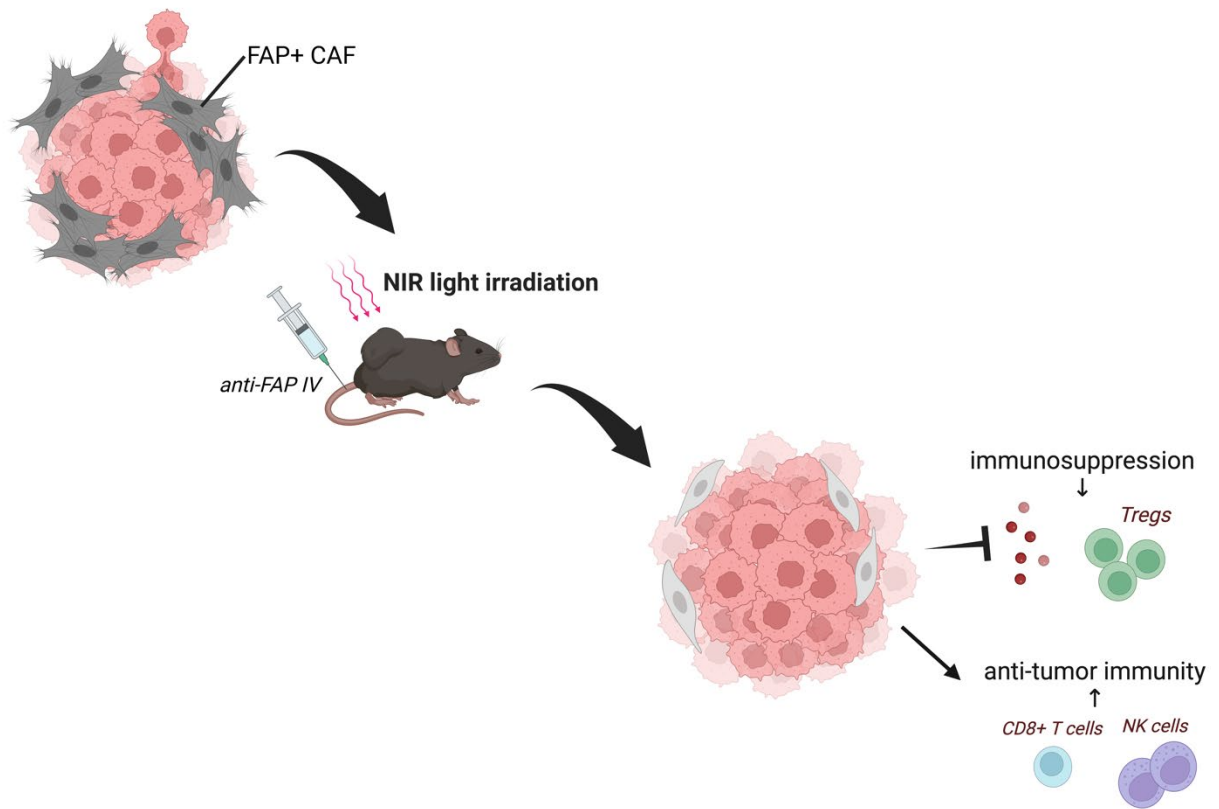


Figure 1.1. Schematic of anti-FAP NIR-PIT and proposed mechanism of immune activation.

FAP+CAFs are selectively and locally targeted within the tumor microenvironment using an intravenous injection of anti-FAP IR700 followed by near-infrared laser light exposure. Following FAP+ NIR-PIT depletion, immunosuppression is decreased, and key anti-tumor immune cells (CD8+T and NK) are activated.

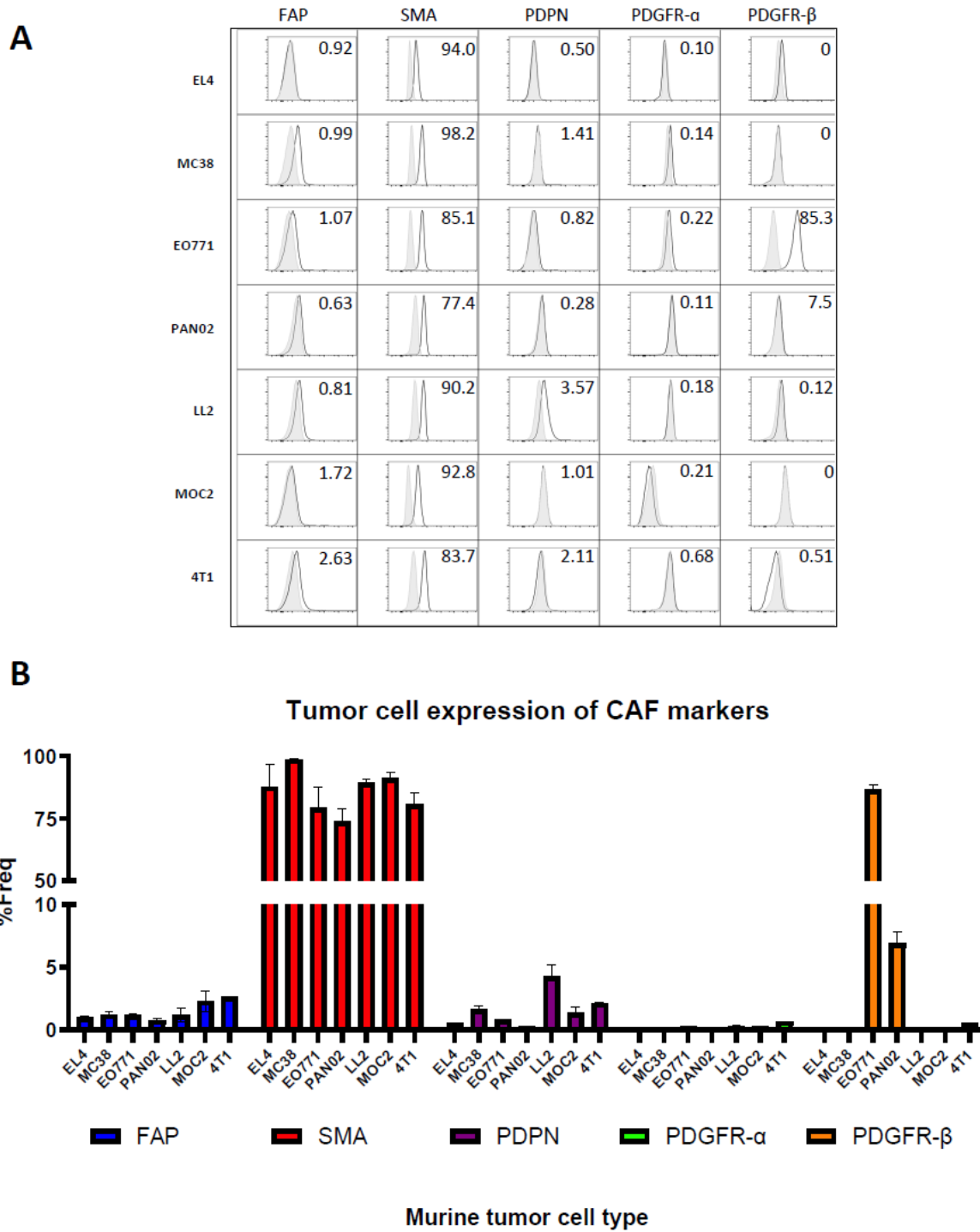


Figure S1. Tumor cell expression of CAF markers in vitro.

Flow cytometry analysis of expression of five major CAF markers in murine tumor cell lines expressed as total percent frequency of live cells (A-B). FAP: fibroblast activation protein; SMA: alpha smooth muscle actin, PDPN: Podoplanin, PDGFR- α : platelet derived growth factor receptor alpha; PDGFR- β : platelet derived growth factor receptor beta. Data represent n=3 replicates per group.

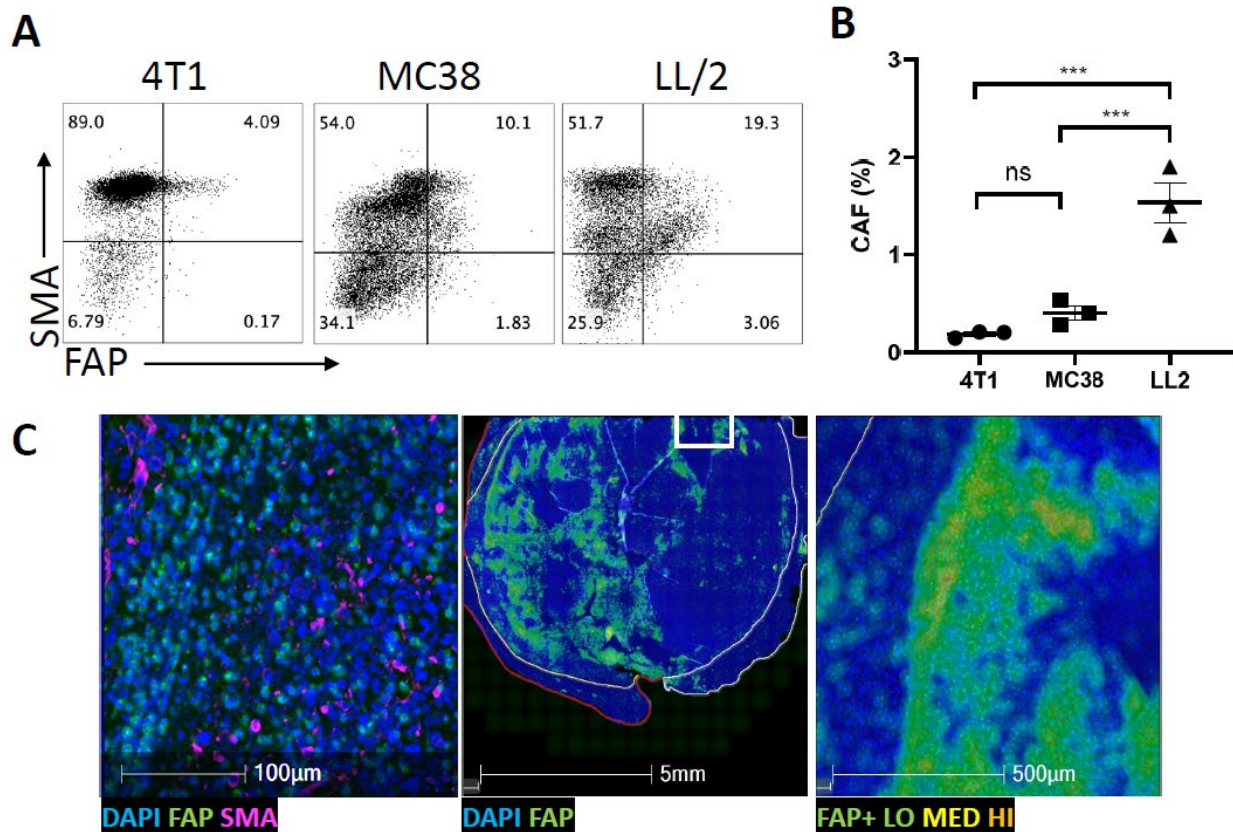


Figure 2. CAFs are present in the TME across several tumor models at steady state.

Representative flow cytometry plots comparing CAF subset marker expression in three murine tumor types (A) Frequency of SMA+FAP+ CAFs analyzed in (A) demonstrate significantly high CAF frequency in LL/2 tumors than the others (B). Data represent n=3 replicates per group. Means \pm SEM are shown. p-values calculated using one-way ANOVA, *** p < 0.001, ns = not significant. Representative immunofluorescent image of an LL/2 tumor shows expression of the activated fibroblast markers α -SMA and FAP and generated heat map of FAP expression (C). Nuclei were counterstained with DAPI. Stromal boundary is represented by yellow line and tumor invasive front by red line.

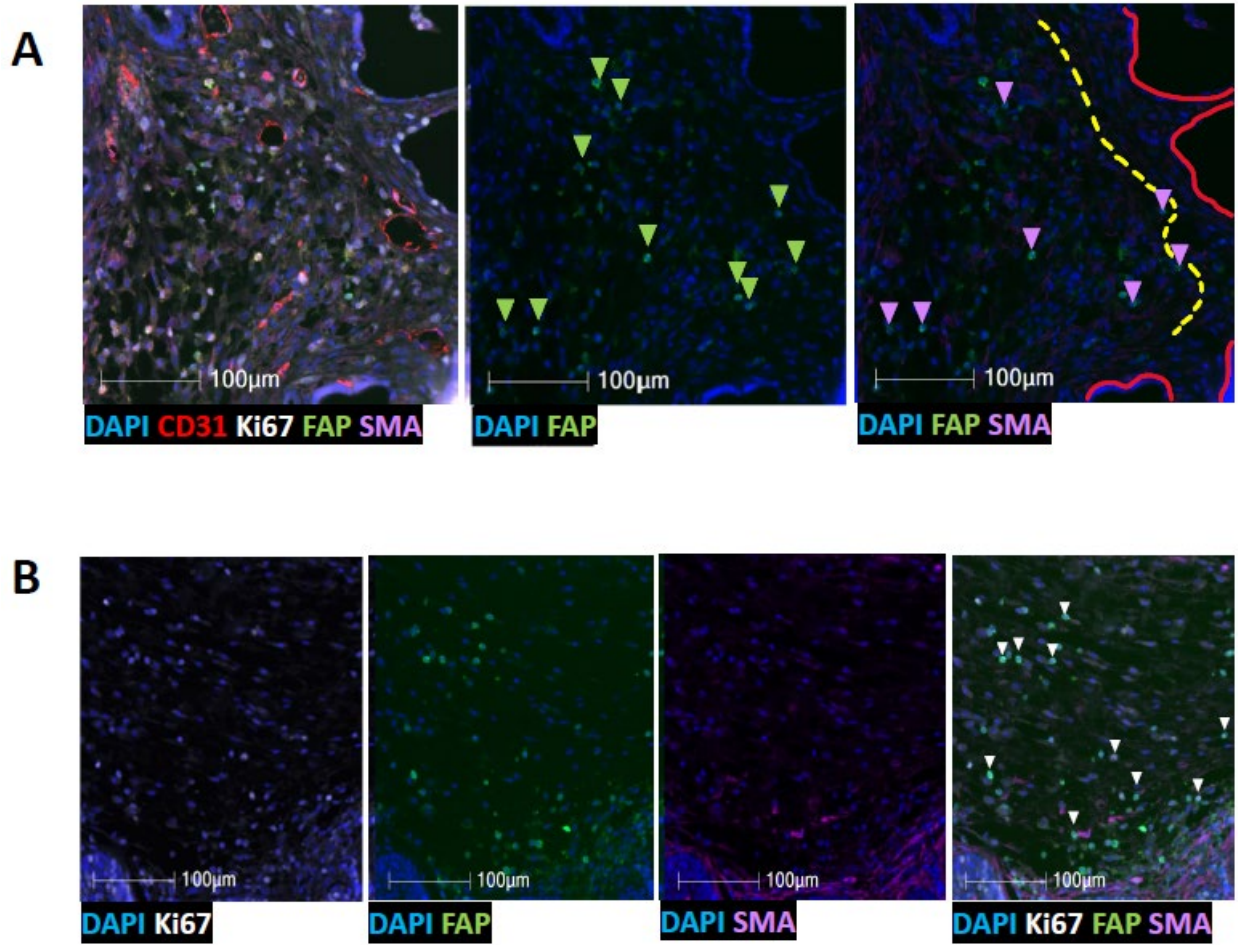


Figure S2. CAFs are present in the MMTV-PyVT TME at steady state.

Immunofluorescent histology of cancer-associated fibroblast (CAF) subset marker expression in the MMTV-PyMT tumor model at steady state (A-B). Representative images show expression of the activated fibroblast markers α -SMA (pink) and FAP (green), α -SMA and FAP co-expression (purple arrowheads) proliferative marker Ki67 (white; white arrowheads) and endothelial marker CD31 (red). Nuclei were counterstained with DAPI (blue). Stromal boundary represented by dashed yellow line and tumor invasive front by solid red line.

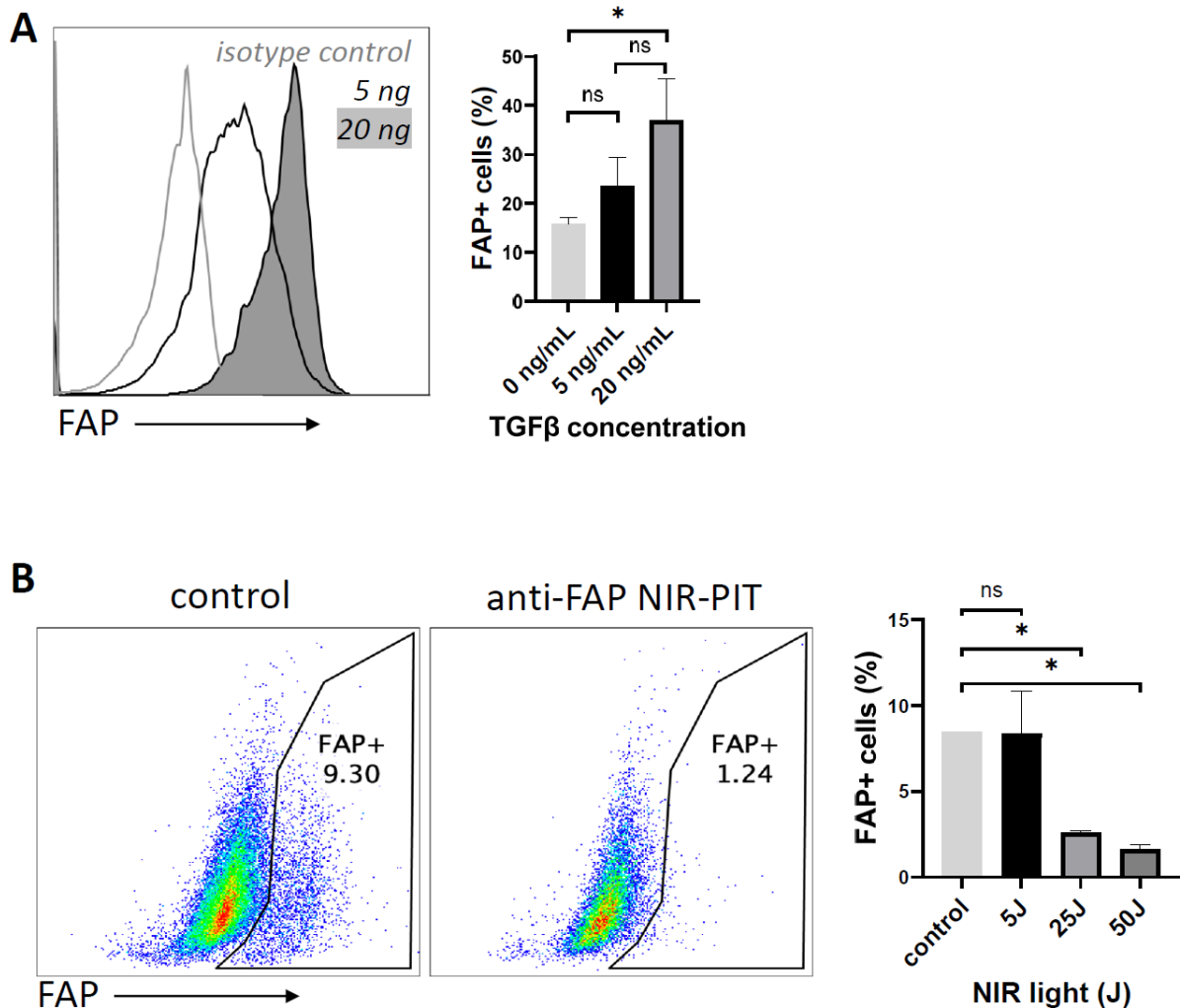


Figure 3. Anti-FAP NIR-PIT induces cell death of FAP⁺ expressing fibroblasts in vitro.

Flow cytometry analysis of NIH3T3 cell stimulation with TGF-β expressed as total percent frequency of Live, FAP⁺ cells (A) and flow cytometry analysis of anti-FAP NIR-PIT in vitro expressed as total percent frequency of Live, FAP⁺ cells (B). Data represent n=3-4 replicates per group. Means ± SEM are shown. *p*-values calculated using one-way ANOVA, * *p* < 0.05, ns = not significant.

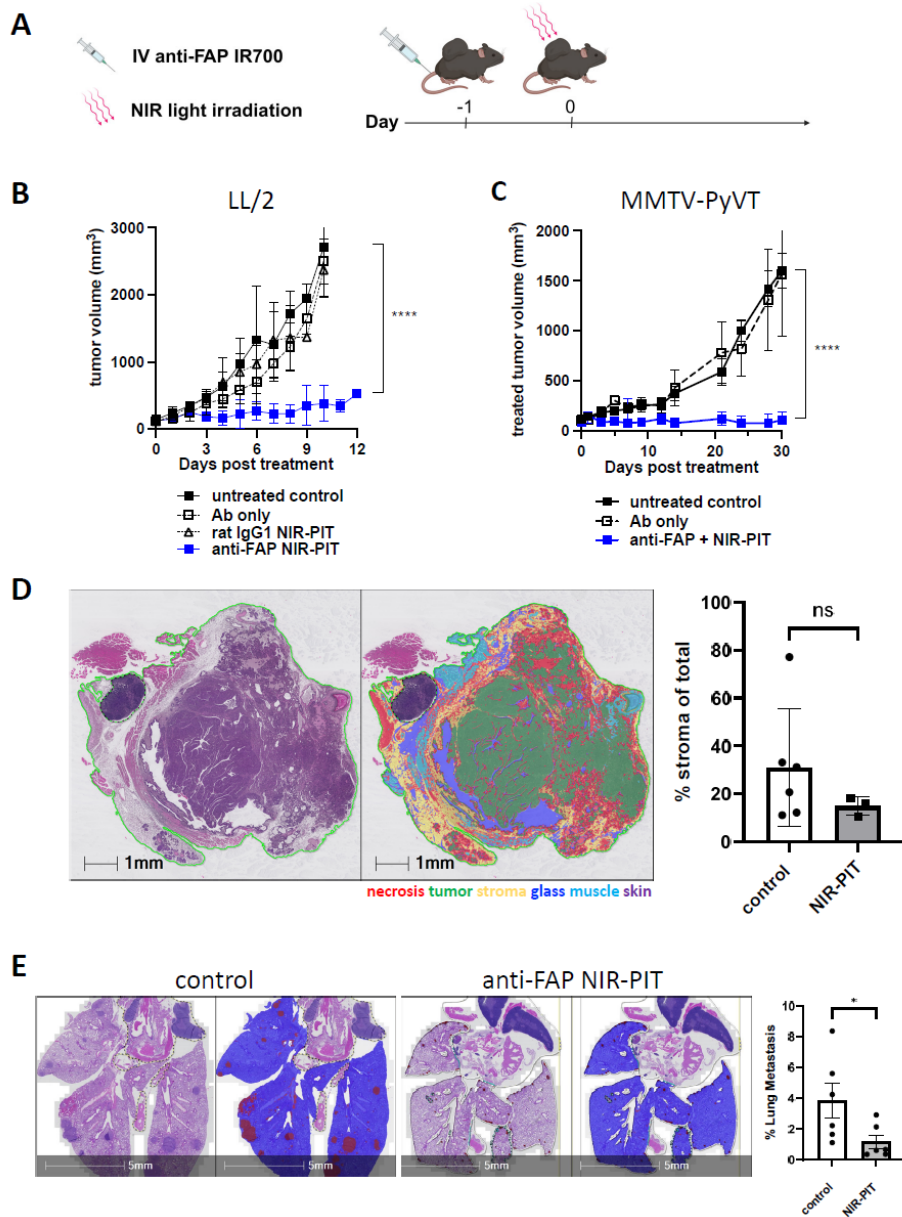


Figure 4. Anti-FAP NIR-PIT suppresses tumor growth and lung metastasis in vivo.

Experimental timeline for in vivo NIR-PIT experiments (A). Experimental group mice were administered an intravenous injection of either unconjugated anti-FAP (Ab only), rat IgG1-IR700 (isotype control; rat IgG1 + NIR-PIT) or anti-FAP IR700 (anti-FAP + NIR-PIT) at Day -1, and both isotype control and anti-FAP groups were administered 50J NIR light exposure at 24h post-injection (Day 0). Tumor volume growth curve for LL/2 (inoculated) tumor experiment (B) and MMTV-PyVT (spontaneous) tumor experiment (C). Data presented as mean \pm SEM. $n=5-6$ per group. p -values calculated using one-way ANOVA, *** $p < 0.0001$. H&E sections with analysis markup from random forest classified tissue regions for LL/2 control and anti-FAP NIR-PIT treatment groups (D). H&E sections with AI classified endpoint lung metastasis for MMTV-PyVT control and anti-FAP NIR-PIT treatment groups (E). Lung metastasis $n=6$ per group. p -values calculated using student's t-test (two-tailed), * $p < 0.05$, ns = not significant.

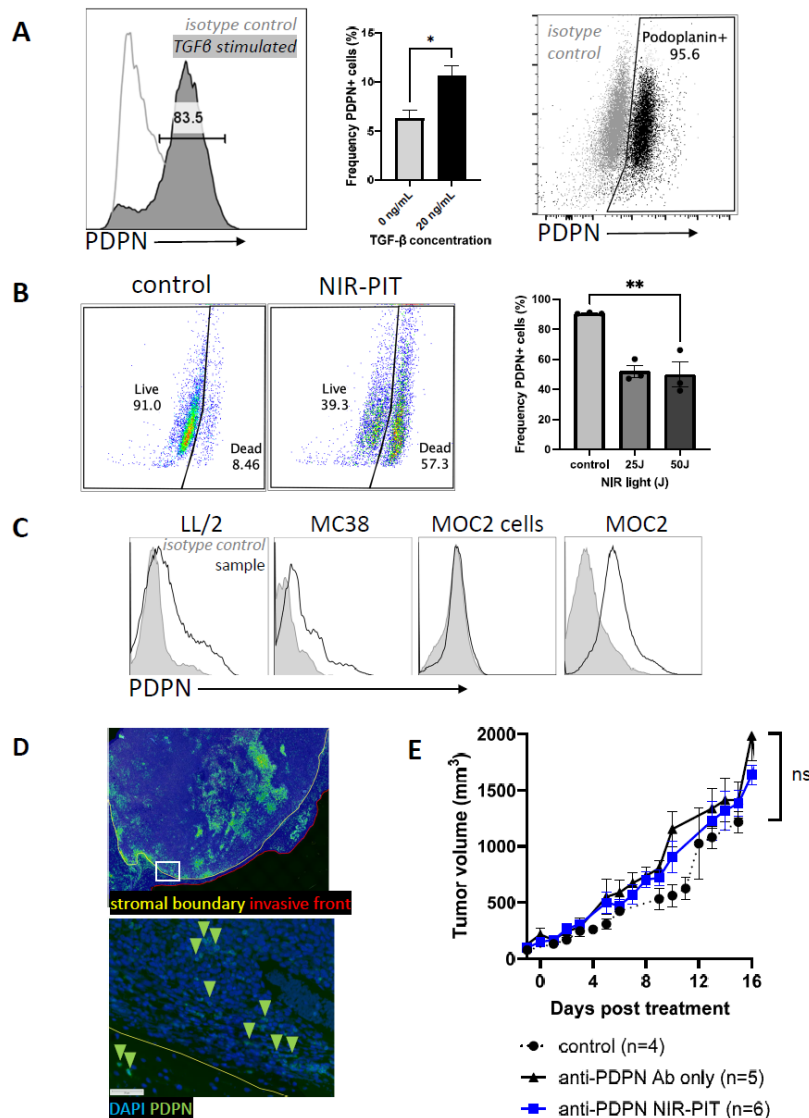


Figure S3. Anti-PDPN NIR-PIT depletes PDPN⁺ cells in vitro but did not suppress tumor growth in vivo.

Flow cytometry analysis of NIH3T3 cell stimulation with TGF-β expressed as total percent frequency of Live, PDPN⁺ cells (A) and flow cytometry analysis of anti-FAP NIR-PIT in vitro expressed as total percent frequency of Live, PDPN⁺ cells (B). Data presented as mean ± SEM. n=3 per group. Flow cytometry analysis of total percent frequency of Live, PDPN⁺ cells within MC38, LL/2 tumors and MOC2 tumors compared with MOC2 tumor cells (C). Representative image and generated heat map of PDPN expression in the MOC2 tumor model at steady state (D). Nuclei were counterstained with DAPI. Tumor volume growth curve for MOC2 (inoculated) tumor experiment (E). Experimental group mice were administered an intravenous injection of either unconjugated anti-PDPN (Ab only), or anti-PDPN IR700 (anti-PDPN + NIR-PIT) and the anti-PDPN IR700 group was administered 50J NIR light exposure at 24h post-injection. Data presented as mean ± SEM. n=4-6 per group. *p*-values calculated using student's t-test (TGF-β stimulation) or one-way ANOVA (in vitro NIR-PIT and tumor growth curve), * *p* < 0.05, ** *p* < 0.005, ns = not significant.

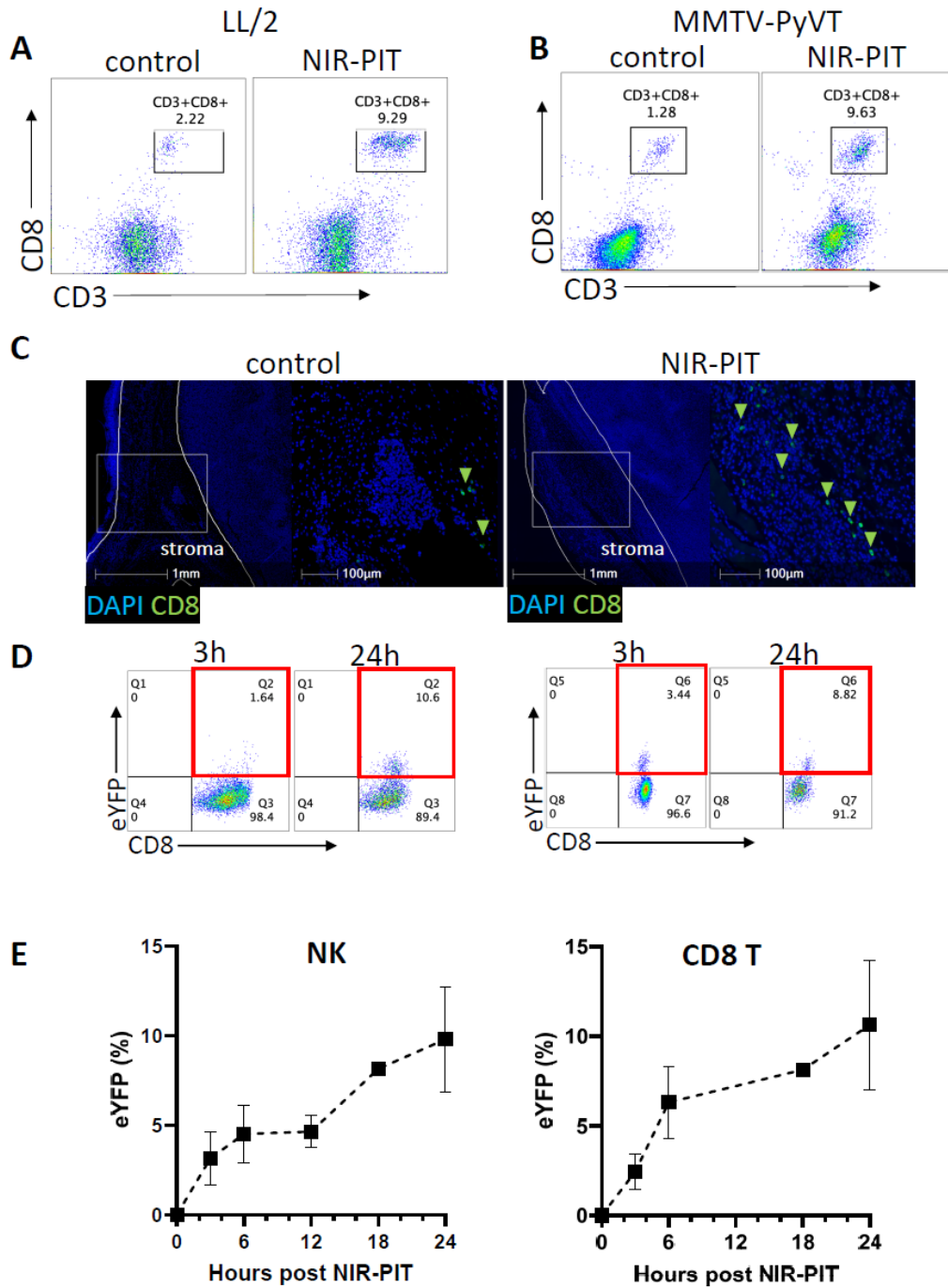


Figure 5. Anti-FAP NIR-PIT increases immune effector cells and IFN- γ in the TME.

Flow cytometry analysis of CD3⁺CD8⁺ T and CD3⁻NK1.1⁺ cells and 24h after anti-FAP NIR-PIT (A-B). Multiplex immunohistochemistry of CD8⁺ T cells 24h after anti-FAP NIR-PIT (C). Flow cytometry analysis of eYFP-IFN- γ reporter mouse CD8⁺T and CD3⁻NK1.1⁺ cells in LL/2 tumors at representative time points (3h, 24h) (D) Endogenous IFN- γ (IFN- γ -eYFP) production by CD3⁻ NK1.1⁺ cells and CD3⁺CD8⁺ T cells from 0h to 24h (E). Data presented as mean \pm SEM. n=3-5 per group.

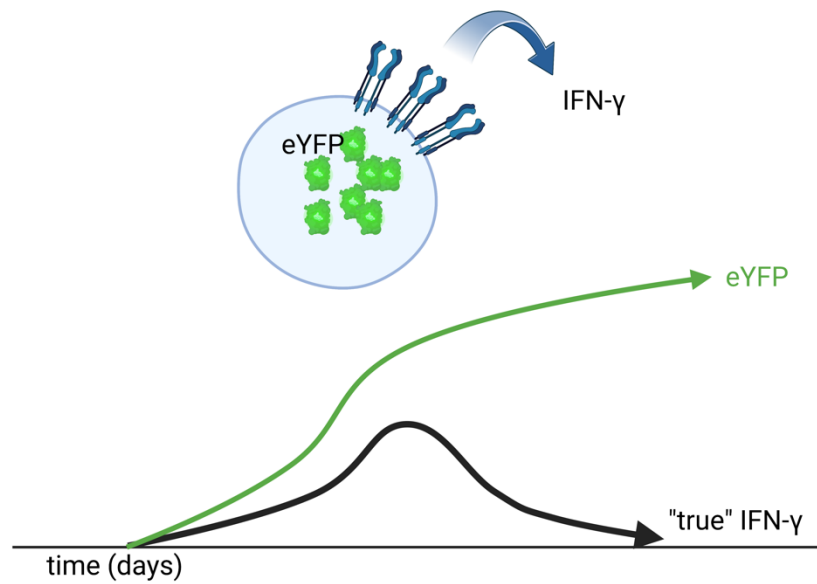


Figure S4. Mechanism of IFN- γ eYFP timecourse

The interferon gamma (IFN- γ) eYFP fluorescent reporter mouse produces eYFP as endogenous IFN- γ is produced. However, there is likely a discrepancy between eYFP signal, which is measured via flow cytometry, and true IFN- γ (unmeasured) due to the longer half-life of eYFP.

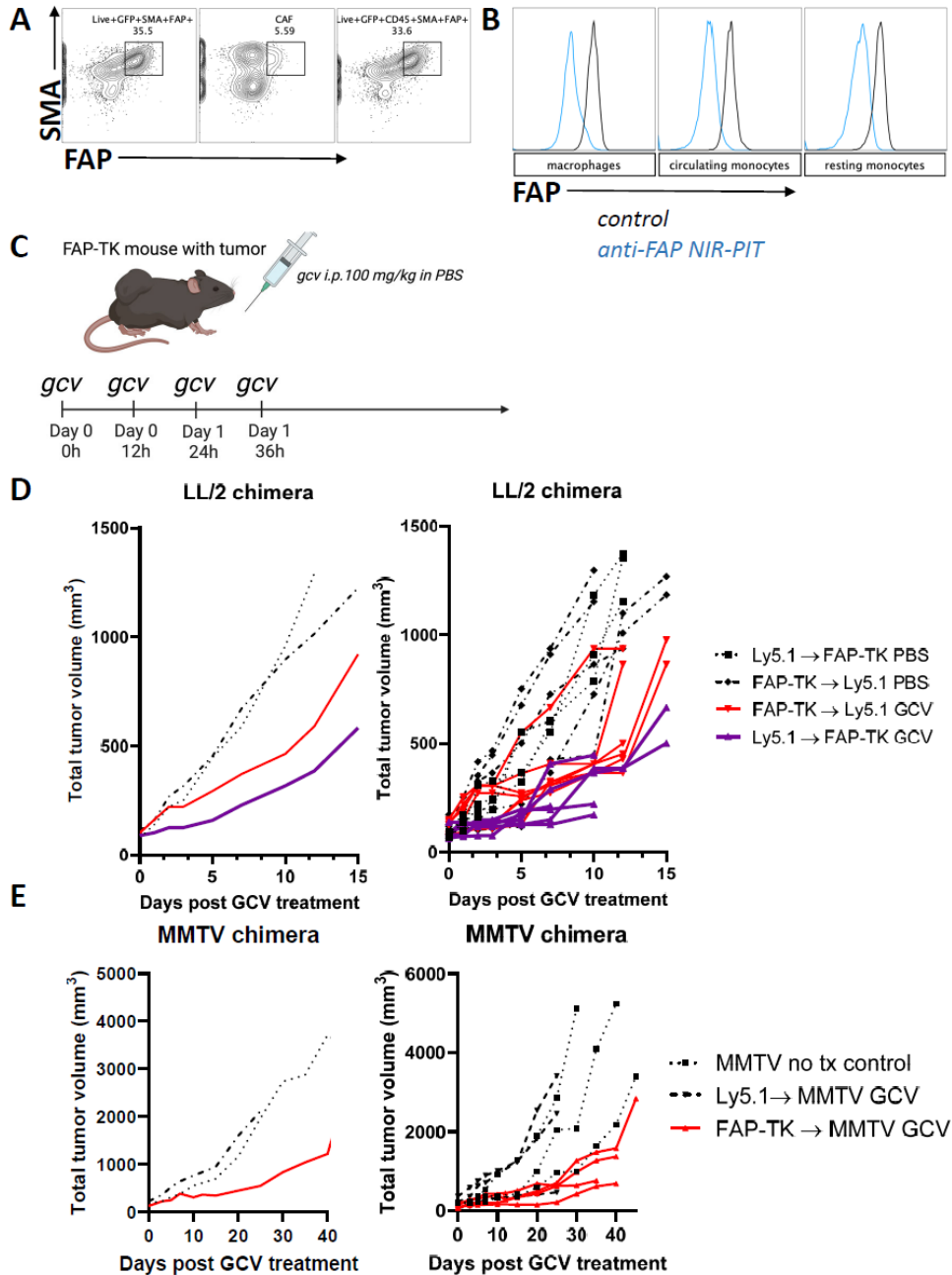


Figure 6. Depletion of FAP⁺ hematopoietic cells contributes to tumor growth suppression.

Flow cytometry analysis of Live⁺GFP⁺FAP⁺SMA⁺ population, Live⁺GFP⁺CD45⁻FAP⁺SMA⁺ population (CAFs) and Live⁺GFP⁺CD45⁺FAP⁺SMA⁺ (leukocyte) population of LL/2 tumor (A). Histograms of Live⁺CD45⁺FAP⁺ macrophage population, circulating monocyte population and resting monocyte population of LL/2 tumor control (black line) of 1h after anti-FAP NIR-PIT depletion (blue line) (B). Bone marrow chimera experimental groups and experimental timeline for ganciclovir administration (C). Tumor growth curves for MMTV-PyVT chimera experimental groups (D) and LL/2 chimera experimental groups (E). Solid red line represents hematopoietic FAP⁺ depletion, solid purple line represents stromal FAP⁺ depletion. PBS = Phosphate Buffered Saline, GCV = Ganciclovir, FAP-TK = Fibroblast Activation Protein Thymidine Kinase.

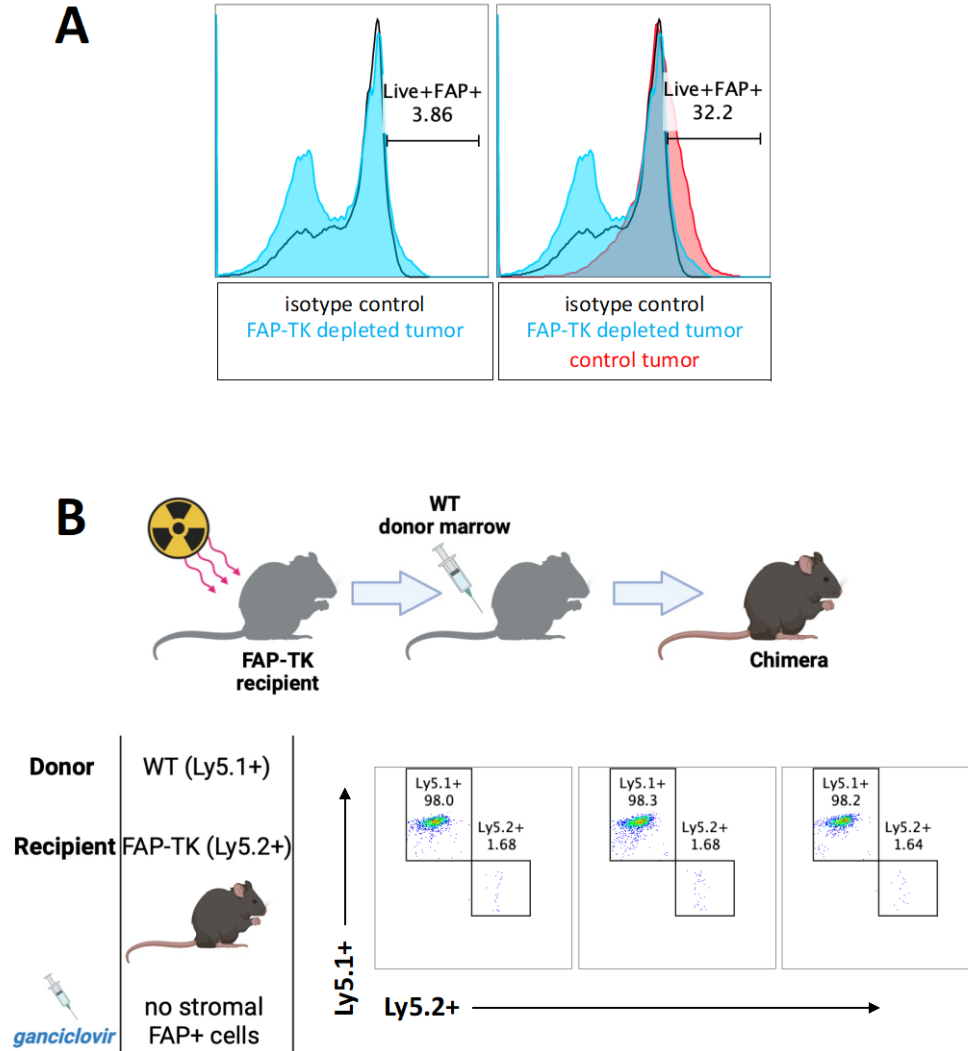


Figure S5. Validation of FAP⁺ depletion in FAP-TK mice and bone marrow chimera mouse models.

Representative histogram showing depletion of Live⁺FAP⁺ cells following ganciclovir administration in FAP-TK LL/2 tumor mouse via flow cytometry analysis (A). Data represents n=3 replicates. Chimera recipients were confirmed to have reconstituted >95% donor marrow using Ly5.1/Ly5.2 flow cytometry analysis on peripheral blood samples taken at least six weeks after bone marrow transfer (B). Data represent n=6-10 replicates per group. FAP-TK = Fibroblast Activation Protein Thymidine Kinase, WT= wild type.

Table S1: Antibodies used for flow cytometry

Reagent	Source	Identifier
Mouse anti-mouse FAP (clone 73.3)	Sigma	MABC1145
Rat anti-mouse FAP (clone 983802)	R&D Systems	AB9727
Mouse anti-mouse α -SMA-PE (clone 1A4)	Novus	NBP2-34522PE
Mouse anti-mouse α -SMA-FITC (clone 1A4)	Sigma	F3777
Armenian Hamster anti-mouse CD3-BV421 (clone 145-2C11)	Biolegend	100336
Anti-mouse CD8a-PECy5 (clone 53-6.7)	Thermo Fisher Scientific	15-0081082
Rat anti-mouse CD11b-PECy7 (clone M1/70)	eBioscience	25-0112-82
Rat anti-mouse polyclonal CD16	Biolegend	101301
Mouse anti-mouse CD45.1-FITC (clone: A20)	Thermo Fisher Scientific	11-0453-85
Mouse anti-mouse CD45.2-PE (clone: 104)	Thermo Fisher Scientific	12-0454-83
Mouse anti-mouse CD45.2-BV 650 (clone: 104)	Biolegend	50-402-986
Rat anti-mouse F4/80-APC	Biolegend	123116
LiveDead Fixable Viability Dye eFlour™ 455 UV	Thermo Fisher Scientific	65-0868-14
Rat anti-mouse Ly6C PE (clone: HK1.4)	Thermo Fisher Scientific	12-5932-82
Syrian Hamster anti-mouse PDPN-PE Cy7 (clone 8.1.1)	Biolegend	25-5381-82
Rat anti-mouse PDGFR- α -Super Bright™ 600 (clone APA5)	Thermo Fisher Scientific	63-1401-82
Rat anti-mouse PDGFR- β -PE (clone APB5)	Thermo Fisher Scientific	14-1402-81
Mouse anti-mouse NK1.1-PE (clone: PK136)	Thermo Fisher Scientific	12-5941-83

Table S2: Antibodies used for histology

Reagent	Source	Identifier
Rabbit polyclonal anti-mouse FAP	Abcam	218164
Rabbit anti-mouse α -SMA (clone EPR5368)	Abcam	Ab124964
Rabbit polyclonal anti-mouse CD3e	Thermo Fisher Scientific	PA1-29547
Rabbit anti-mouse CD8a (clone D4W2Z)	Cell Signaling	989415
Rat anti-mouse CD8a (clone C8/144B)	Invitrogen	MA5-13473
Rabbit anti-mouse CD31 (clone D8V9E)	Cell Signaling	77699S
Rabbit anti-mouse CD45 (clone D3F8Q)	Cell Signaling	70257S
Rabbit anti-mouse Ki67 (clone SP8)	Cell Marque	275R
Rabbit anti-mouse Podoplanin (clone 66)	Invitrogen	MA5-29742

FUNDING

This research was supported by the Intramural Research Program of the National Institutes of Health, National Cancer Institute, Center for Cancer Research (ZIA BC 010656 and ZIA BC 010657).

RG is a Molecular Pathology Fellow in the NIH Comparative Biomedical Scientist Training Program supported by the National Cancer Institute in partnership with Michigan State University.

CHAPTER 3

CONCLUSIONS AND FUTURE DIRECTIONS

CONCLUSIONS AND FUTURE DIRECTIONS

Cancer associated fibroblasts (CAFs) comprise a majority of the stromal cellular compartment in solid tumors, and serve significant functions in immunosuppression, invasion, and angiogenesis. One of the greatest challenges in targeting CAFs is the lack of a pan-specific biomarker as CAFs often express variable phenotypes across tumor and tissue types. As reviewed in Chapter 1, high expression of fibroblast activation protein (FAP) by CAFs is a negative prognostic indicator, and promising intratumoral target as it is most often expressed by immunosuppressive CAFs in several cancers. FAP itself also directly supports tumor growth, invasion, and metastasis as a through extracellular matrix remodeling [1]. We also observed expression of FAP in several murine cancer models examined. Therefore, we chose to use FAP as a CAF target for NIR-PIT. We chose two models, one subcutaneously inoculated (LL/2), one spontaneously occurring with frequent lung metastasis (MMTV-PyVT) to test this therapy. To our knowledge, this work is the first to use anti-FAP NIR-PIT entirely in vivo in an immunocompetent host, as well as the first within a spontaneous mouse tumor model.

As discussed in Chapter 2, our bone marrow chimera modeling sought to untangle the contribution of stromal versus hematopoietic FAP-expressing cells. Although we observed a measurable effect from depletion of the FAP⁺ hematopoietic cells, additional work is required for more meaningful conclusions, as well as fully quantify the contribution of the FAP⁺ hematopoietic cell compartment towards tumor regression. We were also unable to see a measurable distinction between anti-PDPN NIR-PIT treated MOC2 tumor mice and controls. Because this was effective in vitro against murine fibroblasts (NIH3T3) with upregulated PDPN expression, this experiment might be considered for re-evaluation to increase antibody distribution in the tumor, or improving specificity

of the PDPN-IR700 conjugate for CAFs in vivo by increasing PDPN concentration bound to IR700, or considering alternative murine tumors which may express PDPN more highly.

One limitation of NIR-PIT is that NIR light at a wavelength of 690 nm can penetrate and treat cancers at a maximum depth of approximately 1 cm. For our experiments, tumors were present in the subcutis or mammary gland in a mouse model. In clinical applications, for example, fibrotic tumors e.g. hepatocellular carcinoma, pancreatic or colon cancers, NIR light delivered through a catheter needle or endoscope [19, 20] can expand its use on these deeper tumors and also metastatic lesions. It is also possible that additional round(s) of PIT dose could improve tumor efficacy even further. A second round of NIR-PIT could be repeated to prevent tumor regrowth, which occurs months or years later in human patients, in contrast to the experimental mouse tumor models [5].

While much of our knowledge about CAF biology has come from in vitro modeling, it has been repeatedly demonstrated that CAFs in culture do not fully recapitulate the heterogeneity of CAFs in vivo [2-4]. Despite the popularity of human xenografts, immune compromised mice are unable to mount a comprehensive immune response. Moreover, in these models, human cells grow within a murine tumor microenvironment which raises the issue of species incompatibilities and a foreign murine microenvironment. While convenient, co-transplant of human stromal cells (fibroblasts) also do not accurately represent tumor progression or recapitulate metastasis [5]. Preclinical work in immune-competent tumor models including genetically engineered mouse models (GEMM), is critical for insight into clinically relevant cancer biology and CAF ecology in the context of the tumor microenvironment. To this end, we employed the MMTV-PyVT GEMM to evaluate the effects of FAP⁺ depletion using NIR-PIT. The KPC mouse, a spontaneous model of pancreatic ductal adenocarcinoma, could also be considered for future work examining the effects of FAP⁺ depletion, as it is a highly stromagenic cancer [6]. Possible targets which overlap between the

MMTV-PyVT GEMM and the KPC GEMM include FAP and PDGFR- α , which would require minimal changes from the already established protocols and analysis methods described here.

Other Applications for anti-CAF NIR-PIT

NIR-PIT is established as an innovative, safe, and effective tool, which can be used as a single or combination therapy aimed at restoring anti-tumor immunity. NIR-PIT offers a minimally invasive method whereby the antibody conjugate is administered systemically, but only activated at sites where target cells are bound and exposed to NIR light; both conditions need to be met for effective target killing. In addition to its therapeutic use, anti-FAP NIR-PIT could potentially expand our understanding of CAF biology through tumor progression at various stages of tumor development. Unlike tumor-specific antigens used in NIR-PIT, anti-FAP NIR-PIT is also more likely to be effective across a range of tumors as FAP⁺ immunosuppressive cells are present in many tumor types [7]. In this study, the same anti-FAP IR700 conjugate was effective in both Lewis lung murine lung cancer and MMTV murine mammary cancer models.

There are several potential future clinical applications to anti-CAF directed NIR-PIT. Anti-FAP NIR-PIT could be considered as an adjunctive therapy with other cancer drugs, such as cancer-cell directed treatment or immune checkpoint inhibitors. Anti-FAP NIR-PIT in combination with conventional cancer-cell directed therapies could potentially enhance the effect of NIR-PIT alone and overcome the limitations of monotherapy. In previous cancer-cell targeting NIR-PIT, a phenomenon known as the super enhanced permeability and retention (SEPR) effect was observed [8, 9]. In this effect, tumors treated with NIR light undergo a rapid but significant period of increased vascular permeability after cell volume decreased, resulting in enhanced delivery of nano-sized therapeutic agents. By eliminating fibroblasts with anti-FAP NIR-PIT, we may see a similar phenomenon due to reduction of stromal cells in the tumor and subsequent permeability due to a

reduction in tumor pressure. Anti-CAF NIR-PIT could also be considered in the context of other fibrotic conditions. CAFs have been described to contribute to non-malignant disease conditions including cardiac fibrosis [10] and inflammatory bowel disease (IBD) [11] and selective depletion of these cells might help us better understand underlying the role of fibroblasts in the mechanism of disease [12].

One area of research with much recent interest is the use of FAP inhibitors (FAPi) as a PET imaging agent in cancer patients, whose tumors express FAP more highly than those in mice [13]. Radiolabeled FAPi tracers binds to FAP⁺ cells abundant in cancers and can deliver image-enhancing photons and/or ionizing particles directly into tumor stroma. The difference in FAPi expression between tumor stroma and normal tissue is leveraged to better distinguish the tumor from surrounding structures in imaging. Data from this emerging field is limited [14-16] yet highly promising [17], particularly in the detection of peritoneal ovarian and gastric carcinomatosis [18] FAPi PET to might also be beneficial for future diagnostics and identification of human cancer patients who might benefit from anti-FAP therapy.

CAFs not a uniform population of cells, as they may be derived from several different cell types which can express other target markers depending on cell origin and tumor type. Although FAP and PDPN were used in targeting CAFs in our study, other tumor models expressing alternative immunosuppressive CAF markers such as PDGFR- α may also demonstrate efficacy in the NIR-PIT system. In this system, any antibody which can be successfully conjugated to IR700 and bind a target cell efficiently could potentially be investigated as a CAF-directed NIR-PIT therapy.

The in vitro NIR-PIT modeling system using TGF- β stimulated NIH3T3 cells described in this work is also a valuable tool to quickly assess future CAF targets for efficacy. This system requires very few resources, outside of high quality and concentration antibody, IR700 photoactive dye,

NIR light and the target cells. As the quality and number of CAF-directed antibodies increases, this assay provides an excellent screening mechanism for additional CAF-directed NIR-PIT models.

In summary, CAF targeting using anti-FAP NIR-PIT is a highly promising therapy. Recent research in the biology of CAFs in human tumors, as well as FAPi imaging field showing patient tumors expressing high levels of FAP [13] is further encouraging, as this therapy could demonstrate even more benefit in the human cancer clinical setting than preclinical murine studies.

REFERENCES

1. Liu R, Li H, Liu L, Yu J, Ren X. Fibroblast activation protein: A potential therapeutic target in cancer. *Cancer Biol Ther.* 2012; 13: 123-9. doi: 10.4161/cbt.13.3.18696.
2. Puram SV, Tirosh I, Parikh AS, Patel AP, Yizhak K, Gillespie S, Rodman C, Luo CL, Mroz EA, Emerick KS, Deschler DG, Varvares MA, Mylvaganam R, et al. Single-Cell Transcriptomic Analysis of Primary and Metastatic Tumor Ecosystems in Head and Neck Cancer. *Cell.* 2017; 171: 1611-24 e24. doi: 10.1016/j.cell.2017.10.044.
3. Tirosh I, Izar B, Prakadan SM, Wadsworth MH, 2nd, Treacy D, Trombetta JJ, Rotem A, Rodman C, Lian C, Murphy G, Fallahi-Sichani M, Dutton-Regester K, Lin JR, et al. Dissecting the multicellular ecosystem of metastatic melanoma by single-cell RNA-seq. *Science.* 2016; 352: 189-96. doi: 10.1126/science.aad0501.
4. Waise S, Parker R, Rose-Zerilli MJ, Layfield DM, Wood O, West J, Ottensmeier CH, Thomas GJ, Hanley CJ. An optimised tissue disaggregation and data processing pipeline for characterising fibroblast phenotypes using single-cell RNA sequencing. *Sci Rep.* 2019; 9: 9580. doi: 10.1038/s41598-019-45842-4.
5. Wagner KU. Models of breast cancer: quo vadis, animal modeling? *Breast Cancer Res.* 2004; 6: 31-8. doi: 10.1186/bcr723.
6. Hingorani SR, Wang L, Multani AS, Combs C, Deramandt TB, Hruban RH, Rustgi AK, Chang S, Tuveson DA. Trp53R172H and KrasG12D cooperate to promote chromosomal instability and widely metastatic pancreatic ductal adenocarcinoma in mice. *Cancer Cell.* 2005; 7: 469-83. doi: 10.1016/j.ccr.2005.04.023.
7. Monteran L, Erez N. The Dark Side of Fibroblasts: Cancer-Associated Fibroblasts as Mediators of Immunosuppression in the Tumor Microenvironment. *Front Immunol.* 2019; 10: 1835. doi: 10.3389/fimmu.2019.01835.
8. Kobayashi H, Choyke PL. Super enhanced permeability and retention (SUPR) effects in tumors following near infrared photoimmunotherapy. *Nanoscale.* 2016; 8: 12504-9. doi: 10.1039/c5nr05552k.
9. Nakamura Y, Mochida A, Choyke PL, Kobayashi H. Nanodrug Delivery: Is the Enhanced Permeability and Retention Effect Sufficient for Curing Cancer? *Bioconjug Chem.* 2016; 27: 2225-38. doi: 10.1021/acs.bioconjchem.6b00437.
10. Nicolini G, Balzan S, Forini F. Activated fibroblasts in cardiac and cancer fibrosis: An overview of analogies and new potential therapeutic options. *Life Sci.* 2023; 321: 121575. doi: 10.1016/j.lfs.2023.121575.
11. Corsi F, Sorrentino L, Albasini S, Colombo F, Cigognini M, Massari A, Morasso C, Mazzucchelli S, Piccotti F, Ardizzone S, Sampietro GM, Truffi M. Circulating Fibroblast Activation Protein as Potential Biomarker in Patients With Inflammatory Bowel Disease. *Front Med (Lausanne).* 2021; 8: 725726. doi: 10.3389/fmed.2021.725726.

12. Kobayashi H, Furusawa A, Rosenberg A, Choyke PL. Near-infrared photoimmunotherapy of cancer: a new approach that kills cancer cells and enhances anti-cancer host immunity. *Int Immunol.* 2021; 33: 7-15. doi: 10.1093/intimm/dxaa037.
13. Huang R, Pu Y, Huang S, Yang C, Yang F, Pu Y, Li J, Chen L, Huang Y. FAPI-PET/CT in Cancer Imaging: A Potential Novel Molecule of the Century. *Front Oncol.* 2022; 12: 854658. doi: 10.3389/fonc.2022.854658.
14. Fitzgerald AA, Weiner LM. The role of fibroblast activation protein in health and malignancy. *Cancer Metastasis Rev.* 2020; 39: 783-803. doi: 10.1007/s10555-020-09909-3.
15. Loktev A, Lindner T, Burger EM, Altmann A, Giesel F, Kratochwil C, Debus J, Marme F, Jager D, Mier W, Haberkorn U. Development of Fibroblast Activation Protein-Targeted Radiotracers with Improved Tumor Retention. *J Nucl Med.* 2019; 60: 1421-9. doi: 10.2967/jnumed.118.224469.
16. Loktev A, Lindner T, Mier W, Debus J, Altmann A, Jager D, Giesel F, Kratochwil C, Barthe P, Roumestand C, Haberkorn U. A Tumor-Imaging Method Targeting Cancer-Associated Fibroblasts. *J Nucl Med.* 2018; 59: 1423-9. doi: 10.2967/jnumed.118.210435.
17. Chen H, Pang Y, Wu J, Zhao L, Hao B, Wu J, Wei J, Wu S, Zhao L, Luo Z, Lin X, Xie C, Sun L, et al. Comparison of [(68)Ga]Ga-DOTA-FAPI-04 and [(18)F] FDG PET/CT for the diagnosis of primary and metastatic lesions in patients with various types of cancer. *Eur J Nucl Med Mol Imaging.* 2020; 47: 1820-32. doi: 10.1007/s00259-020-04769-z.
18. Gilardi L, Airo Farulla LS, Demirci E, Clerici I, Omodeo Sale E, Ceci F. Imaging Cancer-Associated Fibroblasts (CAFs) with FAPi PET. *Biomedicines.* 2022; 10. doi: 10.3390/biomedicines10030523.
19. Nagaya T, Okuyama S, Ogata F, Maruoka Y, Choyke PL, Kobayashi H. Endoscopic near infrared photoimmunotherapy using a fiber optic diffuser for peritoneal dissemination of gastric cancer. *Cancer Sci.* 2018; 109: 1902-8. doi: 10.1111/cas.13621.
20. Okuyama S, Nagaya T, Sato K, Ogata F, Maruoka Y, Choyke PL, Kobayashi H. Interstitial near-infrared photoimmunotherapy: effective treatment areas and light doses needed for use with fiber optic diffusers. *Oncotarget.* 2018; 9: 11159-69. doi: 10.18632/oncotarget.24329.